Journal of Thermal Analysis and Calorimetry (2023) 148:6645–6686
https://doi.org/10.1007/s10973-023-12184-3

Rheological and thermophysical properties of hybrid nanofluids and their application in flat-plate solar collectors: a comprehensive review

Mohanad A. Alfellag[1,2] · Haslinda Mohamed Kamar[1] · Nor Azwadi Che Sidik[3] · Ali S. Muhsan[4] · S. N. Kazi[5] · Omer A. Alawi[1] · Ummikalsom Abidin[1]

Received: 13 January 2023 / Accepted: 9 April 2023 / Published online: 6 May 2023

Abstract

Conventional working fluids such as water, glycol, and synthetic oils are commonly employed in solar thermal applications, but they have relatively low thermal conductivity, which leads to minimized heat transfer and lower thermal performance. As an alternative, a novel category of fluids known as hybrid nanofluids has proven to be highly beneficial for solar thermal applications due to their enhanced thermophysical properties. Recently, numerous studies have explored hybrid nanofluids as a continuation of nanofluids research for the improvement of the thermophysical properties of mono nanofluids. In this review paper, publications of hybrid nanofluids are in depth analyzed. The review is focusing on hybrid nanofluid preparation methods and characterization procedures, as well as techniques for assessing stability and improving it. The impact of hybrid nanoparticles on thermophysical properties such as thermal conductivity, viscosity, specific heat, and density is extensively reported. Furthermore, the current review provides a comprehensive overview of various experimental, numerical, and theoretical investigations where the hybrid nanofluids in flat-plate solar collectors were studied with a focus on thermal efficiency improvement, which is regarded as the primary parameter for using hybrid nanofluids. Lastly, recent challenges and limitations are outlined, and future recommendations are presented for further investigations.

Keywords Hybrid nanofluids · Stability · Thermophysical properties · Flat-plate solar collectors

Introduction

As the world's population continues to rise at an alarming rate, it is critical to develop more effective methods of using energy resources. Fossil fuels account for more than 80% of global energy output, raising carbon levels in the atmosphere and thereby hastening climate change [1]. As a result, renewable energy sources such as solar energy are encouraged to mitigate the aforementioned disadvantage of fossil fuels [2, 3]. This enormous energy source can be used almost anywhere on the earth without contaminating the air. Solar thermal energy is often regarded as the most ecologically and cost-effective form of energy. Solar thermal collectors are used to harvest thermal energy from solar radiation. The flat-plate solar collector type (FPSC), which collects solar thermal energy and transfers it to the working fluid, is one of the most economical and widely used types of solar collectors. FPSCs are favored over other solar thermal collectors due to their low production cost, ability to collect both diffuse and beam radiation, and absence of need for a sun

✉ Mohanad A. Alfellag
Abdulazez@graduate.utm.my;
mohanadheete@uoanbar.edu.iq

✉ Nor Azwadi Che Sidik
Azwadi@utm.my

1 Department of Thermofluids, School of Mechanical Engineering, Universiti Teknologi Malaysia, UTM Skudai, 81310 Johor Bahru, Malaysia

2 Department of Mechanical Engineering, College of Engineering, University of Anbar, 31001 Ramadi, Iraq

3 Malaysia – Japan International Institute of Technology (MJIIT), University Teknologi Malaysia Kuala Lumpur, Jalan Sultan Yahya Petra, 54100 Kuala Lumpur, Malaysia

4 Department of Mechanical Engineering, Universiti Teknologi PETRONAS, 32610 Bandar Seri Iskandar, Perak Darul Ridzuan, Malaysia

5 Department of Mechanical Engineering, University of Malaya, 50603 Kuala Lumpur, Malaysia

tracking equipment [4]. FPSCs, on the other hand, have low thermal efficiency and convective heat transfer between the circulating fluid and the absorber. [5, 6]. Researchers had aimed to increase FPSCs efficiency by improving collector design and increasing the heat transfer rate between tubes and working fluids: shape of the collector [7, 8], coatings [9, 10], absorber design [11–13], flow turbulence [14–17], porous media [18, 19].

Utilizing highly thermally conductive working fluids, nanofluids, is another feasible and effective way to increase FPSC thermal performance. Nanofluids are produced via dispersing high conductive solid nanoparticles in base fluids, and as a result, the thermophysical characteristics of these fluids are considerably improved. The thermal conductivity of nanofluids is enhanced due to many crucial aspects: particle Brownian motion in fluids, nanoparticles clustering in the base fluid, a liquid layer at the liquid-particle interface, nanoparticles concentration in the base fluid, and size of particle and particle migration [20, 21]. However, by adding nanoparticles to the base fluid, the viscosity experiences a rise, resulting in a rise in pumping power and a decrease in heat transfer capabilities. Nanofluids should be pumped at a low velocity to retain heat transfer rate as classical fluids. As a result, finding the optimal concentration of nanoparticles with low viscosity and good heat conductivity is critical [22]. In addition, one of the essential requirements of nanofluids for the applications of heat transfer is long-term stability. Nanofluid stability is important because it has a strong link to thermal conductivity enhancement [23]. The nanoparticles proneness to aggregation because of the presence of strong van der Waals attractive forces is the major parameter that affects the stability of nanofluids. The enhanced nanofluid thermal conductivity starts to decline as the aggregates sink to the bottom of the container of nanofluids.

The improved thermophysical properties of nanofluids have motivated several researchers to use them as a new class of heat transfer in the use of solar collectors. Hosseini and Dehaj [24] experimentally studied the influence of two types of nanofluids: water-based Al_2O_3 and GO on the performance of parabolic trough solar collector. It was concluded that the highest thermal efficiency of the system was 63.2% for Al_2O_3 and 32.1% for GO. Sheikholeslami and Ebrahimpour [25] attempted to employ Al_2O_3 in linear Fresnel reflector with using multi-way twisted tape numerically. The authors concluded that using such a combination of heat transfer enhancement techniques could lead to augmentation in the thermal efficiency of the solar system. Sheikholeslami and Jafaryar [26] studied the effect of carbon nanotubes (CNT) on the thermal performance of the tube in a concentrated solar system. In addition, swirl flow device was tested as heat transfer enhancement technique. Results revealed that utilizing such techniques can improve the thermal performance of the system. In terms of FPSCs, the most often used nanoparticles in FPSCs are Al_2O_3, SiO_2, CuO, TiO_2, MWCNTs, GNPs [6], and water, ethylene glycol (EG), oil, and molten salt are utilized as the base fluids. Choudhary et al. [27] employed Fe_2O_3/water-EG nanofluids in a FPSC with volume concentrations ranging from 0.2 to 1% and flow rates ranging from 30 to 150 L/h. Thermal efficiency was found to be 15.2% higher when compared to water and EG working fluids. Sundar et al. [28] used water-based Al_2O_3 nanofluid with wire coil as heat transfer augmentation methods for a FPSC. The highest thermal efficiency of 37.73% was reported compared with water. The thermal efficiency of FPSC was improved by 16–34.13% using MWCNTs/water nanofluid with volume concentrations of 0.01–0.1% [29]. Moreover, Alawi et al. [30] investigated the effect of using graphene nanoplatelets with pentaethylene glycol (GNPs/PEG) as a working fluid in a FPSC. Several parameters inputs were employed: nanoparticle mass fractions, volume flow rates, temperatures, and solar radiations. It was reported that the absorber performance had been enhanced by 13.3%.

A novel type of fluid known as hybrid nanofluids was later introduced. Several recent studies had examined hybrid nanofluids as a continuation of nanofluids research. Hybrid nanofluids are formed by dispersing two or more nanoparticles in the base fluid in either composite or mixed form [31]. Various methods were suggested for synthesizing hybrid nanoparticles, namely in situ, thermochemical, mechanical alloying, ball milling, wet chemical, solvothermal, and chemical vapor deposition [32]. Turcu et al. [33] are the first researchers who described synthesizing (MWCNTs/Fe_2O_3) hybrid nanoparticles. Following this, researchers have reported that hybrid nanofluids exhibited better thermal conductivity than regular nanofluids [34–38]. However, pressure loss caused by an increase in friction factor remains a severe issue. The increase in viscosity has a direct impact on pressure drop and requires more pumping power as a result. The pressure drop is proportional to the volume concentration of nanofluids and is greater for hybrid nanofluids [39]. According to several authors [40–42], the friction coefficient and pressure drop were considerably greater for hybrid nanofluids than that for the nanofluids from single nanoparticles. Figure 1 shows the number of articles published over the last 10 years in terms of nanofluids and hybrid nanofluids. It is seen that the attention of researchers on the nanofluids topic has gradually increased. As hybrid nanofluids are new generation of nanofluids, increasing interest in hybrid nanofluids is seen especially during the last three years. Since hybrid nanofluids have proved the enhancement of thermophysical properties compared to mono fluids, it is believed that the attention toward the utilization of hybrid nanofluids will increase shortly.

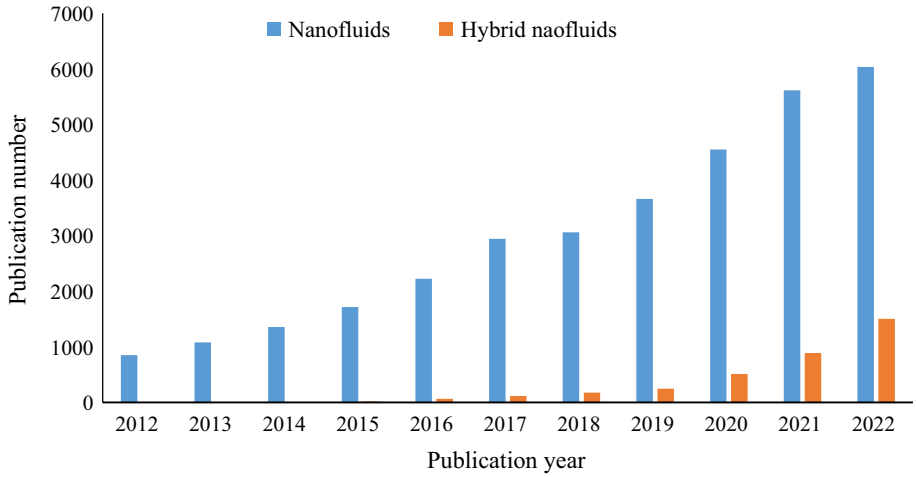

Fig. 1 Number of articles related to mono and hybrid nanofluids published by Elsevier, Springer, and Wiley

Sheikholeslami [43] evaluated the effect of SiO_2-CNT/water hybrid nanofluids on the performance of a Linear Fresnel reflector solar system. Authors employed perforated fins with the shape of horseshoe connected to the bottom of the tube. Based on findings, hybrid nanofluids along with fins can enhance the performance of the system. Ekiciler et al. [44] attempted to test three different types of hybrid nanofluids: Ag-ZnO, Ag-TiO_2, and Ag-Mgo with Syltherm 800 as a base fluid, on parabolic trough solar collector. Volume concentrations of 1–4% were considered. Results indicated that the most suitable type of hybrid nanofluids was Ag-MgO/Syltherm 800. An experimental study was conducted by Henein and Abdel-Rehim [45] to investigate the hybrid nanofluid (MgO-MWCNT/water) on the thermal performance of an evacuated tube solar collector. Four different mixing ratios were considered: 80:20, 70:30, 60:40, and 50:50. The results of the study indicated that the (50:50) ratio of MgO/MWCNT hybrid nanofluid performed better than all other ratios of the hybrid nanofluid at all volume flow rates. Shoeibi et al. [46] numerically studied the impact of using Al_2O_3-TiO_2 hybrid nanofluids on glass cooling of a double-slope solar still. According to the results, the energy efficiency was increased by 28.32% compared with not using hybrid nanofluids. Recently, few articles have been reported in terms of employing hybrid nanofluids in FPSCs. For example, Verma et al. [47] experimentally tested the influence of using CuO-MWCNTs/water and MgO-MWCNTs/water hybrid nanofluids on the thermal performance evaluation of a FPSC. For MgO hybrid nanofluids, the highest augmentation in thermal efficiency of FPSC was 18.05% while for CuO hybrid nanofluids, 20.52%. Thermal efficiency enhancement of FPSC was experimentally assessed using graphene and crystal nano-cellulose (CNC) nanofluids and a combination of graphene-CNC hybrid nanofluids with base fluids of EG and water by Mahamude et al. [48]. The thermal conductivity was increased by 194% in comparison with single nanofluids at 80 ° C, and its viscosity rose to three times of base fluid indicating that hybrid nanofluids can be an excellent replacement to regular absorber working fluid. Moreover, at 0.5 vol%, the maximum thermal efficiency of using graphene-CNC hybrid nanofluid was 15.86%, while the thermal efficiency of using regular water was 4%. Tahat and Benim [49] experimentally evaluated the influence of using Al2O3-CuO (25:75)/water-EG hybrid nanofluids on the thermal efficiency of FPSC system. According to the authors' findings, thermal efficiency had increased to a maximum value of 52%.

In this review, articles related to hybrid nanofluids are comprehensively reviewed. The review focuses on preparation methods of hybrid nanofluids and characterization techniques. Methods of measuring stability and techniques used for enhancing stability are reviewed as well as the influence of hybrid nanoparticles on thermophysical properties, thermal conductivity, viscosity, specific heat, and density. Further, this review explores different experimental, numerical, and theoretical investigations of employing hybrid nanofluids in FPSC focusing on thermal efficiency improvement since it is considered the main parameter for utilizing hybrid nanofluids. Finally, challenges, conclusions, and future remarks are discussed for further investigation. It is also worth mentioning that more than 85% of the reviewed articles in this review were published in the last six years, as depicted in Fig. 2.

Preparation of hybrid nanofluids

Hybrid nanofluid can be produced by dispersing two or more types of different nanoparticles in base fluid with suitable blending in proper environmental conditions. Most common nanoparticles employed for the preparation of hybrid nanofluids are exhibited in Fig. 3. Agglomeration of particles is a crucial issue that may sink due to the action of gravity leading to decreasing the enhanced properties of nanofluids

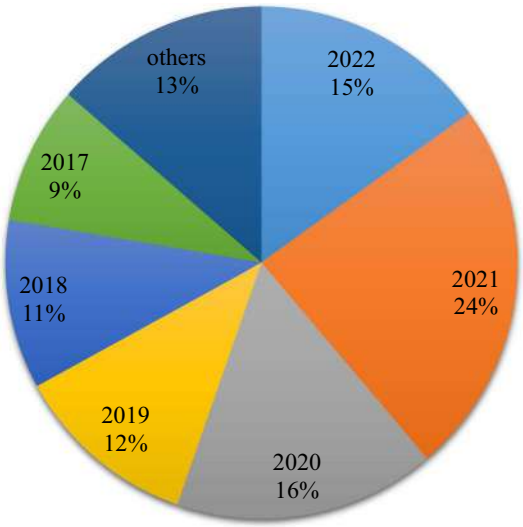

Fig. 2 Breakdown of reviewed articles based on the year of publication

and clogging pipes and valves. Thus, hybrid nanofluids must be prepared in a proper way to avoid these issues. The nanofluid preparation process may commonly be divided into two techniques, namely one-step and two-step techniques. In the single-step approach, the production and suspending of nanoparticles in the base fluid are carried out concurrently. It is considered the most effective strategy for enhancing stability and preventing the creation of oxides and clusters [50]. This approach omits time-consuming steps including storing, drying, and mixing particles in the base fluid. The illustration of the single-step approach is displayed in Fig. 4a. On the other hand, the two-step approach is the most often applied method for synthesizing hybrid nanofluids by researchers. Firstly, the nanoparticles were prepared in dry powder utilizing mechanical or chemical processes. After that, synthesized dry powder is suspended in base fluid: water, or EG with the help of ultrasonication, shown in Fig. 4b. While the two-step approach is advantageous for large-scale production, it has the disadvantage of clumping particles together due to high van der Waals forces prior to distribution in the base fluid, resulting in sedimentation of the particles in the liquid. As a consequence, the heat conductivity decreases. Several chemical and physical ways to resolve this problem have been suggested, including ultrasonic waves, the use of surfactants, and pH adjustments [51]. The following section is the classification of hybrid nanoparticles used to synthesize and prepare hybrid nanofluids.

Metal oxide + metal oxide

Khan et al. [52] used a two-step technique to synthesize and prepare Al_2O_3-SiO_2/water hybrid nanofluids. Al_2O_3 and SiO_2 nanoparticles at a concentration of 0.01% are dispersed in 1000 mL DI water (base fluid) with a mixing ratio of 50:50. The colloid is first stirred for 6 h at 50 ° C in a magnetic stirrer and then homogenized in a homogenizer to accomplish cell disruption, shown in Fig. 5. In another related experiment, Johari et al. [53] synthesized and prepared Al_2O_3-SiO_2 hybrid nanofluids. SiO_2 and Al_2O_3 were both prepared independently using a volume fraction of 0.5% distributed in a 60:40 combination of water/green bio-glycol as base fluids. Due to the fact that Al_2O_3 and SiO_2 nanoparticles exhibit distinct physical phases, their preparation

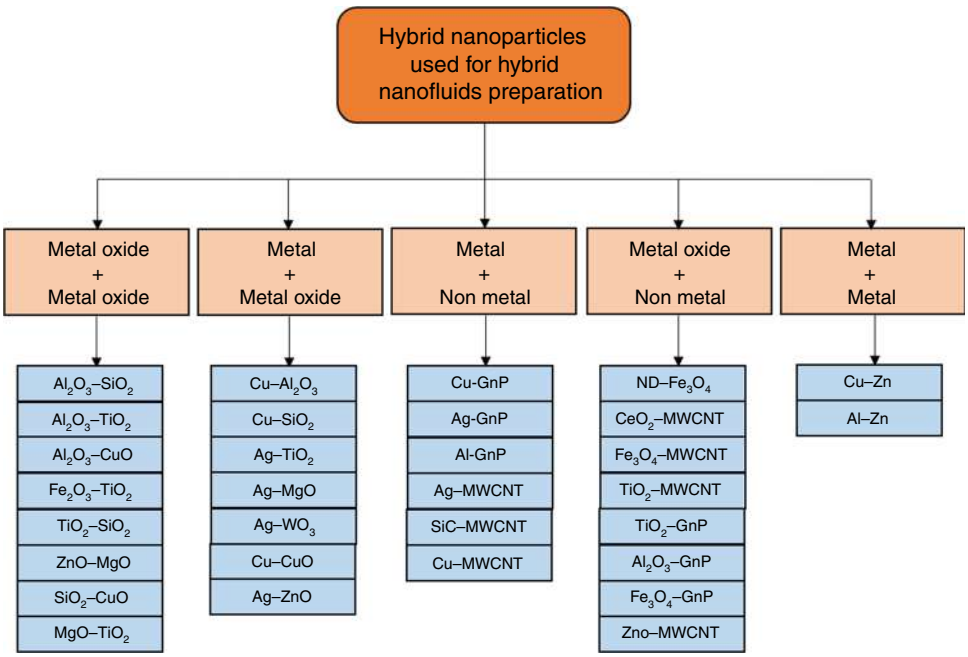

Fig. 3 Classification of nanoparticles used for hybrid nanofluids preparation

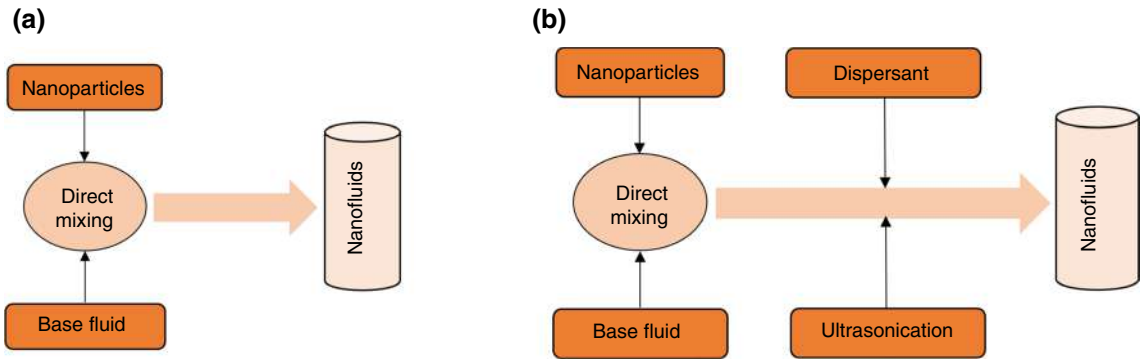

Fig. 4 Illustration of **a** one-step and **b** two-step preparation methods

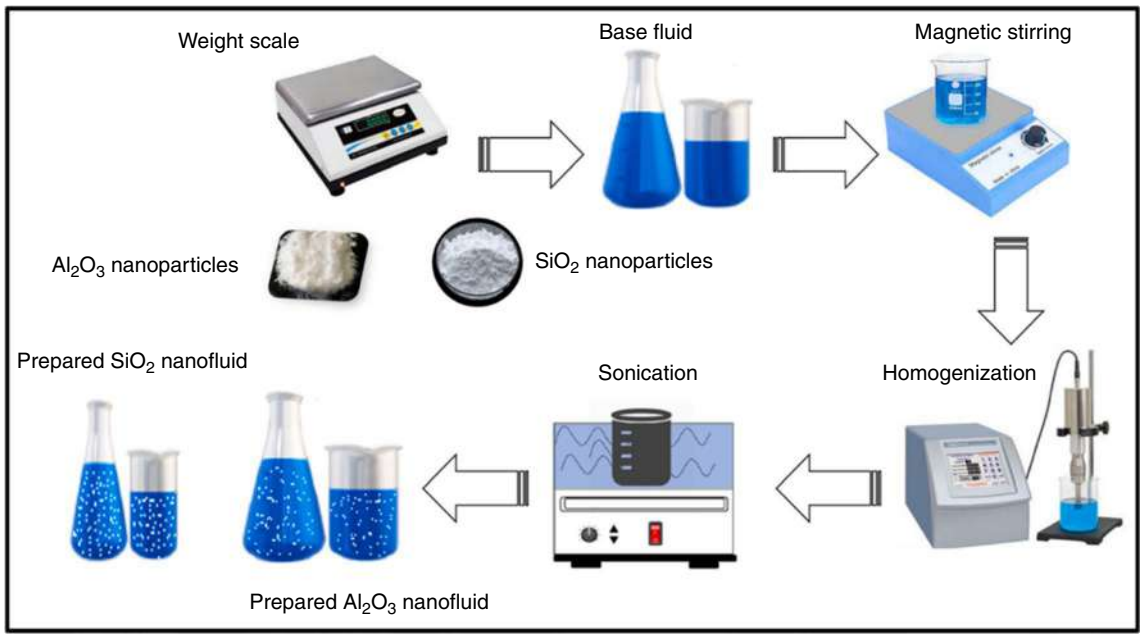

Fig. 5 Schematic illustration of Al_2O_3-SiO_2/water hybrid nanofluids [52]

methods were likewise distinct. Al_2O_3/SiO_2 nanofluids were created in four mixing ratios: 10:90, 30:70, 50:50, and 70:30. Then, they were sonicated for three hours. The preparation of water-based TiO_2-Al_2O_3 hybrid nanofluids was performed by Wanatasanapan et al. [54] using the two-step method. Various mixing ratios of TiO_2-Al_2O_3 nanoparticles were used in this study: 20:80, 40:60, 50:50, 60:40, and 80:20. The nanoparticles were suspended in water firstly using mechanical stirring for 2 h, followed by an ultrasonication technique keeping volume concentration of 1.0%. Ma et al. [55] investigated water-based Al_2O_3-CuO and Al_2O_3-TiO_2 hybrid nanofluids using a two-step technique. The optimal mixing ratio of nanoparticles was selected as 20:80 (Al_2O_3/TiO_2 and Al_2O_3/CuO). Another preparation of Al_2O_3-CuO/water hybrid nanofluids was performed by Zhang et al. [56]. Powders of Al_2O_3 and CuO were purchased and added to DI water followed by mechanical stirring (2000 rpm) for 1 h. Then, nanoparticles were equally suspended in water creating hybrid nanofluids with various mass concentrations. Malika et al. [57] synthesized and prepared Fe_2O_3-TiO_2/water hybrid nanofluids. Fe_2O_3-coated TiO_2 nanosheets were synthesized using hydrothermal reduction. Following this, water-based Fe_2O_3-TiO_2 hybrid nanofluids were prepared utilizing ultrasonication acoustic cavitation method.

The two-step technique was utilized to prepare TiO_2-SiO_2/green bio-glycol hybrid nanofluids which were presented by Zainon and Azmi [58]. Preparation of TiO_2 and SiO_2 nanofluids was firstly performed at several volume fractions of 0.5 – 3%, followed by mixing them with a ratio of 20:80 (TiO_2/SiO_2). Following this, the green bio-glycol base

fluid was added to the mixture preparing the hybrid nanofluid with the help of the dilution process. Synthesizing of MgO and ZnO and nanoparticles was carried out by Vidhya et al. [59] using the co-participation and sol–gel method. Equal amounts of the two nanoparticles were suspended in a mixture of water and EG (60:40) forming ZnO-Mgo hybrid nanofluids. In another investigation, Akilu et al. [60] employed the two-step approach to prepare SiO_2-CuO/C hybrid nanofluids. CuO/C powder was created using solvothermal methods [61], and SiO_2-CuO/C nanoparticles were made in 80:20 (mass concentration) via ultrasonic aided wet mixing method utilizing the technique exhibited in the work performed by Wei et al. [62]. Then, SiO_2-CuO/C hybrid nanofluids were prepared by suspending the solid nanoparticles in the base fluid: glycerol, and EG with a mixing ratio of 60:40 (% by mass).

Metal + metal oxide

Employing the two-step approach, water-based Al_2O_3-Cu hybrid nanofluid was prepared by Ma et al. [63] with volume concentrations of 0.3–1.5 vol%. Nanoparticles of Al_2O_3 of 20, 30, and 50 nm were used. Also, the volume mixing ratio of 80:20 (Al_2O_3/Cu) was kept constant during the experimentation. Similarly, Al_2O_3-Cu hybrid nanofluid with volume concentrations of 0.1–2% was prepared by Suresh et al. [64] via dispersing nanoparticles in pure water. SiO_2-Cu hybrid nanofluids with water and EG as base fluids are synthesized and prepared by Amiri et al. [65]. Firstly, the Stöber technique was applied to produce SiO_2 nanoparticles via hydrolysis and condensation of tetraethyl orthosilicate (TEOS). For about 2 h, the preparation reaction was carried out under stirring. Filtration, washing with ethanol and drying for two hours at temperatures less than 100 ° C were applied. Secondly, for forming SiO_2-Cu nanoparticles, 25 mmol prepared SiO_2 nanoparticles were introduced to 100 ml water in a stirred beaker, followed by adding 11.74 mmol ammonia and 11.16 mmol $CuCl_2$ for 6 h. Following ethanol purification and filtering, the products were dried for two hours at room temperature. Lastly, SiO_2-Cu nanoparticles were dispersed in deionized water and EG and stirred for about 3 h using a magnetic stirrer forming hybrid nanofluids. Using the same nanoparticles, Lahari et al. [66] prepared SiO_2-Cu (50:50)/glycerin-water (30:70) hybrid nanofluids using the two-step method. Cu and SiO_2 nanoparticles are directly suspended in base fluids, and then they were magnetically mixed for one hour and ultrasonicated for two hours producing more stable hybrid nanofluids.

Chawhan et al. [67] synthesized Ag-doped TiO_2 nanoparticles utilizing an ultrasonic-assisted technique. The nanoparticles were filtered and rinsed with ethanol and purified water before being dried at 80 ° C for two hours. Furthermore, the Ag-doped TiO_2 nanoparticles were suspended in water producing Ag-doped TiO_2 hybrid nanofluid. In another study, Esfe et al. [68] prepared Ag-MgO/water hybrid nanofluid. A mixture of 50:50 (Ag/MgO) was suspended in water, forming hybrid nanofluid with volume concentrations range of 0 – 2%. According to Aberoumand and Jafarimoghaddam [69], the electrical explosion of wire (EEW) approach known as a one-step method was utilized in preparing tungsten (III) oxide (WO_3)-silver/transformer oil hybrid nanofluid. One benefit of using EEW method is its capacity to produce nanoparticles from any substance capable of forming a thin wire.

Metal + non-metal

Using the two-step technique, Kishore et al. [70] prepared Cu-graphene/water hybrid nanofluid. Cu nanoparticles with a diameter of 30–50 nm and GnP nanoplatelets with a diameter of less than 2 μm are employed for the preparation procedure, and hybrid nanoparticles with two mixing ratios: 30:70 and 70:30 (Cu/GnP), were employed in this study. Dispersing hybrid nanofluids in water yielded producing Cu-graphene hybrid nanofluids with 0.01 and 0.02% volume fractions. According to Ma et al. [71], a mixed ratio of 1:1 of GnP/Ag nanoparticles was used for preparing GnP-Ag/water hybrid nanofluid with three mass concentrations: 0.001, 0.002, and 0.003%. A magnetic stirrer was utilized for the reason of evenly suspending the nanoparticles in the base fluid. Likewise, GnP-Ag/water hybrid nanofluid was prepared by Yarmand et al. [72] using the two-step technique. Graphene nanoplatelets were functionalized first since they are hydrophobic and not able to disperse directly into the water. Then, Ag was mixed with functionalized GnP with a mass ratio of 1:6. Specific amounts of water were added to the composition making hybrid nanofluids with several concentrations.

Li et al. [73] synthesized and prepared SiC-MWCNTs hybrid nanofluids for solar applications. Firstly, powders of SiC and MWCNTs were mixed with a ratio of 8:2 (SiC/MWCNTs). Then, hexane was added to the mixture followed by stirring for 20 min and then ultrasonication and drying process. The dry product was dispersed in ethylene glycol, base fluid, forming SiC-MWCNTs hybrid nanofluid with mass fractions range of 0.01–1%. Munkhbayar et al. [74] prepared Ag-MWCNTs hybrid nanofluid via the single-step technique utilizing the pulsed wire evaporation (PWE) approach. The apparatus utilizes four major elements: a high-voltage direct current power source, a high-voltage gap switch, a capacitor bank, and a condensation/evaporation chamber. MWCNT nanofluids were put into a 500-ml bottle, which was subsequently placed in the PWE instrument. Then, using the PWE approach, Ag nanoparticles were synthesized and directly contacted the base fluid within wall

of the chamber. Finally, Ag-MWCNT hybrid nanofluid was obtained with different concentrations.

Metal oxide + non-metal

Sundar et al. [75, 76] used chemical co-precipitation and in situ growth method to synthesize nanodiamond (ND)/Fe_3O_4 nanoparticles with a mixing ratio of ND/Fe_3O_4 of 72:28% (mass ratio) [75] and 28:72% (mass ratio) [76]. The synthesized nanoparticles were suspended in two base fluids, namely water and EG. Several mixture ratios were used in reference [75]: 20:80, 40:60, 60:40 (mass ratio) of EG/W, while in reference [76], just one mixing ratio was employed, 40:60 (mass ratio) of EG/W. Both studies utilized concentrations of 0.05, 0.1, and 0.2%. The same procedure was repeated by Said et al. [77] and Saleh and Sundar [78] to synthesize and prepare nanodiamond-Fe_3O_4 hybrid nanofluids with mixing ratios of base fluids of 40:60% and 60:40% (water/ethylene glycol).

Tiwari et al. [79, 80] applied the two-step approach for preparing CeO_2-MWCNT hybrid nanofluids. They mixed 80:20% (mass ratio) of CeO_2/MWCNT nanoparticles and dispersed them in several base fluids, namely water, Therminol VP-I, EG, and silicon oil. A range of concentrations of 0.25–1.5 vol% was employed. Some other recent studies utilized various nanoparticles with multi-walled carbon nanotubes (MWCNTs) to prepare hybrid nanofluids. In an investigation performed by Said et al. [81], water-based Fe_3O_4-MWCNT hybrid nanofluids were prepared using the in situ growth method with the approach of chemical reduction. Several particle concentrations were utilized: 0.05, 0.1, 0.2, and 0.3%. Moreover, Fe_3O_4-F-MWCNT nanoparticles were prepared and mixed with equal volume by Harandi et al. [82]. Then, the mixture was dispersed in ethylene glycol to form hybrid nanofluids with volume fractions of 0.1–2.3 vol%. In another Fe_3O_4-F-MWCNT hybrid nanofluids preparation investigation [83], the chemical reduction technique was used which entails treating MWCNT with strong acids and establishing a carboxyl (–COOH) connection between Fe_3O_4 and MWCNT. Fe_3O_4-MWCNT nanoparticles were mixed in water to achieve concentrations range of 0.05–0.3%.

Alawi et al. [84] employed the two-step method for preparing MWCNTs-TiO_2 hybrid nanofluid following sequencing steps. Functionalization of MWCNT was firstly performed, and then, MWCNT and TiO_2 nanofluids were prepared. After that, the prepared nanofluids with a mixing ratio of 40:60% (MWCNT/TiO_2) were dispersed in water forming hybrid nanofluids with mass fractions range of 0.025–0.1%. Another similar investigation was performed by Safi et al. [85] synthesizing and preparing MWCNTs-TiO_2 hybrid nanofluids. Functionalized MWCNTs and TiO_2 nanoparticles were prepared utilizing solvothermal technique. A wide range of MWCNTs-TiO_2 concentrations of 0.02–0.08 mass% was employed and mixed in water as base fluid. Graphene nanoplatelets had been used with TiO_2 [86], Al_2O_3 [87], and Fe_3O_4 [88] nanoparticles producing hybrid nanofluids. The two-step technique had been applied for the hybrid nanofluids preparation with a concentrations range of 0 – 1%.

Metal + metal

Mechiri et al. [89] investigated the synthesis and preparation of Cu–Zn hybrid nanofluid. Cu and Zn nanoparticles were prepared using mechanical milling. Nanoparticles were mixed with ratios of 50:50, 75:25, and 25:75 (Cu/Zn). Following this, compositions were suspended in vegetable oil for volume concentrations of 0.1 – 0.3% and then ultrasonicated for 3 h each. Other similar studies were carried out by Kumar et al. and Mechiri et al. [90, 91]. In situ Cu–Zn hybrid nanoparticles were synthesized. Equal amounts of Cu and Zn nanoparticles were suspended in vegetable oil producing hybrid nanofluids. Pual et al. [92] prepared Al/Zn nanoparticles via mechanical alloying, and nanoparticles were suspended in ethylene glycol base fluid utilizing ultra sonicator producing Al-Zn hybrid nanofluid. Table 1 summarizes preparation methods of hybrid nanofluids for various publications.

Characterization of hybrid nanofluids

Techniques of characterization are necessary to successfully characterize the hybrid nanofluids that have been produced. Researchers have used various methods, namely X-ray diffraction (XRD), transmission electronic microscope (TEM), scanning electronic microscope (SEM), Fourier transmission infrared (FTIR), energy-dispersive X-ray spectroscopy (EDX), dynamic light scattering (DLS), energy-dispersive X-ray spectroscopy (EDS), high-resolution transmission electron microscopy (HRTEM), Raman, field emission scanning electron microscopy (FE-SEM). XRD is used for estimating the characteristic peaks of the materials, and TEM and SEM are utilized for studying the microstructure and morphology of hybrid nanoparticles [95]. FTIR is employed to investigate the surface chemistry of solid particles as well as liquid particles, while DLS is utilized for estimating the average nanoparticle size in base liquid. Also, Raman is used to investigate the G-band and D-band of the carbon-related hybrid nanoparticles [96]. Figure 6 shows the TEM, FTIR, and XRD results of Ag-TiO_2 hybrid nanoparticles [67]. Characterization techniques employed by scholars in this literature are provided in Table 2.

Table 1 A summary of preparation methods of hybrid nanofluids for various publications

Category	Nanoparticles	Base fluid	Method of preparation	References
Metal oxide + metal oxide	Al_2O_3-SiO_2	Water, water/bio-glycol	Two-step	[52, 53]
	TiO_2-Al_2O_3	Water	Two-step	[54, 55]
	Al_2O_3-CuO	Water	Two-step	[55, 56]
	Fe_2O_3-TiO_2	Water	Two-step	[57, 93]
	TiO_2-SiO_2	Water/bio-glycol	Two-step	[58]
	ZnO-Mgo	Water/bio-glycol	Two-step	[59]
	SiO_2-CuO/C	Glycerol/ethylene glycol	Two-step	[60]
	MgO-TiO_2	Water	Two-step	[94]
Metal + metal Oxide	Al_2O_3-Cu	Water	Two-step	[63, 64]
	SiO_2-Cu	Water and ethylene glycol	Two-step	[65]
	SiO_2-Cu	glycerin	Two-step	[66]
	Ag-doped TiO_2	Water	Two-step	[67]
	Ag-MgO	Water	Two-step	[68]
	Ag-WO_3	Transformer oil	One-step	[69]
Metal + non-metal	Cu-GnP	Water	Two-step	[70]
	Ag-GnP	Water	Two-step	[71, 72]
	SiC-MWCNTs	EG	Two-step	[73]
	Ag-MWCNTs	Water	One-step	[74]
Metal oxide + non-metal	ND-Fe_3O_4	Water/bio-glycol	Two-step	[75–78]
	CeO_2-MWCNT	water, Therminol VP-I, EG, silicon Oil	Two-step	[79, 80]
	Fe_3O_4-MWCNT	Water, ethylene glycol	Two-step	[81–83]
	TiO_2-MWCNTs	Water	Two-step	[84, 85]
	TiO_2-GnP	Water	Two-step	[86]
	Al_2O_3-GnP	Therminol	Two-step	[87]
	Fe_3O_4-GnP	Kerosene	Two-step	[88]
metal + metal	Cu – Zn	Vegetable Oil	Two-step	[89–91]
	Al – Zn	water	Two-step	[92]

Stability of hybrid nanofluids

Because nanoparticles are often hydrophobic, they are not able to be dispersed in the majority of heat transfer fluids without the addition of surface treatments, surfactants, or dispersants [97]. Additionally, without these particular procedures, the nanoparticles would agglomerate, resulting in additional issues such as sedimentation, clogging, and a decrease in the mixture's thermal conductivity. Thus, it is critical to study the parameters affecting the hybrid nanofluids dispersion stability and methods of stability enhancement. The following section discusses several ways for evaluating and improving the stability of hybrid nanofluids, shown in Fig. 7. This approach has the disadvantage of being time-consuming.

Stability evaluation methods

Nanofluids evaluation stability can be assessed using popular methods including sedimentation method, zeta potential, and spectral absorbance analysis as discussed below in detail.

Sedimentation method

Sedimentation method is a very easy technique for determining the stability of a nanofluid. After preparing the hybrid nanofluid, it is maintained static inside a glass tube, and the particles settling are monitored continually via the use of photographs. The time required to capture photos is related to the quality of the hybrid nanofluids during preparation. Various researchers have utilized the sedimentation approach to study the stability of hybrid nanofluids [63, 73, 98–106]. For instance, the sedimentation observation after 72 h of preparing Al_2O_3-ZrO/Jatropha oil-based hybrid nanofluids is shown in Fig. 8 [107].

Zeta potential test

The zeta potential test is considered the most popular method for determining the stability of the hybrid nanofluids. Dispersed particles are surrounded by a liquid layer of fluid which consists of two parts: the stern layer, which

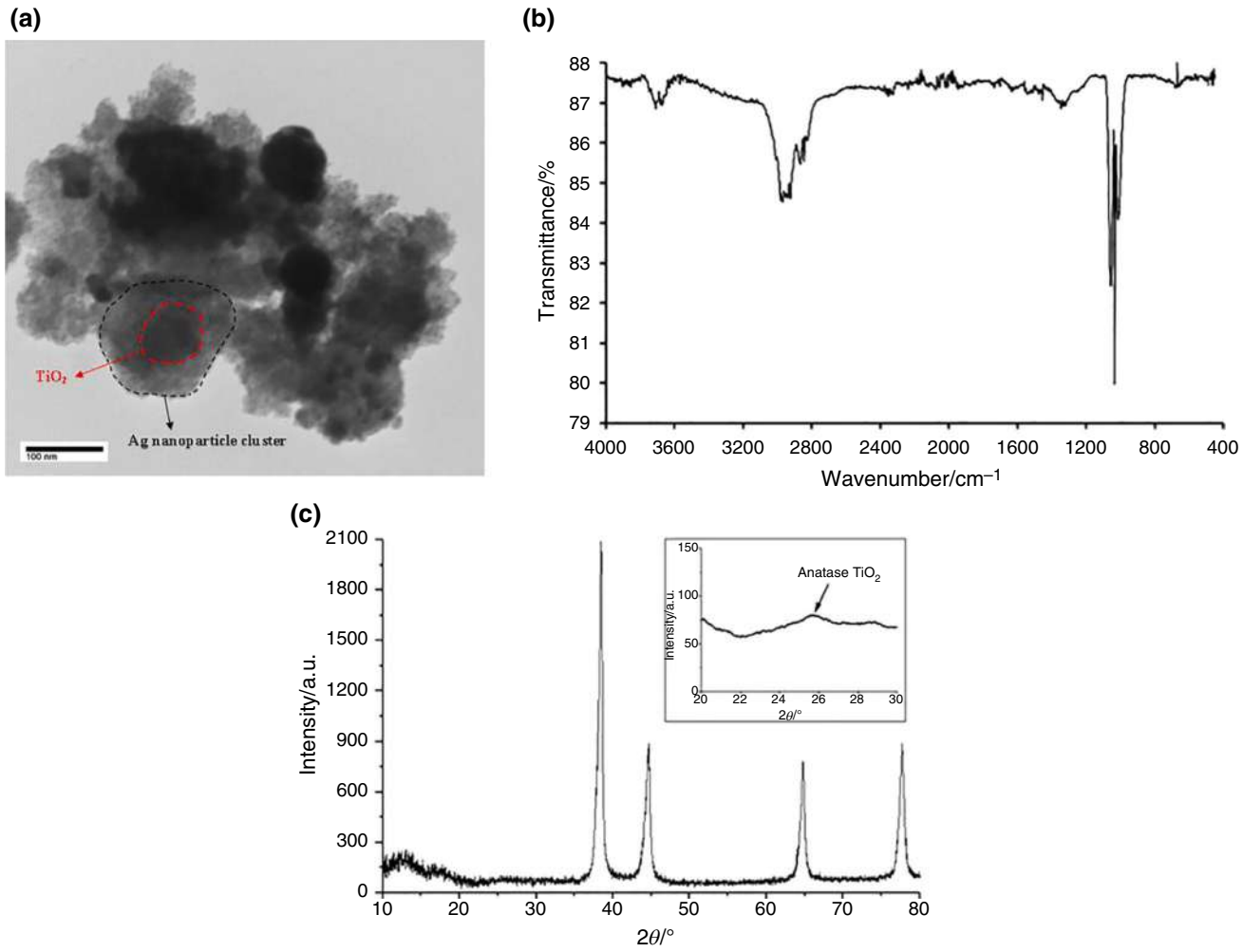

Fig. 6 **a** TEM, **b** FTIR spectra, **c** X-ray diffraction pattern of Ag-doped TiO_2 hybrid nanoparticles [67]

Table 2 Characterization methods employed by researchers in this literature

Characterization technique	References
X-ray diffraction (XRD)	[54, 59, 60, 63, 64, 67, 68, 71, 75, 85, 88, 94, 98, 102, 104, 122, 123, 135, 163, 169, 170, 174]
Scanning electronic microscope (SEM)	[56, 64, 65, 70, 71, 75, 81, 85, 90, 93, 94, 98, 107, 122, 123, 125, 170]
Field emission scanning electron microscopy (FESEM)	[57, 60, 65, 84, 90, 98, 100, 102, 123, 143, 172, 174]
Transmission electronic microscope (TEM)	[54, 55, 63, 67, 88, 98, 100, 104, 113, 117, 127, 135, 161, 163, 168]
High-resolution transmission electron microscopy (HRTEM)	[54, 75, 84, 104]
Fourier transmission infrared (FTIR)	[38, 57, 59, 67, 71, 75, 85, 88, 98, 99, 104, 124, 135, 163, 170, 174]
Energy-dispersive X-ray Spectroscopy (EDS)	[59, 107, 123]
Energy-dispersive X-ray spectroscopy (EDX)	[60, 65, 70, 84, 100, 123, 124]
Dynamic light scattering (DLS)	[57, 88, 90, 99, 170, 175]
Raman	[71, 82, 83, 104]

contains firmly bound ions, and the diffuse layer, which contains weakly bound ions. A stable entity is formed by ions and particles inside an imaginary boundary in the diffuse layer. Due to gravitation, any particles that migrate beyond this boundary will remain within this bulk phase and the potential on the boundary is named as zeta potential. Zeta

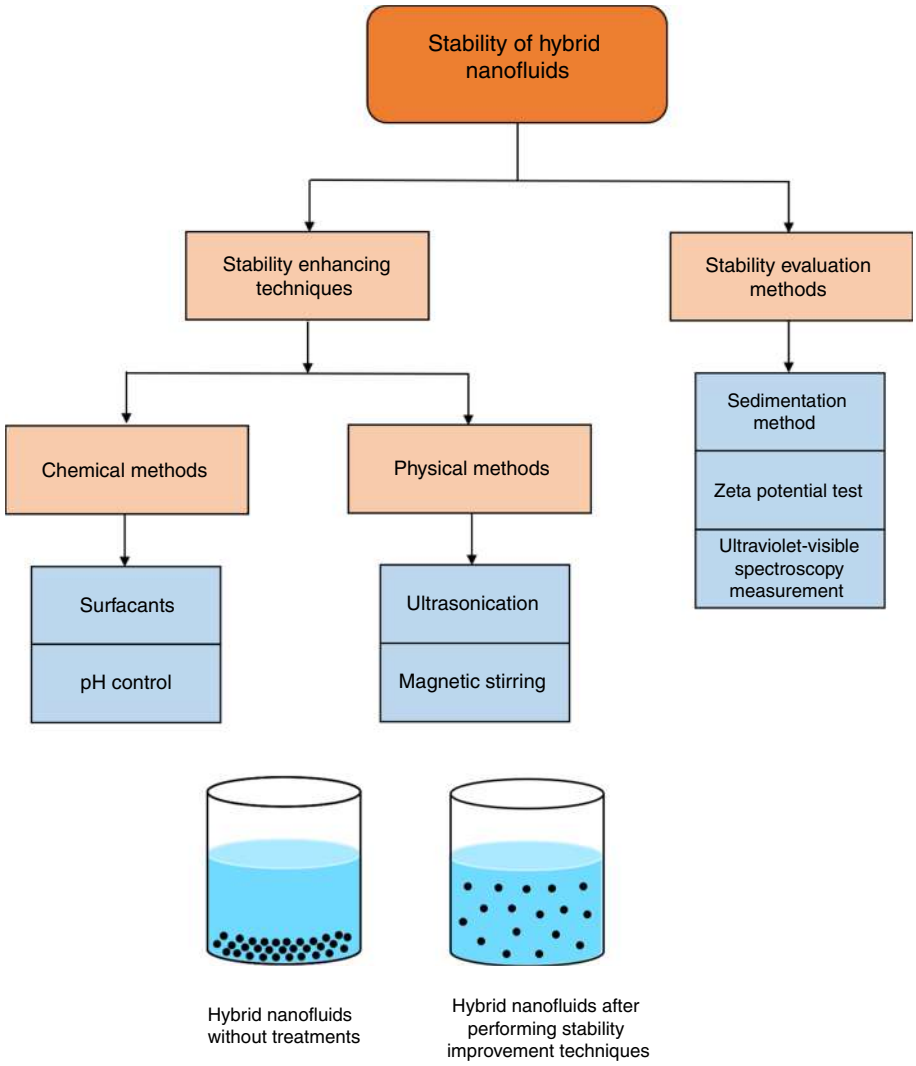

Fig. 7 Hybrid nanofluids evaluation and enhancement techniques

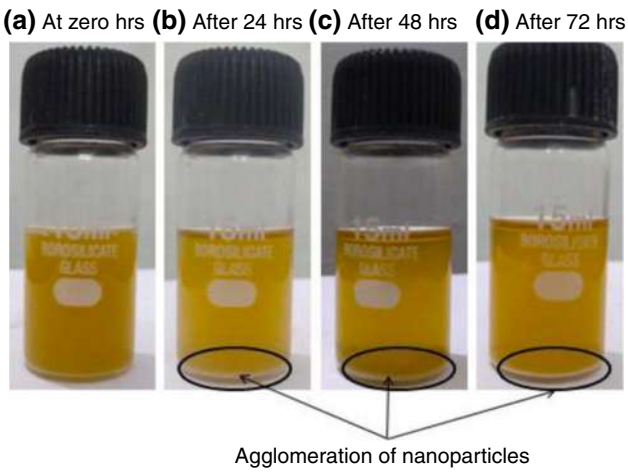

Fig. 8 Sedimentation analysis of Al_2O_3-ZrO/Jatropha oil-based hybrid nanofluid [107]

potential value increases as the forces of electrostatic repulsive between nanoparticles rise. An increase in the zeta potential reveals that nanofluids are more stable [22, 53, 108]. Several studies [50, 59, 104] indicated that nanofluids with zeta potential values higher than ± 30 mV are regarded as good stable nanofluids while nanofluids with zeta potential values above ± 60 mV have outstanding stability.

Bakhtiari et al. [86] utilized the zeta potential test for evaluating the stability of TiO_2-Graphene/water hybrid nanofluids. The measured zeta potential was − 47.6 mV revealing good stable hybrid nanofluids. Mane et al. [109] inspected the effect of several dispersants: chitosan, sodium dodecyl benzoic sulfate (SDBS), and gum Arabica (GA) on the zeta potential of CuO-Fe_3O_4/water hybrid nanofluids. It was concluded that using chitosan increased the zeta potential revealing better stability in comparison with others. The stability of SiC-MWCNTs hybrid nanofluids was performed by Li et al. [73] for different mass concentrations. Results exhibited that the zeta potential value reduced with

increasing mass concentration and standing time, shown in Fig. 9, the same trend was reported by Li et al. [103]. Despite this, after 30 days of storage, the value of zeta potential was 45 mV which indicates a good stable nanofluid. CeO_2-MWCNT/water hybrid nanofluids prepared by Tiwari [80] showed good stability after 90 days of preparation with the highest zeta potential value of 50 mV. According to Johari [53], moderate stability of Al_2O_3-SiO_2 hybrid nanofluids with a value of zeta potential of 23 mV was observed. In addition, moderate stability of Al_2O_3-CuO hybrid nanofluid with a potential value of − 26.49 mV was observed by Wanatasanappan et al. [105]. A recent investigation by Jin et al. [104] on the Cu-CNT and Ag-CNT hybrid nanofluids stability showed relative potential values which were relatively low: -37.6 mV and − 33.7 mV, respectively, and it may be accounted for the metal nanoparticles presence. Vidhya et al. [59] employed the zeta potential technique to test the stability of the ZnO-MgO hybrid nanofluid. They concluded that the potential values for all examined volume concentrations: 0.0125–0.1%, were between 45 and 60 mV indicating that the nanofluids were in good stability. Mousavi et al. [94] tested the stability of MgO-TiO_2/water hybrid nanofluids with several concentrations and mixing ratios. They found that the hybrid nanofluids were stable with a minimum potential of 30 mV and a maximum value of 38.93 mV.

Ultraviolet–visible spectroscopy measurement

Another effective method for determining the stability of hybrid nanofluids is ultraviolet–visible spectroscopy measurement. This technique is most commonly utilized when the nanoparticle dispersed in the base fluid exhibits an absorption peak that is between 190 and 1100 nm in wavelength [110, 111]. The particles dispersed in the base fluid have a proclivity for absorbing visible and ultraviolet light. Stability is determined via monitoring the absorption peak characteristics and how they change over time with a UV–VIS spectrophotometer. The decrease in absorbance with time suggests that the nanofluid suspension is unstable [112]. In the UV–VIS spectrophotometer, the absorbance peak of the provided nanofluid must be firstly determined. As the concentration of suspension increases, absorbance rises as well demonstrating a linear connection between absorbency and concentration. Once a desired concentration of suspension is prepared to investigate relative stability, the sedimentation process begins. Following that, the stability of nanofluids will be assessed via monitoring supernatant concentration by employing a UV–VIS spectrophotometer at several intervals [22]. The drawback of this method is that it is ineffective for nanofluids with a high concentration or those that are dark in color, since high concentration nanofluids induce high incoming light absorption and lower scattered light intensity, lowering data quality.

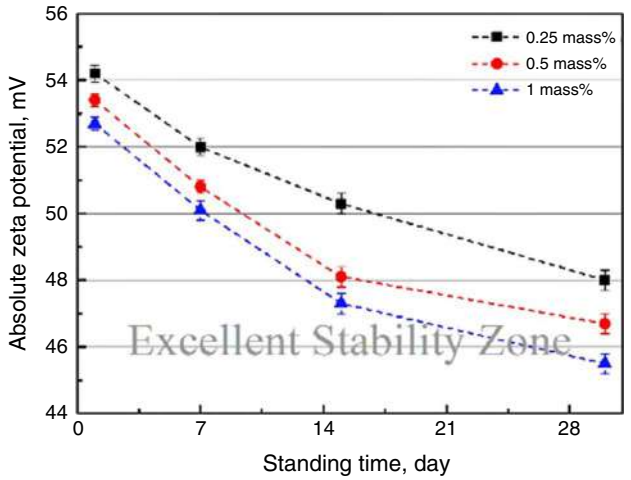

Fig. 9 Zeta potential of SiC-MWCNTs nanofluids as a function of standing time [73]

Sandhya et al. [98] evaluated GNPs-CNC hybrid nanofluid stability utilizing UV–Vis spectroscopic technique for different volume concentrations. The UV–VIS spectrums revealed that the hybrid nanofluid at 0.2% volume concentration had the highest absorption peak (with 200–400 nm wavelength range) which yields greater hybrid nanofluid stability. Shajan et al. [87] studied the stability of GNP-Al_2O_3 hybrid nanofluid. Results indicated that, at high wavelengths, UV absorbance value decreased with increasing sedimentation period. After 14 days of storage, the absorbance value of 0.658 was found which promised a good stable suspension. The stability of Al_2O_3-CuO and Al_2O_3-TiO_2 hybrid nanofluids was assessed by Ma et al. [55] as a function of wavelength using UV–Vis investigation. Results yielded that Al_2O_3-TiO_2 hybrid nanofluid is more stable than Al_2O_3-CuO at all ranges of wavelengths.

Stability determination of TiO_2-SiO_2 hybrid nanofluid by measuring the absorbance ratio throughout sedimentation time was performed by Hamid et al. [101, 113] and Nabil et al. [114] using the UV–Vis spectrophotometer. It was indicated that rising sonication time up to 120 min over 336 h of sedimentation time yielded an absorbance ratio of 70% [101, 113] which means stable suspension. The optimal value reference of the absorbance ratio is 100%. However, Nabil et al. [114] found that a sonication time of 90 min with the same sedimentation period yielded the highest absorbance ratio of around 80%. In another related study, Zainon and Azmi [58] applied the same technique with the same nanoparticles to evaluate the suspension stability. They achieved an absorbance ratio of about 90%, which means excellent stability, with a sonication time of 3 h and sedimentation period of 336 h, as explained in Fig. 10.

Stability enhancing techniques

Chemical methods

Surfactants

This is one of the most applied strategies for preventing nanoparticle sedimentation. The use of surfactants, also known as dispersants, may help nanoparticles stay stable in aqueous solutions [115]. The reason behind this is that with the help of surfactants, nanoparticle surfaces are changed from hydrophobic to hydrophilic and vice versa depending on the requirement. Surfactants can be classified into four groups depending on the composition of the head: anionic surfactants which are negatively charged heads, non-ionic surfactants which do not have charges in their heads, amphoteric surfactants which have zwitterionic head groups, and cationic which have positively charged heads [116]. The type of dispersant to be used is determined by the particle characteristics as well as the desired fluid. Tiwari et al. [80] tested the stability of CeO_2-MWCNT hybrid nanofluid employing six different surfactants, namely sodium dodecyl benzene sulfonate (SDBS), polyvinyl pyrrolidone (PVP), sodium dodecyl sulfate (SDS), gum Arabic (GA), cetyltrimethylammonium bromide (CTAB), and distearyl dimethylammonium chloride (DDC). Authors stated that better stability was achieved when increasing the amounts of surfactants to a certain point. However, any additional increase in the amount of surfactant used in the mixture will diminish the stability of the suspension. In addition, CTAB surfactant, which is cationic, exhibited the best stability up to 30 days after preparation. Days 30–90, the SDBS surfactant was crucial in the hybrid nanofluid stability. The same research group, Tiwari et al. [79], had proven that the organic salt type Benzalkonium chloride (BAC) surfactant produced the best results among other surfactants in terms of stability of CeO_2-MWCNT hybrid nanofluid up to the 30th day, and hence, the use of BAC surfactant is suggested when preparing long-term stable nanofluids. Ma et al. [55] studied the influence of SDS, PVP, and CTAB dispersants on the stability of Al_2O_3-CuO and Al_2O_3-TiO_2 hybrid nanofluids. According to the findings, PVP had been discovered to be the most effective surfactant for maintaining the stability of hybrid nanofluids after 25 days, as illustrated in Fig. 11.

Many researchers had utilized popular dispersants to stabilize nanofluids including CTAB [55, 59, 67, 68, 70, 80, 99], SDBS [56, 80, 93, 117], SDS [55, 80, 94, 99, 118, 119], PVP [55, 80, 117, 120], GA [99, 120], BAC [79], potassium lauryl sulfate (PLS) [79], sodium deoxycholate (SDC) [117].

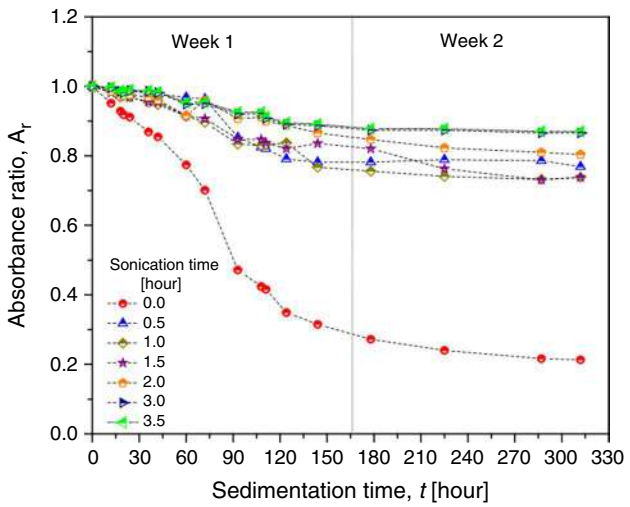

Fig. 10 Variation of absorbance ratio for different sonication times [58]

pH control

The stability of nanoparticles is directly related to their electrokinetic characteristics. As a result, adjusting the pH of nanoparticles can assist in improving their stability. It has been shown that nanoparticles are more stable at pH levels that are distant from the isoelectric point (IEP), which is known as the point at which the particles' surface charge and the zeta potential values are both zero [121]. Wanatasanapan et al. [54] concluded that TiO_2-Al_2O_3 hybrid nanofluids within all mixing ratios: 20:80, 40:60, 50:50, 60:40, and 80:20 showed high stability since they exhibited pH values slightly lower than the pH of the base fluid. In Suresh et al. [64] study, the pH values of the synthesized water-based Al_2O_3-Cu hybrid nanofluids were determined to be approximately 6. A stable dispersion is thought to be accomplished because the pH range (6) is near to that of normal water. Also, it was discovered that when the concentration of the hybrid nanofluid grows, the pH rises. This suggests that the hybrid nanofluids stability is reliant on the nanoparticles' volume fraction. In another related investigation performed by Suresh et al. [122], the stability of water-based Al_2O_3-Cu hybrid nanofluid was assessed via measuring pH values. It was revealed that pH values were about 5.5 which is distant from the isoelectric point (IEP) meaning high stability. A stable TiO_2-CuO/C hybrid nanofluid was achieved by Akilu et al. [123] with a pH value of 10, accounting for the strong electrostatic repulsion between the nanoparticles. Qing et al. [124] inspected the SiO_2-graphene/naphthenic oil hybrid nanofluid stability under 4 different pH values, 9 – 12. Authors stated that a pH value of 11 showed the maximum stability, while a pH value of 12 revealed the lowest stability. According to Tiwari et al. [80], optimized pH values, 9 and 9.5, were obtained with the utilization of SDBS and CTAB dispersants. Zhang et al. used NaOH to regulate the pH value

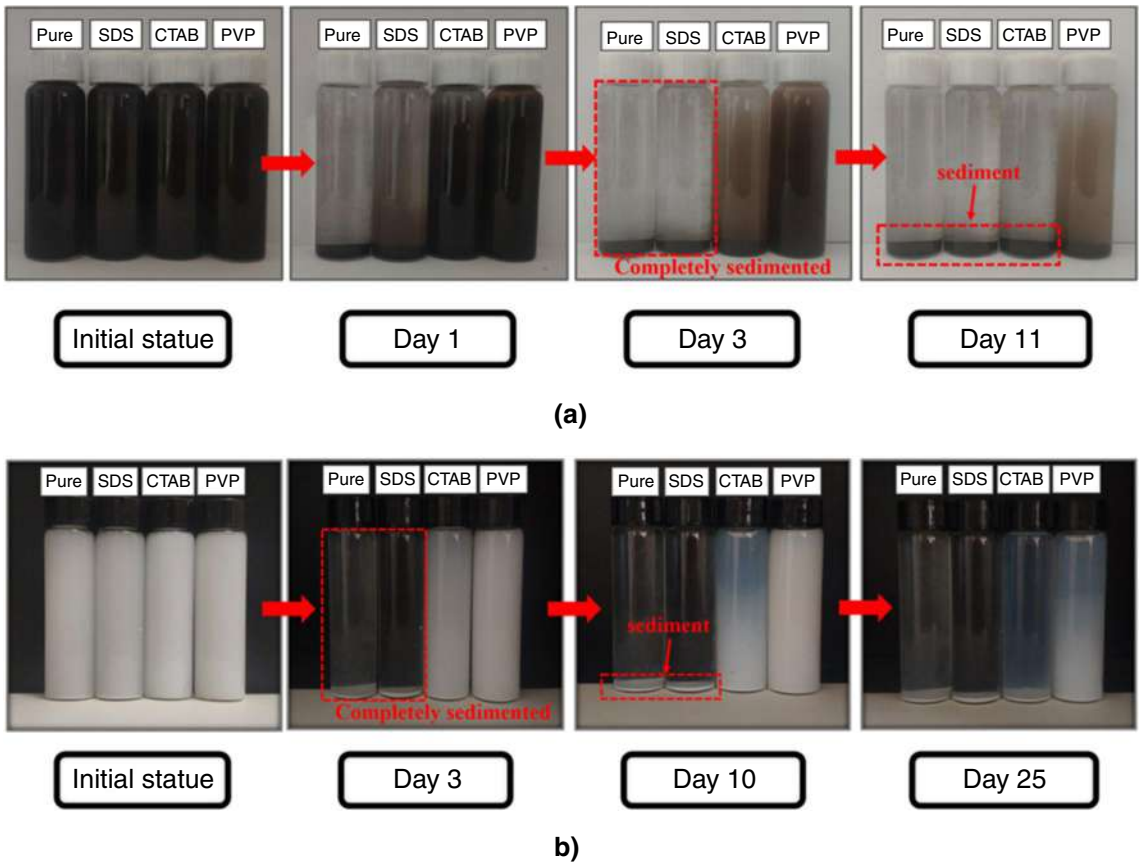

Fig. 11 Stability of **a** Al_2O_3-CuO and **b** Al_2O_3-TiO_2 hybrid nanofluids for various surfactants [55]

of Al_2O_3-CuO/water to 9.5 resulting in good stability [56]. In another study, Yıldırım et al. [125] described that the highest pH value of 7.9 of Al_2O_3-MoS_2 hybrid nanofluid was obtained at a mixing ratio of 2:1, shown in Fig. 12, achieving higher stability among other tested concentrations.

Physical methods

Ultrasonication

Ultrasonication is a common approach used by scholars to stabilize nanofluids. Ultrasonic devices can distribute nanoparticles uniformly in the base fluid and break up clusters via applying high-frequency vibrations, with no change in nanoparticle surface characteristics [32, 126]. Mousavi et al. [94] indicated that ultrasonication time is considered one of the most important factors affecting hybrid nanofluids stability. Increasing sonication time to a certain point yielded to more stable MgO-TiO_2 hybrid nanofluid and then experienced slightly lower stability, as Tiwari et al. [79, 80] concluded. At a mass mixing ratio of 50:50 (MgO/TiO_2), the optimal sonication time was 70 min for all volume concentrations

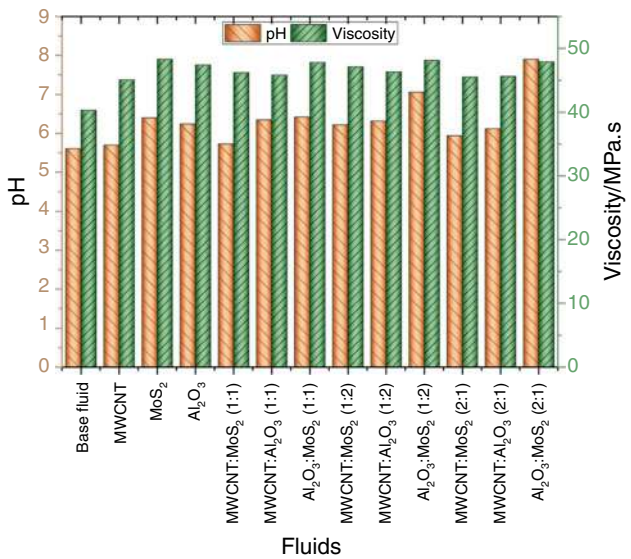

Fig. 12 pH values of tested nanofluids [125]

examined while at mixing ratios of 80:20 and 20:80 (MgO/TiO_2), the best sonication time appeared to be 60 min. Asadi and Asadi [127] used an ultrasonic processor to obtain super dispersion of MWCNT-ZnO hybrid nanofluid, and the suspension was stable for one week. A probe sonicator was utilized by Xian et al. [117] to stabilize TiO_2-graphene/water-EG hybrid nanofluid. It was concluded that a longer sonication time for tested samples reveals better stability. During the preparation process of TiO_2-SiO_2/water-EG hybrid nanofluid which is performed by Hamid et al. [113], ultrasonic bath was used to stabilize the solution with several sonication times. 120 min of sonication time was employed in this study since it yielded to high stability to the solution. Amiri et al. [65] employed a 250-W sonicator for two hours to stabilize SiO_2-Cu hybrid nanofluid. The solution gave stable for two weeks at least.

Magnetic stirring

Magnetic stirring is considered the most common technique utilized for dispersing nanoparticle clusters. This approach is essential for mixing nanoparticles in base fluids during hybrid nanofluids production. Magnetic bead spins because of an external outside magnetic field and stirring of the particle fluid mixture. It is necessary to control the stirring speed to create high-quality hybrid nanofluids, as too fast stirring might lead to promoting bubble production, and these bubbles may attach to the side of the beaker during shifting, affecting the mass fraction during research [128]. Various investigations dealing with using magnetic stirring can be found in [60, 65, 85, 103, 117, 126, 127, 129, 130]. Table 3 summarizes measurement and stabilization techniques employed by researchers.

Thermophysical properties of hybrid nanofluids

Employing nanoparticles significantly alters the thermophysical properties of hybrid nanofluids, namely thermal conductivity, viscosity, density, and specific heat of any type of hybrid nanofluid. A variety of factors influencing this modification: material type, size, and shape of the nanoparticles used, temperature, and the volume concentration of dispersed nanoparticles are discussed in the following sub-sections.

Thermal conductivity

Thermal conductivity is a critical thermophysical parameter that dictates the heat transfer characteristics of hybrid nanofluids. Improvement of thermal conductivity is linked to convection currents between nanoadditives and base fluids. High thermal conductivity yields to increase in the thermal performance of the thermal system. The thermal conductivity of hybrid nanofluids is highly affected via the kind and concentration of nanoparticles, the type of base fluid, and the operating temperatures [131, 132]. Researchers have utilized several apparatuses to measure the thermal conductivity, such as KD2 pro thermal properties analyzer, and scholars also proposed correlations based on experimental data for estimating the thermal conductivity, as displayed in Table 4.

Experimental investigations

Various studies have analyzed and assessed the performance of convective heat transfer of hybrid nanofluids to increase the thermal conductivity of these nanofluids and improve the heat transfer rate. Kumar and Sahoo [133] investigated the thermal conductivity of Al_2O_3-CuO (50:50) hybrid nanofluids with several mass concentrations of propylene glycol (PG) and EG binary base fluids, the volume fraction of 1.5%, and temperatures ranging from 50 to 70 °C. The influence of various nanoparticle shapes on thermal conductivity, such as cylindrical, spherical, platelets, brick, and blades had been studied in this investigation. It was found that Al_2O_3-CuO hybrid nanofluid had a greater thermal conductivity in PG binary base fluid than in EG base fluid. In addition, for both base fluids, increasing temperature and volume concentration yielded a remarkable augmentation in thermal conductivity. Spherical nanoparticles exhibited the highest results in terms of thermal conductivity compared with other shapes. An experimental investigation was carried out by Ma et al. [134] for investigating the influence of various mixing ratios of nanoparticles and base fluids on the thermal conductivity of Al_2O_3-TiO_2/EG-W, Al_2O_3-CuO/EG-W, and Al_2O_3-Cu/EG-W hybrid nanofluids. The study was performed with a temperature range of 20–60 ° C and a volume concentration of 1%, and a thermal constant analyzer (Hotdisk TPS2500) was utilized for performing the measurements. Results revealed that a mixing ratio of nanoparticles of 20:80 yielded the highest thermal conductivity among other ratios. According to a sensitivity analysis, it was shown that the influence of nanoparticle mixing ratios on thermal conductivity was more notable as compared to the base fluid mixing ratios. Also, the thermal conductivity of tested hybrid nanofluids was enhanced via increasing both temperatures and nanoparticle concentrations, and the Al_2O_3-TiO_2 hybrid nanofluid outperformed other nanofluids. The influence of temperatures and nanoparticles fractions of GO-$C_{O3}O_4$/water hybrid nanofluid on thermal conductivity was examined by Said et al. [135]. A range of temperature of 20 – 60 ° C and a range of volume concentration of 0 – 0.2% had been employed in this study. KD2 pro (Decagon Devices Inc., USA) was employed to measure thermal conductivity, and the average of 15 readings at 5-min intervals was

Table 3 Summary of measurement and stabilization methods used by researchers

Hybrid nanofluids	Stabilization method	Measurement method	Stability period	References
CeO_2-MWCNT/water, silicone oil, EG, and Therminol VP-I	Surfactants (BAC, CTAB, ALS, PLS) 30–240-min Ultrasonication pH value	Zeta potential test	90 days	[79]
CeO_2-MWCNT/water	SDBS, SDS, CTAB, DDC, GA, PVP) 30–180-min Ultrasonication 8–11 pH value 4-h magnetic stirring	Zeta potential test	90 days	[80]
Al_2O_3-CuO/water Al_2O_3-TiO_2/water	Surfactants (SDS, PVP and CTAB) 60-min Ultrasonication 20-min magnetic stirring	Sedimentation Spectral absorbance analysis test	25 days	[55]
Al_2O_3-CuO/water	SDBS 1-min Ultrasonic vibration 8.5 pH value 1-h mechanical stirring	Sedimentation Zeta potential test	14 days	[56]
ZnO-Mgo/water-EG	CTAB 90-min Ultrasonication 4-h magnetic stirring 9 pH value	Sedimentation Zeta potential test	30 days	[59]
Ag-dopedTiO_2/water	CTAB 2-min Ultrasonication	Sedimentation	30 days	[67]
Ag-MgO/water	CTAB 3-h Ultrasonication 5.4 pH value	–	Several hours	[68]
Cu-GnP/water	CTAB Ultrasonication	Sedimentation	30 days	[70]
Fe_2O_3-TiO_2/water	SDBS 9-h ultrasonication bath 45-min magnetic stirring 5-min homogenization	Sedimentation test	20 h	[93]
TiO_2-GnP/water-EG	CTAB, SDC, SDS and SDBS 90-min Probe ultrasonication 30-min magnetic stirring	Sedimentation test Zeta potential test Spectral absorbance analysis test	40 days	[117]
Ag-GnP/water	GA 180-h ultrasonication 180-min magnetic stirring	Sedimentation test	30 days	[71]
MgO-TiO_2/water	SDS 80–100-min Probe ultrasonication 1-h magnetic stirring	Zeta potential test	More than 3 days	[94]
TiO_2-Al_2O_3/water	PVP 2-h ultrasonication 6.7–6.8 pH value 2-h mechanical stirring	Sedimentation test Zeta potential test	30 days	[54]
Al_2O_3-Cu/water	SLS 6-h ultrasonication 6 pH value	Zeta potential test	Stable	[64]
Al_2O_3-Cu/water	SLS 6-h ultrasonication 5.5 pH value	–	Stable	[122]
TiO_2-CuO/C /EG	2-h ultrasonication 6–7 pH value	Zeta potential test	Stable	[123]
SiO_2-GnP/naphthenic oil	4-h ultrasonication 9–12 pH value 24-h stirring	Zeta potential test Spectral absorbance analysis test	14 days	[124]
Al_2O_3-MoS_2	60-min ultrasonication 5.6–7.9 pH value 60-min magnetic stirring 1-h mechanical stirring	–	Stable	[125]

Table 3 (continued)

Hybrid nanofluids	Stabilization method	Measurement method	Stability period	References
MWCNT-Al_2O_3-MoS_2	1-h ultrasonication 2-h magnetic stirring	–	7 days	[127]
TiO_2–SiO_2/water-EG	2-h bath ultrasonication 1-h mechanical stirring	–	Stable	[113]
SiO_2-Cu/water	2-h ultrasonication 3-h magnetic stirring	–	14 days	[65]
Al_2O_3-Cu/water	60-min ultrasonication 15-min magnetic stirring	Sedimentation test	7 days	[63]
Cu-CNT/water-EG Ag-CNT/water-EG	ultrasonication 30-min stirring	Sedimentation test Zeta potential test Spectral absorbance analysis test	6 months	[104]

Table 4 Correlations proposed by researchers estimating thermal conductivity of hybrid nanofluids

Hybrid nanofluids	Correlation	Range	References
SiO_2-TiO_2/water-EG	$\frac{K_{nf}}{K_{bf}} = \left(1+\frac{\varphi}{100}\right)^{5.25}\left(1+\frac{T}{70}\right)^{0.076}$	$0 \le \varphi \le 3\%$ $30 \le T \le 70$ ° C	[149]
Al_2O_3-Cu/EG	$\frac{K_{nf}}{K_{bf}} = \frac{(9.6128+\varphi)}{9.3885-0.000107597T^2} - \frac{0.0041099}{\varphi}$	$0.125 \le \varphi \le 2\%$ $25 \le T \le 50$ ° C	[150]
ZnO-Ag/water	$\frac{K_{nf}}{K_{bf}} = 1 + 0.0008794\varphi^{0.5899}T^{1.345}$	$0.125 \le \varphi \le 2\%$ $25 \le T \le 50$ ° C	[151]
SiO_2-P25/water-EG	$k_{nf} = k_{bf} * 1.0156\left(1+\frac{T}{70}\right)^{0.0848}\left(1+\frac{\phi}{100}\right)^{3.474}$	$0.5 \le \varphi \le 1.5\%$ $20 \le T \le 60$ ° C	[38]
GO-Al_2O_3/water	$\frac{k_{nf}}{k_{bf}} = 0.0031*\left(T^{1.185}\right)*\left(\varphi^{0.863}\right) + 1.006$	$0.1 \le \varphi \le 1\%$ $25 \le T \le 50$ ° C	[137]
GNP-Al_2O_3/TH55	$k(\varphi, T) = 0.1055 + 0.6761\varphi + 0.001097T - 3.247\varphi^2 - 0.02626\varphi T$ $-1.515e^{-05}T^2 + 0.08627\varphi^2 T + 0.0002225\varphi T^2 + 7.288e^{-08}T^3$	$0.01 \le \varphi \le 0.1\%$ $25 \le T \le 65$ ° C	[87]
TiO_2-Graphene/Water	$\frac{k_{nf}}{k_{bf}} = 1.0033 + 0.078846 \times \left(T^{0.40488}\right) \times \left(\varphi^{0.69671}\right)$	$0.005 \le \varphi \le 0.5\%$ $25 \le T \le 75$ ° C	[86]
ND-Fe_3O_4/water-EG	$k_{nf} = 1.041 \times k_{bf}\left[(1+\varphi)^{0.39} \times \left[\frac{T_{min}}{T_{max}}\right]^{0.383\times10^{-1}}\right]$	$0.05 \le \varphi \le 0.2\%$ $T_{min} = 20$ ° C $T_{max} = 60$ ° C	[76]
Al_2O_3-MWCNTs	$k_{nf}/k_{bf} = A + B \times T + C \times \varphi + D \times T \times \varphi + E \times \varphi^2$ $+F \times T \times \varphi^2 + G \times \varphi^3$	$0.02 \le \varphi \le 0.8\%$ $25 \le T \le 50$ ° C	[138]
SiO_2-MWCNTs/EG	$\frac{K_{nf}}{K_{bf}} = 1.01 + 0.007685T\varphi - 0.5136\varphi^2 T^{-0.1578} + 11.5\varphi^3 T^{-1.175}$	$0.025 \le \varphi \le 0.86\%$ $30 \le T \le 50$ ° C	[152]
TiO_2-MWCNTs/EG-water	$\frac{k_{nf}}{k_{bf}} = 1 + 0.0187\varphi^{0.6719}T^{0.6913}$	$0.0625 \le \varphi \le 1\%$ $20 \le T \le 60$ ° C	[37]
CeO_2-MWCNT/water	$k_{nf} = k_{bf}\left(1 + 0.580453 \times \left(\frac{T}{T_0}\right)^{1.54358} \times \varphi^{0.356853}\right)$	$0 \le \varphi \le 1.5\%$ $30 \le T \le 50$ ° C $T_0 = 30$ ° C	[80]
Al_2O_3-SWCNTs	$\frac{K_{nf}}{K_{bf}} = 0.963 + 0.008379 \times \left[\varphi^{0.4439} \times T^{0.9246}\right]$	$0.04 \le \varphi \le 2.5\%$ $30 \le T \le 50C$	[153]
MgO-FMWCNTs/EG	$\frac{K_{nf}}{K_{bf}} = 0.8341 + 1.1\varphi^{0.243}T^{-0.289}$	$0.05 \le \varphi \le 0.6\%$ $25 \le T \le 50$ ° C	[154]

K_{nf}, K_{bf}, φ, T are thermal conductivity of hybrid nanofluids, thermal conductivity of base fluid, volume concentration, and temperature, respectively

considered. It was noted that increasing both temperature and particle concentration yielded augmentation in hybrid nanofluid thermal conductivity. A maximum thermal conductivity enhancement of 19.14%, compared to water, was achieved. The thermal conductivity of GO-Si/water hybrid nanofluids was tested experimentally by Vardaru et al. [136]. The study considered the influence of nanoparticle mixing ratios (0.2 – 0.8) and temperature (25 – 50 ° C) on thermal

conductivity. Authors used a KD2 pro analyzer and thermostat bath for measuring thermal conductivity. Authors concluded that a mixing ratio of 0.8:0.2 (GO/Si) exhibited higher enhancement in thermal conductivity. Maximum improvement of thermal conductivity of 7.97% was achieved at a temperature of 50 ° C. In another study employed GO nanoparticles, Taherialekouhi et al. [137] tested the thermal conductivity of GO-Al_2O_3/water hybrid nanofluid at temperature range of 25 – 50 ° C and volume concentrations of 0.1 – 1% with the help of KD2 pro (Decagon Devices Inc., USA). Such device measure thermal conductivity with a range of 0.2 – 2 W m^{-1} K^{-1} and -50 to + 150 ° C. According to the results, the relative thermal conductivity coefficient was improved by 33.9% when the temperature was raised from 25 ° C to 50 ° C and the volume fraction was increased from 0.1% to 1%, as indicated in Fig. 13. Similar trend was observed by Askari et al. [88] where Fe_3O_4-graphere hybrid nanofluids were tested. They found that thermal conductivity was augmented by increasing both temperature and mass concentration achieving the highest enhancement of 31%. Thermal conductivity coefficient variation of SiO_2-P25/water-EG hybrid nanofluid was evaluated by Ba et al. [38] for several volume concentrations: 0.5, 1, and 1.5% at five different temperatures, 20, 30, 40, 50, and 60 ° C. A modified transient plane source technique was used to measure thermal conductivity. To ensure that the desired temperature is maintained throughout the experiment, a temperature-controlled oven was utilized. All the samples were placed in the oven for 30 min to achieve the desired temperature. Each sample was measured three times, and the mean value was recorded as the final result. Authors used an equal mixing ratio of SiO_2 and P25 nanoparticles, 1:1, for all experiments, and also, employed a mixing ratio of 5:1 for water and EG base fluids. A maximum enhancement in thermal conductivity, 12%, was achieved at a temperature of 60 C and 1.5% volume concentration.

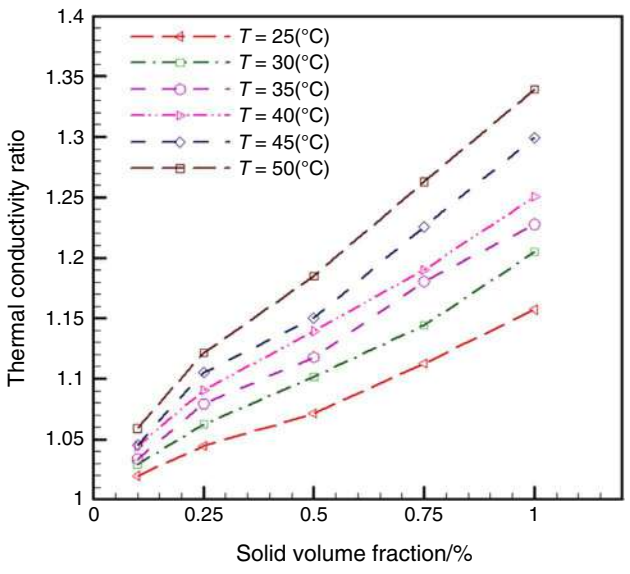

Fig. 13 Relative thermal conductivity coefficient of GO- Al_2O_3/water hybrid nanofluid as a function of volume concentration [137]

Bakhtiari et al. [86] evaluated the thermal conductivity of water-based TiO_2-graphene hybrid nanofluids with a volume concentration range of 0.005 – 0.5% and temperature range of 25–75 ° C employing KD 2 Pro (Decagon, USA). According to the data, the rise in thermal conductivity with increasing solid volume concentrations is more evident at higher temperatures. Nevertheless, the impact of volume fraction rise on thermal conductivity was greater than that of temperature. At a volume concentration of 0.5% and a temperature of 75 °C, the thermal conductivity was 27.84% greater than the base fluid. A similar trend was noted by Arani and Pourmoghadam [138] who examined the thermal conductivity of EG-based Al_2O_3-MWCNTs hybrid nanofluid with a temperature range from 25 ° C to 50 ° C and nanoparticles volume concentrations of 0.02–0.8% without adding any surfactants. Findings showed that the thermal conductivity was increased while increasing both temperature and volume fraction. The influence of volume fraction on thermal conductivity was more noticeable than temperature. In another related investigation, Asadi et al. [139] tested Al_2O_3-MWCNT/thermal oil hybrid nanofluid with temperature and concentration ranges of 25 – 50 ° C and 0.125 – 1.5%, respectively. KD2 pro analyzer was employed in this study. Three repetitions were conducted for each measurement set and the resulting average values were recorded. Additionally, a hot water bath was utilized to regulate and maintain the desired temperature during the process of measuring thermal conductivity. Findings exhibited that thermal conductivity augmented linearly with increasing both temperature and concentration achieving a highest enhancement of 45%.

Shajan et al. [87] assessed the influence of graphene nanoplatelets (GNP) fraction and temperature on the thermal conductivity GNP-Al_2O_3/TH55 hybrid nanofluid. Hybrid nanofluids were evaluated with GNP loadings range of 0.01 – 0.1% and temperatures of 25 – 65 ° C using KD2 pro (Decagon Devices Inc., USA). Findings exhibited that the thermal conductivity was increased by 6.5 – 18.72% when increasing particle loading from 0.01% to 0.1% at the highest temperature, 65 ° C. Moreover, the thermal conductivity of hybrid nanofluids was augmented by 3.03% compared with GNP/TH55 mono nanofluid while it was augmented by 10.28% in comparison with Al_2O_3/TH55 mono nanofluid. Moradi et al. [37] inspected the thermal conductivity of TiO_2-MWCNTs/EG-water hybrid nanofluid taking into consideration the effect of temperature, which ranged between 20 ° C and 60 ° C, and volume concentration, which ranged between 0.0625 and 1%. According to the experiment data, the thermal conductivity was augmented as the

volume concentration and temperature rose. The study indicated that the highest augmentation in thermal conductivity was 34.31%. Further, the findings showed that thermal conductivity was more sensitive at high temperatures compared to lower temperatures. Effect of using several surfactants (CTAB, SDBS, SDS, DDC, GA, PVP), different mixing ratios of hybrid nanofluid to surfactants (5:0, 4:1, 3:2, 2:3, 1:4), sonication time (30 – 180 min), volume concentration (0.25 – 1.5%), and temperature (30 – 50 ° C) on thermal conductivity of CeO_2-MWCNT (80:20)/water hybrid nanofluid was evaluated by Tiwari et al. [80]. Authors employed Hot Disk (TPS-500) analyzer for measuring the thermal conductivity. The measurements were taken multiple times for each temperature and concentration, and then, a mean value was recorded. The thermal conductivity of hybrid nanofluids using surfactants was positively influenced when increasing the mixing hybrid nanofluid to surfactant ratio up to a certain ratio, 3:2. After that, thermal conductivity experimented with a declining trend. Increasing sonication time up to 90 min yielded increasing thermal conductivity, and then, it started to decrease. In addition, it was revealed that increasing both temperature and volume concentration can enhance thermal conductivity. Researchers concluded that a maximum 27.38% improvement in thermal conductivity was obtained with CTAB, 3:2 mixing ratio, 90 min sonication time, 1.5% volume concentration, and 50 ° C temperature. Pourrajab et al. [140] performed an investigation dealing with the effect of Ag nanoparticles and MWCNTs-COOH nanoparticles on enhancing the thermal conductivity of hybrid nanofluid using KD2 Pro (Decagon Devices, Inc., USA). Several concentrations of water-based MWCNTs-COOH nanofluid, 0.004 – 0.14%, and a concentration of Ag of 0.04% were employed in this study with a 20–50 ° C range of temperature. The highest augmentation of thermal conductivity of 47.3% was noted for hybrid nanofluid having 0.16% MWCNT-COOH and 0.004% Ag nanoparticles at 50 ° C. MWCNTs-Ag/water hybrid nanofluid showed higher performance as compared with single-nanoparticle nanofluids as illustrated in Fig. 14 indicating that hybrid nanofluids are the nanofluids of the future.

Sundar et al. [76] and Saleh and Sundar [78] performed investigations dealing with the thermal conductivity enhancement of nanodiamond-Fe_3O_4/water-EG hybrid nanofluid. 60:40% water-EG mixture base fluid was used by [76] while a mixture of 40:60% water-EG was utilized by [78]. Both studies performed experiments at particle concentrations of 0.05% to 0.2% and temperatures ranging from 20 ° C to 60 ° C. According to findings, the highest thermal conductivity of 12.79% [76] and 14.65% [78] indicated that the influence of increasing EG base fluid is more effective than water. Another related study employing nanodiamond-Fe_3O_4 hybrid nanofluids was performed by Sundar et al. [75]. Outcomes indicated that thermal conductivity was

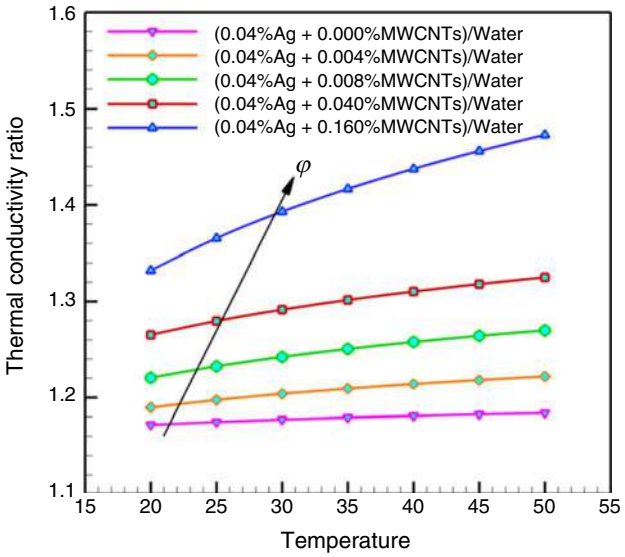

Fig. 14 Influence of Ag and MWCNT mixing ratio on thermal conductivity [140]

linearly augmented via increasing both temperatures (20–60 ° C) and volume concentrations (0–0.2%). Experiments were performed at volume fractions range of 0.019–0.075% and temperature range of 25–50 ° C.

Artificial intelligence (AI) investigations

Due to the number of factors that appear to impact the thermal conductivity of nanofluids, the accuracy of theoretical models of thermal conductivity prediction is limited [141]. Numerous researchers have suggested different correlation models determining the thermal conductivity of hybrid nanofluids. Recently, artificial neural networks have been offered as an alternate method for estimating the thermal conductivity of hybrid nanofluids. Thermal conductivity of fly ash-copper (80:20 vol.%) hybrid nanofluid in temperatures ranging between 30 ° C and 60 ° C and a volume concentration range of (0–4.0%) was predicted by Kanti et al. [142] employing artificial neural network (ANN) and multi-gene genetic programming (MGGP) techniques. The results revealed that the thermal conductivity of hybrid nanofluid augmented with temperature and concentration. The highest thermal conductivity was achieved at 60 ° C for a concentration of 4 vol.%. Further, ANN model showed more accurate results estimating the thermal conductivity of proposed hybrid nanofluids compared with MGGP model. Malika and Sonawane [143] used ANN and response surface methodology (RSM) techniques to study the influence of nanoparticle concentrations (0.2–1 vol%), temperatures (25–45 ° C), size of particles (20–60 nm), and ultrasonication time (0–40 min) on thermal conductivity of Fe_2O_3-SiC/water hybrid nanofluid. A more accurate predicted thermal

conductivity was obtained by the ANN method compared with the RSM method, as shown in Fig. 15. It was revealed that the best thermal conductivity was noted at a concentration of 0.8 vol%, a temperature of 40 ° C, a particle diameter of 30 nm, and ultrasonication time of 30 min. In another related work, ANN technique was utilized by Rostami et al. [144, 145] to estimate the thermal conductivity of SiO_2/water–ethylene glycol (50:50) hybrid nanofluid [144] and MWCNT-CuO/water hybrid nanofluid [145]. Experiments were firstly performed using seven different volume concentrations ranging from 0 to 5% [144], and 0.05–6% [145] with a temperature range of 25–50 ° C. Authors noted that thermal conductivity augmented with rising nanofluid temperature and volume concentration of the nanofluid due and this enhancement can be accounted for the increase in nanoparticle collisions as well as the weakening of molecular bonds in fluid layers. After, the ANN method was applied predicting the nanofluid thermal conductivity and authors stated that the ANN method showed better performance with fewer errors compared to the fitting method.

Wole-Osho et al. [141] tested the thermal conductivity of Al_2O_3-ZnO/water hybrid nanofluid with three different mixing ratios, namely 1:2, 1:1, and 2:1 (Al_2O_3/ZnO). The experiments were performed with various volume concentrations (0.33, 0.67, 1.0, 1.33 and 1.67%) with a range of temperatures of 25–65 ° C. Moreover, authors utilized artificial intelligence approaches, ANN, and adaptive neuro-fuzzy inference system (ANFIS), for predicting thermal conductivity. According to their findings, Al_2O_3-ZnO/water hybrid nanofluid with a mixing ratio of 1:1 yielded the highest thermal conductivity as compared with other mixing ratios, 1:2 and 2:1, at all examined temperatures and volume concentrations. Further, maximum thermal conductivity augmentation of 36%, 35%, and 40% was found for hybrid nanofluids with mixture ratios of 1:2, 1:1, and 2:1, respectively, at a temperature of 65 ° C and a volume concentration of 1.67%. ANN model performed better performance in terms of predicting thermal conductivity. Locally weighted linear regression (LWLR) was used by Pourrajab et al. [146] as a computing technique predicting the thermal conductivity of hybrid nanofluids in water, EG, and water/EG mixtures. For validation, several related recent correlations [82, 114, 129, 147, 148] were compared with LWLR. Authors findings revealed that LWLR offered a good prediction of thermal conductivity with a maximum error of less than 1.5%. Additionally, via performing a sensitivity analysis, it was concluded that temperature, volume concentration, and nanoparticles size were the most effective factors while water/EG mixing ratio showed less importance in terms of assessing hybrid nanofluid thermal conductivity. A summary of thermal conductivity improvement of hybrid nanofluids performed by various researchers is displayed in Table 5.

Viscosity

Viscosity is a crucial characteristic of fluid-based thermal applications. The viscosity of the fluid affects pressure drop, pumping power, and convective heat transfer coefficient [155]. Therefore, viscosity merits the same consideration as thermal conductivity owing to its very significant effect on heat transfer [127, 156]. The viscosity of hybrid nanofluids, compared to base fluids, should be thoroughly examined

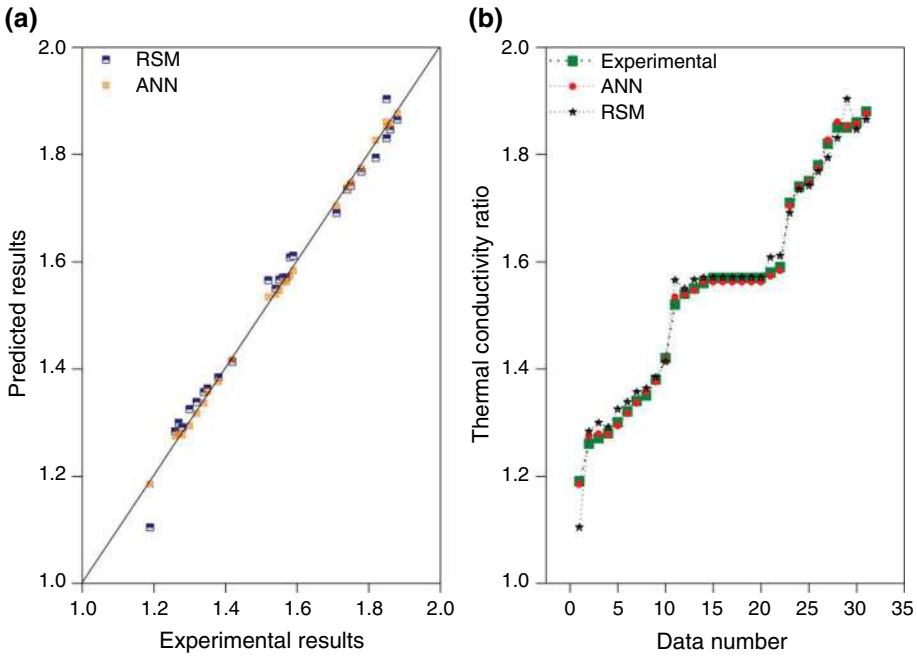

Fig. 15 Prediction of thermal conductivity of Fe_2O_3-SiC/water hybrid nanofluid using ANN and RSM [143]

Table 5 Thermal conductivity enhancement of various hybrid nanofluids performed by researchers

Hybrid nanoparticles	Base fluids	Outcomes	References
Al_2O_3-CuO	PG, EG/water	Using Spherical nanoparticles, PG base fluid exhibited the highest thermal conductivity	[133]
Al_2O_3-TiO_2 Al_2O_3-CuO Al_2O_3-Cu	Water/EG	Optimum nano particles mixing was 20:80, and Al_2O_3-TiO_2 hybrid nanofluid outperformed other nanofluids	[134]
Go-Co_3O_4	Water	Maximum thermal conductivity enhancement of 19.14%, compared to water at 60 ° C and 0.2 vol%	[135]
GO-Si	Water	A maximum thermal conductivity enhancement of 7.97% was achieved	[136]
GO-Al_2O_3	Water	The relative thermal conductivity coefficient was improved by 33.9% at 50 C and 1 vol%	[137]
SiO_2-P25	Water/EG	A maximum enhancement in thermal conductivity, 12%, was achieved at a temperature of 60 ° C and 1.5% volume concentration	[38]
Fe_3O_4-graphere	Kerosene	Maximum thermal conductivity of 31% was achieved	[88]
TiO_2-Graphene	Water	The thermal conductivity was 27.84% greater than the base fluid at 75 ° C and 0.5 vol%	[86]
Al_2O_3- MWCNTs	EG	The influence of volume fraction on thermal conductivity was more noticeable than temperature	[138]
Al_2O_3-MWCNT	Thermal oil	Thermal conductivity augmented linearly with increasing both temperature and concentration achieving a maximum enhancement of 45%	[139]
Al_2O_3-GNP	TH55	Thermal conductivity was increased by 18.72% at 65 ° C and 0.1 vol%	[87]
TiO_2-MWCNTs	Water/EG	The highest rise in thermal conductivity was 34.31%. thermal conductivity was more sensitive at high temperatures compared to lower temperature	[37]
CeO_2- MWCNT	Water	A maximum 27.38% improvement in thermal conductivity was obtained	[80]
Ag-MWCNTs-COOH	Water	The highest augmentation of thermal conductivity of 47.3% was noted for hybrid nanofluid having 0.16% MWCNT-COOH and 0.004% Ag nanoparticles at 50 ° C	[140]
ND-Fe_3O_4	Water/EG	The highest thermal conductivity of 12.79% was obtained at 60 C and 0.2%	[76]
ND-Fe_3O_4	Water/EG	The highest thermal conductivity of 14.65% was obtained 60 ° C and 0.2%	[78]
ND-Fe_3O_4	Water	Thermal conductivity was linearly augmented by increasing both temperatures and volume concentrations	[75]
fly ash-copper	Water	The highest thermal conductivity was achieved at 60 ° C for a concentration of 4 vol. percent hybrid nanofluid. ANN model showed more accurate results estimating thermal conductivity of proposed hybrid nanofluids compared with MGGP model	[142]
Fe_2O_3-SiC	Water	A more accurate predicated thermal conductivity was obtained by ANN method compared with RSM method	[143]
Al_2O_3–ZnO	Water	Maximum thermal conductivity enhancement of 40% was found. ANN model performed better performance in terms of predicting thermal conductivity compared with ANFIS	[141]

and analyzed before considering employing them in solar thermal applications. Many researchers proposed correlations for estimating the viscosity of hybrid nanofluids, as shown in Table 6.

Experimental investigations

Most researchers have evaluated the influence of temperature and volume concentration on the viscosity of hybrid nanofluids. Nadooshan et al. [157] evaluated the viscosity of EG-based Fe_3O_4-MWCNTs (1:1)/hybrid nanofluid at temperatures range of 25–50 ° C, volume concentration ranging from 0.1% to 1.8%, and shear range of 12.24–73.44 s^{-1}. Brookfield DV-1 prime digital viscometer was employed in this research. The viscometer's precision was within ± 1% of the maximum value that the viscometer could measure. To obtain more accurate results, experiments were conducted at each volume fraction and temperature for different shear rates. This process helps to account for any variations in the experimental conditions and ensures that the results are reliable. The findings exhibited that hybrid nanofluids showed a Newtonian behavior at volume concentrations (0.1–0.8%), while it demonstrates a non-Newtonian behavior at volume concentrations (0.8–1.8%). Furthermore, researchers concluded that viscosity increased with respect to rising volume concentration and decreasing temperature. Another related study dealing with evaluating the viscosity of Fe_3O_4-MWCNTs (80:20)/water hybrid nanofluids was performed by Giwa et al. [158]. Volume concentrations and temperatures ranges of 0.1–1.5% and 15–55 ° C, respectively, were used in this study. Researchers employed vibro-viscometer (SV-10; A&D, Tokyo, Japan) as a viscosity measurement device with ± 3% accuracy It can be seen that the effect of temperature on viscosity was higher than that of volume fraction, and also findings were compared with references [157, 159, 160] and showed a good agreement

Table 6 Correlations proposed by researchers estimating the viscosity of hybrid nanofluids

Hybrid nanofluids	Correlation	range	Ref
Fe_3O_4-MWCNTs/water	$\frac{\mu_{nf}}{\mu_{bf}} = \frac{-2.0987+(4.65\varphi)^{0.0969}+(0.8702T)^{0.2633}+(62323.1365\varphi^2)}{(143.1076T^2)}$	$0.1 \le \varphi \le 0.8\%$ $25 \le T \le 75$ ° C	[157]
Fe_3O_4-MWCNTs/water	$\frac{\mu_{hnf}}{\mu_{bf}} = 1.031 + 0.0025T + 0.1386\varphi$	$0.1 \le \varphi \le 1.5\%$ $15 \le T \le 55$ ° C	[158]
Al_2O_3-MWCNT/water	$\mu_{nf} = 1.41467 + 5.197 \times 10^{-3}R - 1.37 \times 10^{-2}T$	$15 \le T \le 55$ ° C	[161]
WO_3-MWCNT/water-EG	$\frac{\mu_{nf}}{\mu_{bf}} = \frac{0.1708+(-0.0028T)+(-0.0131\varphi T)+(0.0003\varphi)^{0.1443}}{\exp\left((-1.5776\varphi^2)+(-0.6442T^{0.1443})+\left(-0.1882\left(\frac{T}{\varphi}\right)^{0.1443}\right)\right)}$	$0.1 \le \varphi \le 0.6\%$ $25 \le T \le 50$ ° C	[163]
ZnO-MWCNT/engine oil	$\mu_{nf} = 796.8 + 76.26\varphi + 12.88T + 0.7695\varphi T + \frac{-196.9T-16.53\varphi T}{\sqrt{T}}$	$0.125 \le \varphi \le 1\%$ $5 \le T \le 55$ ° C	[127]
Al_2O_3-TiO_2/EG	$\mu_{nf} = 7.1074 + 3.65\varphi - 0.14097T + 0.05176\varphi T + 0.907\varphi^2 + 0.00092T^2$	$0.02 \le \varphi \le 0.1\%$ $30 \le T \le 80$ ° C	[168]
Al_2O_3-ZnO/water	$\mu_{nf} = (a_1 + a_2T_f + a_3T_f^2 + a_4R + a_5R^2 + a_6\varphi + a_7\varphi^2\mu_{bf}),\ R = 0.9334$	$0.33 \le \varphi \le 1.67\%$ $25 \le T \le 65$ ° C	[169]
TiO_2-SiO_2/bio-glycol	$\frac{\mu_{nf}}{\mu_{bf}} = 1.0753\exp\left(13.91 \times \frac{\varphi}{100}\right) + \left(0.0619 \times \frac{T}{80}\right)$	$0.5 \le \varphi \le 3\%$ $30 \le T \le 70$ ° C	[58]
SiO_2-graphite/water	$\frac{\mu_{nf}}{\mu_{bf}} = 1.00527 \times \left(T^{0.00035}\right) \times (1+\varphi)^{9.36265} \times \left(\frac{w_G}{w_{SiO_2}}\right)^{-0.028935}$	$0.001 \le \varphi \le 0.02\%$ $15 \le T \le 60$ ° C	[171]
Ag-Mgo/water	$\frac{\mu_{nf}}{\mu_{bf}} = 1.123 + 0.3251\varphi - 0.08994T + 0.002552T^2 - 0.00002386T^3 + 0.9695\left(\frac{T}{\varphi}\right)^{0.01719}$	$0.0625 \le \varphi \le 1\%$ $25 \le T \le 50$ ° C	[178]
ND-Fe_3O_4/water-EG	$\mu_{nf} = \mu_{bf}\left[1.67922 + 2.71766\phi - 0.69741\left(\frac{T_{min}}{T_{max}}\right)\right]$	$0 \le \varphi \le 0.2\%$ $T_{min} = 20$ ° C $T_{max} = 60$ ° C	[77]
ND-Fe_3O_4/water-EG	$\mu_{nf} = 1.366 \times \mu_{bf}\left[(1+\varphi)^{2.08} \times \left[\frac{T_{min}}{T_{max}}\right]^{-0.279}\right]$	$0 \le \varphi \le 0.2\%$ $T_{min} = 20$ ° C $T_{max} = 60$ ° C	[76]

μ_{nf}, μ_{bf}, φ, T are viscosity of hybrid nanofluids, viscosity of base fluid, volume concentration, and temperature, respectively

with them. Relative to the base fluid, a maximum increase of 35.7% of hybrid nanofluid viscosity was noticed. Giwa et al. [161, 162] tested water-based Al_2O_3-MWCNT and γ-Al_2O_3-MWCNT hybrid nanofluid with 0.1% volume concentration. Different mixture ratios of Al_2O_3 and MWCNT were used (90:10, 80:20, 60:40, 40:60, and 20:80) (Al_2O_3/MWCNT) with temperatures ranging from 15–55 ° C. Results of both studies revealed that viscosity increase of 24.56% (80:20) and 26.3% (90:10) was observed for Al_2O_3-MWCNT/water and γ-Al_2O_3-MWCNT/water hybrid nanofluid, respectively, at 55 °C and 0.1 vol%, shown in Fig. 16. Zhu et al. [163] investigated the dynamic viscosity of WO_3-MWCNT/water-EG (80:20) hybrid nanofluid. A range of volume concentrations of 0.1–0.6% and temperatures of 25–50 ° C were used. The Brookfield DV2 viscometer (± 1% accuracy) is employed to measure the viscosity. The findings indicated that viscosity increased as volume concentration increased at a constant temperature. In contrast, viscosity of the fluid decreased as temperature rose at a fixed volume concentration.

Influence of nanoparticle concentrations and temperatures on dynamic viscosity of engine oil SAE40-based SiO2-MWCNTs hybrid nanofluids had been carried out by Afrand et al. [164]. Experiments were conducted with volume concentrations range of 0–0.1% and temperature of 25–60 ° C. Brookfield CAP 2000 + Viscometer was used in this study. The viscometer operates at a medium to high shear rate and utilizes the cone-plate geometry. It also has an integrated temperature control system to regulate the temperature of the test sample material during the experiment. It was found that a Newtonian fluid behavior at all examined ranges of temperatures and concentrations. Also, it was revealed that the dynamic viscosity was augmented with increasing volume fractions and reduced with rising temperature. A similar trend was observed by Amini et al. [165] using the same nanoparticles employed by Ref. [164] but with a different base fluid, glycerol. A maximum increase of 37.5% and 105.4% was found by both research teams. Esfe et al. [166] assessed the effect of volume concentration and temperature on the viscosity of TiO_2-MWCNT (70:30)/SAE50 hybrid nanofluid. Authors used volume fractions of 0–1% and temperatures of 25–50 ° C and also various shear rates using CAP2000 rotary viscometer. It was revealed that the hybrid nanofluids showed non-Newtonian behavior at all concentrations. When predicting viscosity using empirical correlations, authors concluded that temperature, as an independent

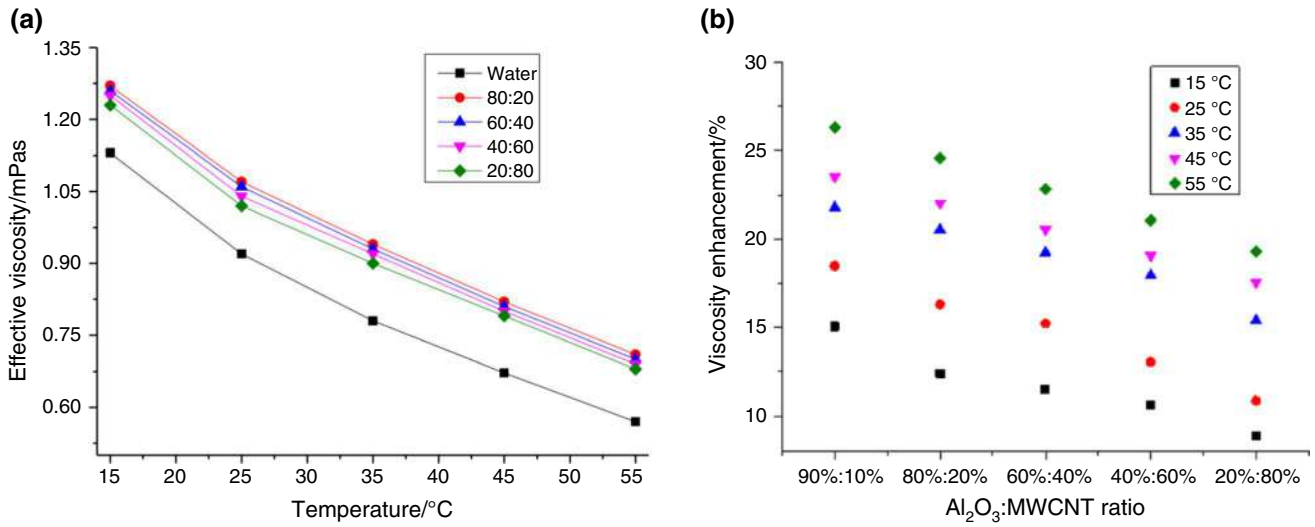

Fig. 16 Viscosity of water-based **a** Al_2O_3-MWCNT [161] and **b** γ- Al_2O_3-MWCNT hybrid nanofluid [162]

factor, is important in predicting viscosity, and the second independent parameter in the proposed correlation can be shear rate or volume fraction. However, these two independent characteristic factors cannot accurately predict nanofluid viscosity when utilized in an empirical correlation as two independent parameters. The rheological behavior of water-based Al2O3-TiO2 hybrid nanofluid was tested by Moldoveanu et al. [167]. A modular rheometer (Physica MCR 501, Anton Paar) with a Peltier system for temperature control was employed by authors. The most significant finding is that the tested nanofluids exhibited non-Newtonian behavior. In contrast, the Newtonian behavior of Al_2O_3-TiO_2 (80:20)/EG hybrid nanofluid was observed by Urmi et al. [168]. Experiments were carried out with volume concentrations ranging from 0.02% to 0.1% and temperatures of 30–80 ° C. Viscosity was noted to be raised with increasing concentrations and decreasing temperatures.

Wole-Osho et al. [169] inspected the influence of particle mixing ratio on the dynamic viscosity of Al_2O_3-ZnO hybrid nanofluids. In this study, the Brookfield DV-I PRIME digital viscometer was employed to measure the viscosity of the fluid. To maintain a consistent temperature during the viscosity measurements, the viscometer was equipped with a temperature bath that kept the samples at a constant temperature. Researchers used three different mixing ratios of Al_2O_3 and ZnO (1:1, 2:1, and 1:2) of nanoparticles at volume concentrations ranging from 0.33 to 1.67% and temperature range of 25–65 ° C. Findings showed that viscosity enhanced with increasing volume concentration, and it reduced with rising temperature. Also, it was seen that a mixture ratio of (2:1) yielded a maximum increase of 96.37% in dynamic viscosity at 1.67% volume concentration and 25 ° C. The dynamic viscosity of water-based CuO-TiO_2 hybrid nanofluids was assessed by Asadi et al. [170]. A digital viscometer (Brookfield DV2-Pro) was utilized, and at the same time, a thermal bath was used to regulate and stabilize the temperature of the samples during the viscosity measurements. After preparing and examining the hybrid nanofluids using techniques mentioned earlier in the literature, dynamic viscosity was measured with a range of 0.1–1% of volume concentration and 25–50 ° C of temperature. Additionally, the influence of shear stress was examined. According to researchers' findings, prepared hybrid nanofluids were found to be Newtonian, and a maximum increase in dynamic viscosity took place at 1 vol% and 25 ° C. It was also found that rising the temperature had resulted in a decrease in viscosity indicating a positive effect on hybrid nanofluid thermal properties, shown in Fig. 17. Dynamic viscosity of TiO_2-SiO_2(20:80)/water-bio-glycol(40:60) hybrid nanofluids was measured by Zainon and Azmi [58] with volume concentration and temperature ranges of 0.5–3% and 20–80 ° C, respectively. It was concluded that the dynamic viscosity remained almost constant for all examined volume concentrations. However, a slight rise in viscosity was noted at the temperature of 80 ° C. Dalkılıç et al. [171] performed an experimental investigation measuring the viscosity of SiO_2-graphite hybrid nanofluids using a capillary tube viscometer. Authors used Cannon–Fenske Opaque Viscometer as a viscosity measurement device. To maintain a constant temperature during the experiment, the hybrid nanofluids were placed in a measurement tank with circulating water. A cooler/heater unit was used to regulate the temperature of the tank and keep it at the desired level. Additionally, a reference thermometer was submerged into the measurement tank to ensure that the temperature remained consistent throughout the experiment. The viscometer was placed into the

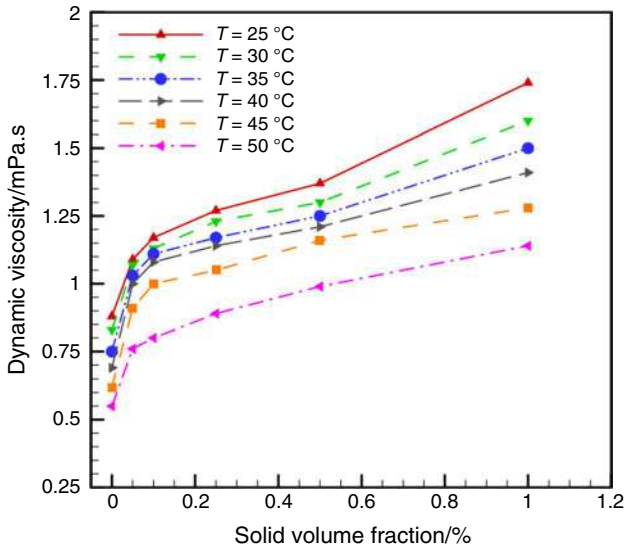

Fig. 17 Variations of the viscosity versus solid concentration in different temperatures of CuO-TiO_2/water hybrid nanofluids [170]

measurement tank to conduct the viscosity measurements. Several mixing ratios of SiO_2 and graphite, 20:80, 40:60, 60:40, 80:20, and four volume concentrations, 0.1, 0.5, 1, and 2%, with a range of temperature of 15–60 ° C were used in experimentations. Highest increase in viscosity of 36.12% was observed. Similarly, the viscosity of SiO_2-graphene (70:30)/water hybrid nanofluids was assessed by Kazemi et al. [172]. Non-Newtonian pseudoplastic behavior was exhibited.

Artificial intelligence (AI) investigations

ANN and MGGP modeling were implemented by Kanti et al. [173] to predict and optimize the viscosity data of fly ash-Cu hybrid/water nanofluid collected from the experimental investigation. The dynamic viscosity of fly ash-Cu hybrid (80:20)/water hybrid nanofluid was experimentally evaluated with a volume concentration range of 0–4% with a temperature range of 30–60 ° C. It was revealed that the dynamic viscosity of hybrid nanofluid increased with concentration and decreased with temperature. The contact between the water molecules and the nanoparticles causes an increase in viscosity. At 30 ° C, hybrid nanofluid nanoparticles had the highest effective viscosity of 1.45. Using the ANN model, the optimal number of neurons in the hidden layer is 7 for hybrid nanofluid. Also, the results of a statistical analysis showed that the MGGP model exhibited an outstanding performance for fly ash-Cu hybrid nanofluid viscosity compared with the ANN model. In another study, ANN and RSM modeling along with experiments were performed by Chu et al. [174] for investigating the rheological behavior of MWCNT-TiO_2/5W40 hybrid nanofluid at concentrations of 0.05–1% and temperatures of 20–60 ° C. According to the study results, dynamic viscosity on hybrid nanofluid raised with increasing volume concentration and decreasing of both shear rate and the temperature reaching a maximum increase of 790%. Numerically, utilizing ANN and RSM approaches was acceptable predicting viscosity. However, the accuracy of the ANN method, with an error of less than 5%, was greater than that, 5–10%, of the RSM method as indicated in Fig. 18. In another investigation, Toghraie et al. [175] used ANN technique to evaluate viscosity of WO_3-MWCNTs/engine oil hybrid nanofluid for different volume concentrations, temperatures, and shear rates. The experimental findings indicated that the effect of increasing temperatures on viscosity was more noticeable than increasing volume concentrations. In addition, it was found that ANN outputs closely match the experimental data points, and the optimal neuron number for this data set was 39. Therefore, utilizing ANN method may reduce experimental costs by eliminating the need for further tests. For saving time and cost, Jamei et al. [176] used the MGGP technique for assessing the viscosity of oil-based hybrid nanofluids. Gene expression programming (GEP) and multi-variate linear regression (MLR) methods were utilized for the reason of comparison with the MGGP model. Authors used 679 previous experimental data points including temperature, volume concentration, density, and size of nanoparticles as input for the model, and relative viscosity was set as an output. Results exhibited outstanding performance of the present approach in predicating relative viscosity. Said et al. [177] applied three different machine learning methods: support vector machine (SVM), ANN, and boosted regression tree (BRT) predicting viscosity of rGO-Fe_3O_4-TiO_2/EG hybrid nanofluids based on experimental data for a range of temperature and nanoparticles volume concentrations. Results of BRT method were more accurate compared to others. A summary of the viscosity of different hybrid nanofluids carried out by various researchers is displayed in Table 7.

Specific heat and density

Another significant parameter of hybrid nanofluids is specific heat. Solids often have a lower specific heat than liquids. As a result, when solid nanoparticles are added to the base fluid, the specific heat decreases. However, a greater specific heat value is required for an optimum coolant to remove more heat [156]. Additionally, the density of the hybrid nanofluid is an essential feature. Increased particle loadings increase the hybrid nanofluids density, which decreases with increasing temperature. It is the determining factor responsible for the sedimentation of nanoparticles in the base fluid [96].

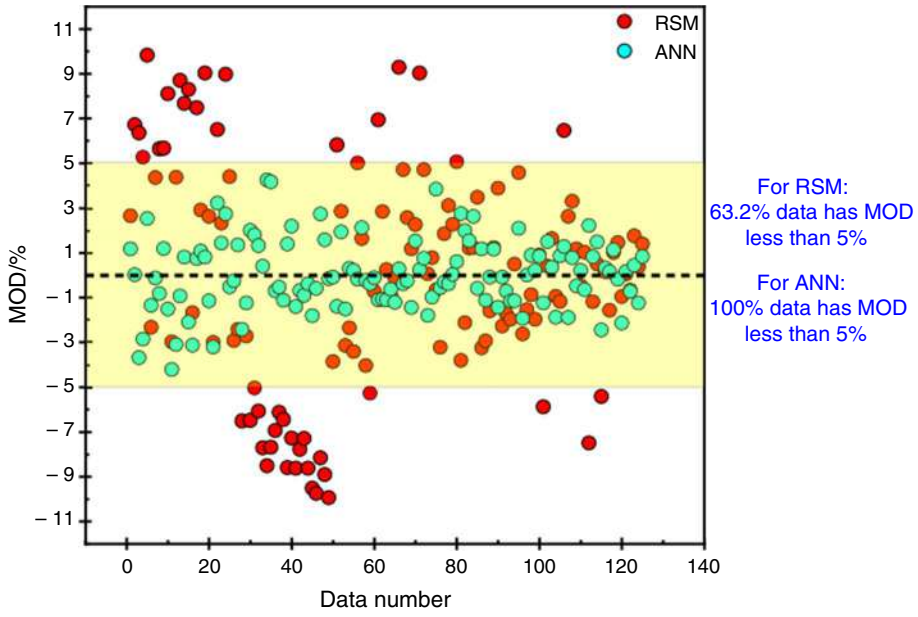

Fig. 18 Distribution of error of employing ANN and RSM [174]

Table 7 Viscosity of various hybrid nanofluids performed by researchers

Hybrid nanoparticles	Base fluids	Remarks	References
Fe_3O_4-MWCNTs	EG	Viscosity increased concerning rising volume concentration and decreasing temperature	[157]
Fe_3O_4-MWCNTs	Water	A maximum increase of 35.7% of hybrid nanofluid viscosity was noticed. the effect of temperature on viscosity was higher than that of volume fractions	[158]
Al_2O_3-MWCNT	Water	Viscosity increased up to 24.56% at 55 ° C and 0.1 vol%	[161]
γ-Al_2O_3-MWCNT	Water	Viscosity increased up to 26.2% at 55 ° C and 0.1 vol%	[162]
WO_3-MWCNT	Water-EG	Findings indicated that viscosity rises as volume concentration increased at a constant temperature. In contrast, the viscosity of the fluid decreased as temperature rose at a fixed volume concentration	[163]
SiO_2-MWCNTs	SAE40	Newtonian fluid behavior at all studied range of temperatures and concentrations with 37.5% increase in viscosity	[164]
SiO_2-MWCNTs	Glycerol	Maximum increase of viscosity of 105.4% was found	[165]
TiO_2-MWCNT	SAE50	Hybrid nanofluid results showed non-Newtonian behavior at all concentrations	[166]
Al_2O_3-TiO_2	Water	The most significant finding is that the tested nanofluids exhibited non-Newtonian behavior	[167]
Al_2O_3-TiO_2	EG	Results showed Newtonian behavior. Viscosity was found to be raised with increasing concentrations and decreasing temperatures	[168]
Al_2O_3-ZnO	Water	Maximum viscosity enhancement was 96.37% at 1.67 vol% and 25 ° C	[169]
CuO-TiO_2	Water	Prepared hybrid nanofluids were found to be Newtonian, and a maximum increase in dynamic viscosity took place at 1 vol% and 25 ° C	[170]
TiO_2-SiO_2	Water-bio-glycol	Dynamic viscosity remained almost constant for all examined volume concentrations. However, a slight rise in viscosity was noted at the temperature of 80 ° C	[58]
SiO_2-graphite	Water	Highest increase in viscosity of 36.12% was observed	[171]
SiO_2-graphene	Water	Non-Newtonian pseudoplastic behavior was exhibited	[172]
fly ash-Cu	Water	Statistical analysis showed that the MGGP model exhibited an outstanding performance for fly ash-Cu hybrid nanofluid viscosity compared with ANN	[173]
MWCNT-TiO_2	5W40	Maximum increase of 790% of viscosity was noted. the accuracy of ANN method, with error of less than 5%, was greater than that, error of 5–10%, of RSM method	[174]
WO3-MWCNTs	Engine oil	ANN outputs closely match the experimental data points, and the optimal neuron number for this data set was 39	[175]
rGO-Fe_3O_4-TiO_2	EG	Results of BRT methods were more accurate compared to others	[177]

Experimental investigations

Moldoveanu and Minea [179] evaluated the specific heat capacity of Al_2O_3-SiO_2/water hybrid nanofluids with several mixing ratios of nanoparticles. Measurements of specific heat were conducted at room temperature with the use of a Mettler-Toledo DSC apparatus. The aluminum capsules used for the measurements had a volume of 40 mL, and all probes had a mass ranging from 4 to 6 mg. The measurement accuracy was within 1% and a cooling system of type RCS40 was employed. To ensure accuracy, three tests were conducted for each determination and the average value was used for interpretation. Their main conclusion is that specific heat is highly reduced with the addition of nanoparticles. Also, they proposed an equation predicting the specific heat capacity of the tested nanofluids as a function of density of nanoparticle and base fluid (ρ_p and ρ_{bf}), nanoparticle size (d_p), and concentration (φ):

$$c_{p_{nf}} = \left(\frac{\rho_p}{\rho_{bf}}\right)^{0.2}\left(1+\frac{d_p}{50}\right)^{0.4167}\left(1-\frac{\varphi}{100}\right)^{2.272} c_{pbf} \quad (1)$$

In another investigation, Gao et al. [180] evaluated the specific heat of graphene oxide-Al_2O_3/water hybrid nanofluids taking into consideration the effect of the temperature and mass fraction. Experiments were conducted at a temperature range of (20–70 ° C) and mass fractions of (0.05–0.15%). The cooling method was adopted in this research using heat capacity evaluation equipment (BRR-II/II, Xiangtan Xiangyi instrument Co. LTD, China). Based on findings, the nanoparticle mass fraction has a greater impact on the specific heat of hybrid nanofluids at lower temperatures. The specific heat increases as the temperature rises, which influences the specific heat more than the nanoparticle mass fraction. Specific heat and density of metal oxides (CuO, MgO, SnO_2) with MWCNT water-based hybrid nanofluids was assessed by Tiwari et al. [181] with various volume concentrations (0.25–1.5%), temperatures (25–50 C) and sizes (20–50 nm). The specific heat capacity was evaluated employing differential scanning calorimetry (Setaram C80D), and density was evaluated by the density meter (DMA 5000, Anton Paar). Every experiment was performed four times for each sample in order to minimize errors. Based on findings, a highest decrease in the specific heat of 15% as compared with base fluid was noted at 1.5 vol%, 25 ° C, and 20 nm diameter for MgO-MWCNT hybrid nanofluids. It was also found that the specific heat of hybrid nanofluid increases as density decreases while decreasing as density increases. Authors had proposed a correlation determining specific heat as a function of temperature (T and T_0), concentration (φ), size (d_{np} and d_0), and density (ρ_{nf} and ρ_{bf}):

$$Cp_{nf} = Cp_{bf}\left(1-10.6364\times\left(\frac{T}{T_0}\right)^{-0.771}\times\varphi^{0.448}\times\left(\frac{d_{np}}{d_0}\right)^{-0.474}\times\left(\frac{Cp_{np}}{Cp_{bf}}\right)^{1.027}\times\left(\frac{\rho_{nf}}{\rho_{bf}}\right)^{-2.742}\right) \quad (2)$$

Saleh and Sundar [78] evaluated the influence of temperature and volume concentration of ND-Fe_3O_4/water-EG hybrid nanofluids on specific heat and density. Researchers used a range of temperature of 20–60 ° C and a volume concentration range of 0–0.2%. The specific heat of hybrid nanofluids was measured using a differential scanning calorimeter (DSC 2920 instrument, TA Instruments), which has an accuracy of ± 2.5%. The DSC device is equipped with a refrigerated cooling system for precise temperature control during the measurements while the Archimedes principle was adopted for evaluating the density. It was noted that specific heat increased with rising temperature and decreased with increasing particle loading. However, in terms of density, as the temperature rose, the density decreased while it rose with increasing the volume concentration, shown in Fig. 19. Such a trend was also observed by Oliveira et al. [182] using ND-Ag/EG hybrid nanofluids. Authors had proposed equations to estimate specific heat and density of hybrid nanofluid depending on experimental data as follows:

$$C_{p,hnf} = C_{p,bf}\left[(1+\varphi)^{-0.129\times10^{-1}}\times\left[\frac{T_{min}}{T_{max}}\right]^{-0.238\times10^{-3}}\right] \quad (3)$$

$$\rho_{hnf} = \rho_{bf}\left[(1+\varphi)^{0.414\times10^{-1}}\times\left[\frac{T_{min}}{T_{max}}\right]^{0.1106\times10^{-3}}\right] \quad (4)$$

where T_{min} = 20 ° C and T_{max} = ° 60 C. Specific heat and density of TiO_2-SiO_2 hybrid nanofluids were evaluated by Zainon and Azmi [58] with volume concentration and temperature ranges of 0.5–3% and 20–80 ° C. The DA-130 N model portable density meter was employed to measure the density using the resonant frequency oscillation method with an accuracy of ± 0.0001 g/cm^3. Data were manually recorded for each sample, and the measurement was repeated at different concentrations, with a minimum of three repetitions. According to their findings, specific heat increased with rising temperature and decreased with increasing volume concentration. Also, increasing concentration led to an increase in density while rising temperature yielded a density reduction. The results of the present study were consistent with Saleh and Sundar [78], Gao et al. [180], Akilu et al. [183]. Wanatasanappan et al. [105] inspected the influence of different mixing ratios of Al_2O_3 and CuO nanoparticles on both specific heat and density. Several mixing ratios were used: 20:80, 40:60, 50:50, and 60:40 (Al_2O_3/CuO), at a volume

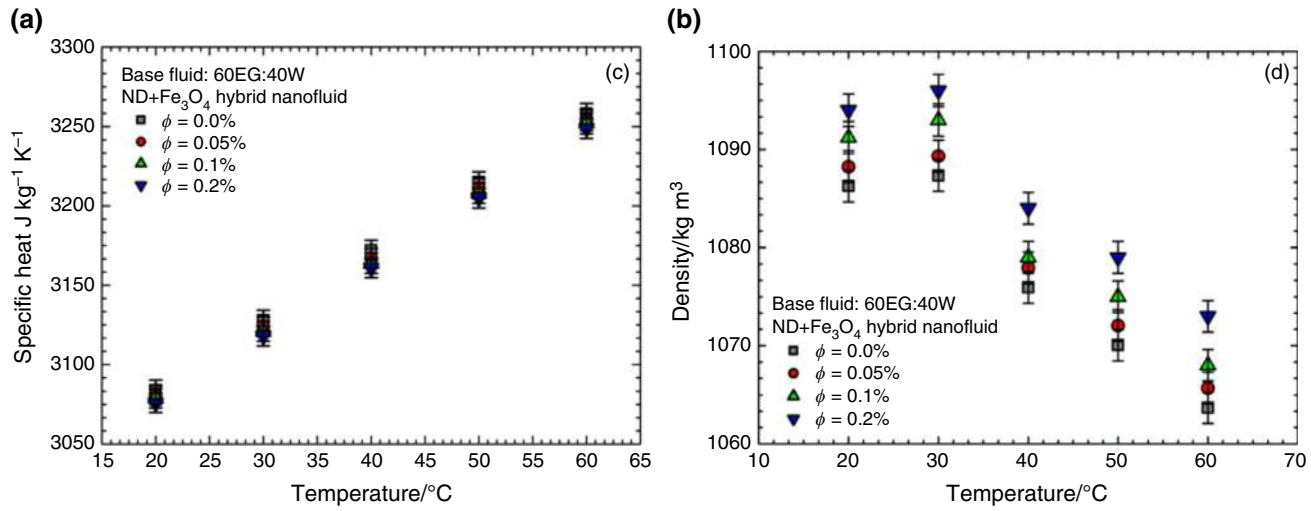

Fig. 19 **a** Specific heat and **b** density of ND- Fe3O4/water-EG hybrid nanofluids [78]

concentration of 1%. The DSC Q20 instrument from TA Instruments was utilized to determine the specific heat capacity of nanofluids. Six scans were carried out to obtain average values and minimize the possibility of system errors. The Rudolph density meter DDM 2909 (± 0.0001 g/cm3 accuracy) was utilized to measure the density of the samples. A total of five readings were obtained and averaged to analyze the results. It was shown that the specific heat capacity of base fluid was higher than that of hybrid nanofluids, and specific heat reduced as increasing the Al_2O_3 ratio. In terms of density, hybrid nanofluids at all mixing ratios showed an increasing trend compared with base fluid. Suspending equal amounts of nanoparticles, 50:50, led to the lowest density with an improvement of 2.33% compared with base fluid.

Artificial intelligence (AI) investigations

ANN modeling was designed by Çolak et al. [184] for estimating the specific heat of Cu-Al_2O_3 hybrid/water hybrid nanofluids. Values of specific heat were experimentally measured at different volume concentrations with a temperature range of 20–65 ° C, and the results obtained were utilized in the ANN model. It was indicated that the data obtained from modeling were in agreement with experimental results with an average deviation of 0.005%. Experiments were conducted by Kumar et al. [185] evaluating thermophysical properties including specific heat and density of water-based MWCNT/Al_2O_3, TiO_2, ZnO, and CeO_2 hybrid nanofluids, and they also performed ANN modeling optimizing experimental data. Researchers used volume concentration and temperature ranges of 0.25–2% and 25–50 ° C, respectively. The specific heat capacity was observed to rise with rising temperatures, and it was also shown to decline with increasing concentrations of the nanoparticles. The specific heat capacity was reported to rise by 5% with rising temperatures for all tested hybrid nanofluids. As concentrations of hybrid nanofluids increased, a degradation of 5–10% was seen on average. In addition, density was shown to be decreased with rising temperature while experiencing an increasing trend with increasing volume concentrations. The results of the ANN method matched the experimental data showing that a single model can accurately estimate the thermophysical parameters of hybrid nanofluids. Sepehrnia et al. [186] stated that the utilization of the ANN method in predicting the viscosity of ZnO-MWCNT/5W30 engine oil hybrid nanofluids revealed better accuracy compared to theoretical correlations. In another study, Said et al. [135] used an algorithm named Marine Predators Algorithm to optimize specific heat capacity and density of rGO-Co_3O_4 hybrid nanofluids achieving the goal of the proposed study.

Application of hybrid nanofluids in flat-plate solar collectors

Flat-plate solar collector (FPSC) is the most common type of solar thermal units, and it is used in low-temperature applications up to 90 °C, such as space heating, swimming pools heating, and household hot water generation, as well as sun cooling systems due to the ability to convert sunlight into thermal energy [187]. Details of a FPSC are shown in Fig. 20, and it consists of the following [39, 188];

1. Glazing one or more glass sheets. Its function is to minimize heating losses of convection and radiation.
2. Tubes they act as a heat exchanger transferring heat to working fluids. Heat transfer can be maximized using

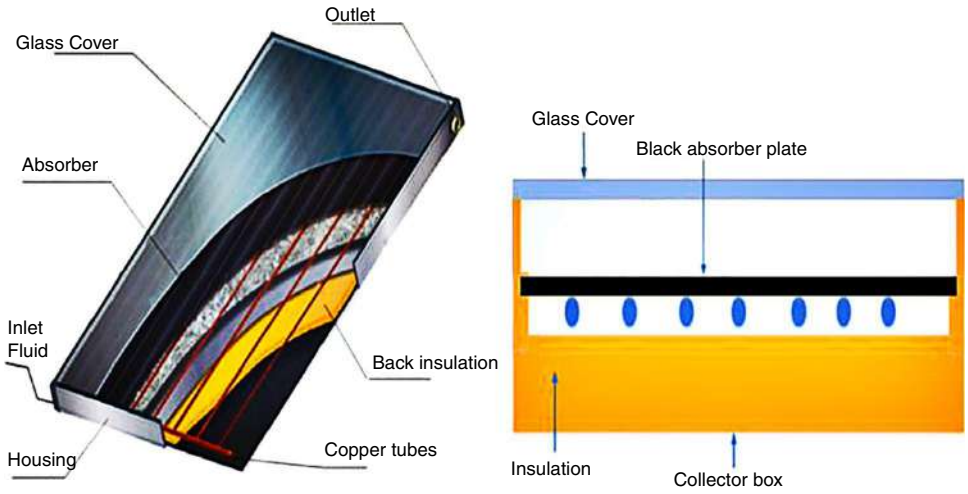

Fig. 20 Schematic of a flat-plate solar collector [39, 198]

heat transfer enhancing techniques inside the tubes: corrugations, grooves, fins, etc. [189].

3. Absorber it is used for collecting solar energy and transferring heat to the tubes and then working fluids. Its surface is typically having high absorption and low emittance. The absorber could be flat, grooved, or modulated.
4. Insulation it is important because it reduces the thermal losses from the bottom and sides of the collector to the surrounding.
5. Casing all parts mentioned above are enclosed in a casing for protection from water, dust, and others.

FPSCs have the benefits of being inexpensive to produce, collecting both beam and diffuse radiation, and is permanently fixed in place, so no tracking of the sun is necessary [190]. Utilizing nanofluids in the FPSC increases its efficiency, which is further boosted when particle loadings are raised. Initial investigations with nanofluids containing a single nanoparticle revealed an increase in collector thermal efficiency [191–197]. More recently, researchers have made an effort to utilize hybrid nanofluids in flat-plate solar collectors for more enhancement in thermal performance experimentally, numerically, and theoretically.

Experimental studies

Verma et al. [47] experimentally examined the influence of employing CuO-MWCNTs/water and MgO-MWCNTs/water hybrid nanofluids on the energetic and exergetic performance evaluation of a FPSC. Experiments were conducted with volume concentrations ranging from 0.25 to 2% and a flow rate range of 0.5 L min^{-1} to 2 L min^{-1} under given ambient conditions. Findings revealed that the optimal operating conditions for the FPSC were with volume fractions of 0.75–1% and mass flow rate of 0.025–0.03 kg s^{-1}. For MgO hybrid nanofluid, the maximum improvement in thermal efficiency of FPSC was 18.05%, while for CuO hybrid nanofluids was achieved. Thus, authors concluded that MgO-MWCNTs/water hybrid nanofluids are preferred in terms of thermal efficiency and cost as compared with CuO-MWCNTs/water hybrid nanofluids. However, it was noted that using MWCNT/water mono nanofluids have superior efficiency compared to hybrid nanofluids, as indicated in Fig. 21. Hussein et al. [199] formed hybrid nanofluids by dispersing covalent functionalized-graphene nanoplatelets (CF-GNPs) with hexagonal boron nitride (h-BN) with covalent functionalized-multi-wall carbon nanotubes (CF-MWCNTs) in water. The prepared nanofluids had been tested in a FPSC system with volume flow rates of 2–4 L min^{-1}. Several mass concentrations (0.05, 0.08, and 0.1%) were used by utilizing Tween-80 (Tw-80) as a surfactant. It was noted the performance of using hybrid nanofluids

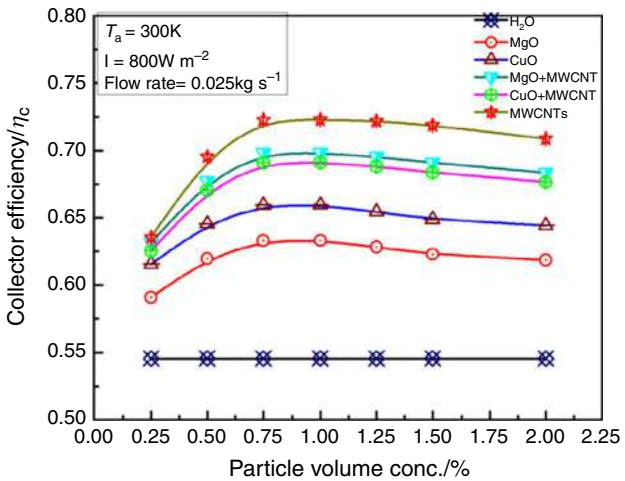

Fig. 21 Efficiency of FPSC vs volume concentration of tested nanofluids [47]

in a FPSC is superior to single nanofluids. In addition, the maximum efficiency of FPSC of 85% was obtained at a mass concentration of 0.1% and 4 L min^{-1}, which was 20% higher than water as a working fluid under the same conditions. In another similar experimental study, hybrid nanofluids consisting of boron nitride and functionalized carbon nanotubes were employed by Ahmed et al. [200] in a FPSC system. Tween-80 surfactant was used, and an optimized mixing ratio of 40:60 was adopted in this research. The findings indicated that incorporating an amount of hBN/CF-CNTs (0.1 mass%) with a flow rate of 4 L min^{-1} had a significant impact on collector efficiency, increasing it by up to 87% compared to the conventional working fluid employed in FPSC. The thermal efficiency of a FPSC was studied by Elshazly et al. [201] using MWCNT, Al_2O_3, and a hybrid MWCNT/Al_2O_3 (50:50%) as a working fluid. Four volume concentration percentages were examined for each type of nanofluid (0.5, 0.025, 0.01, and 0.005%), with three different mass flow rates for each concentration. The results demonstrated that the use of hybrid MWCNT/Al_2O_3 (50:50) led to a considerable increase in efficiency by 29%.

A study on the thermal performance of a flat-plate collector employing hybrid nanofluid (Cu-MWCNTs/water) and using grey relational analysis (GRA) was carried by Mausam et al. [202]. The research demonstrated how hybrid nanofluids can be beneficial and valuable in solar energy harvesting systems that incorporate flat-plate collectors by enhancing the heat transfer mechanism. Maximum thermal efficiency of 68.69% was achieved. Fe_3O_4-MWCNTs hybrid nanofluids were investigated by Saleh and Sundar [203] in a FPSC under thermosyphon circulation to evaluate the heat transfer, friction factor, and thermal efficiency using various concentrations of 0.05% to 0.3% and volume rates of 0.1 L min^{-1} to 0.75 L min^{-1}. The FPSC achieved better performance in terms of thermal efficiency due to the enhanced thermophysical properties of the proposed hybrid nanofluids. Researchers indicated that the highest improvement in thermal conductivity and viscosity of 28.46% and 50.4% were obtained at 0.3 vol% and 60 ° C as compared to water. Furthermore, Nusselt number was augmented with increasing particle concentration, and a maximum value of Nusselt number and friction factor values of 18.68% and 18.91% was obtained at daytime hour of 13:00 and Reynolds number of 1413. Thermal efficiency of the FPSC was noted to be increased by 28.09% at 0.3 vol% confirming that the use of Fe_3O_4-MWCNTs hybrid nanofluids in FPSCs is advantageous as compared to the working fluid of water. Thermal efficiency enhancement of a FPSC was experimentally assessed using graphene and crystal nano-cellulose (CNC) nanofluids and a combination of graphene-CNC hybrid nanofluids with water and EG as base fluids by Mahamude et al. [48]. Thermal conductivity of the proposed hybrid nanofluids was increased by 194% compared with mono nanofluids at 80 ° C, and its viscosity rose to 3 times of base fluid indicating that hybrid nanofluids can be an excellent replacement to regular absorber material. Moreover, at 0.5 vol%, maximum thermal efficiency of using graphene-CNC hybrid nanofluid was 15.86%, while thermal efficiency of using regular water was 4%. ND–Co_3O_4 hybrid nanofluids were utilized by Sundar et al. [204] for experimentally assessing the thermal efficiency, heat transfer, friction factor of a FPSC thermosyphon system. 0.05–0.15% volume concentrations and 0.56–1.35 L min^{-1} volume flow rates were tested. As a result of the enhanced thermophysical characteristics of hybrid nanofluids, the FPSC was able to achieve both a greater coefficient of heat transfer and an increased thermal efficiency in comparison with the results obtained using water. The findings indicated that the Nusselt number increased by 21.23%, with a highest friction factor penalty of 1.13 times when compared to water. While the thermal efficiency of water is only 48% at day time hour of 13, the collector thermal efficiency was determined to be 59% for 0.15% mass concentration, as shown in Fig. 22.

Some researchers have tested metal oxides hybrid nanofluids in FPSCs. Mono and hybrid nanofluids of metal oxides of Al_2O_3 and TiO_2 were prepared with the addition of CTAB surfactant for better stability by Farajzadeh et al. [205]. The prepared nanofluids were investigated experimentally and numerically in a FPSC system, shown in Fig. 23, with a mass concentration of 0.1% at volume flow rates (1.5 L min^{-1}, 2 L min^{-1}, and 2.5 L min^{-1}). Findings indicated that employing Al_2O_3, TiO_2, and Al_2O_3-TiO_2 nanofluids led to an augmentation in thermal efficiency of the FPSC by 19%, 21%, and 26%, respectively, in comparison with water as a working fluid. In terms of cost, authors revealed that using a mixture of proposed nanofluids can lead to a reduction in price

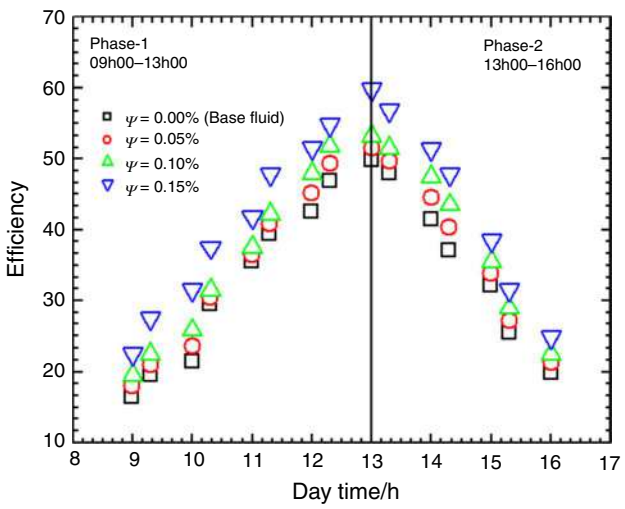

Fig. 22 Variation of FPSC efficiency employing ND-Co_3O_4 hybrid nanofluids vs day time [204]

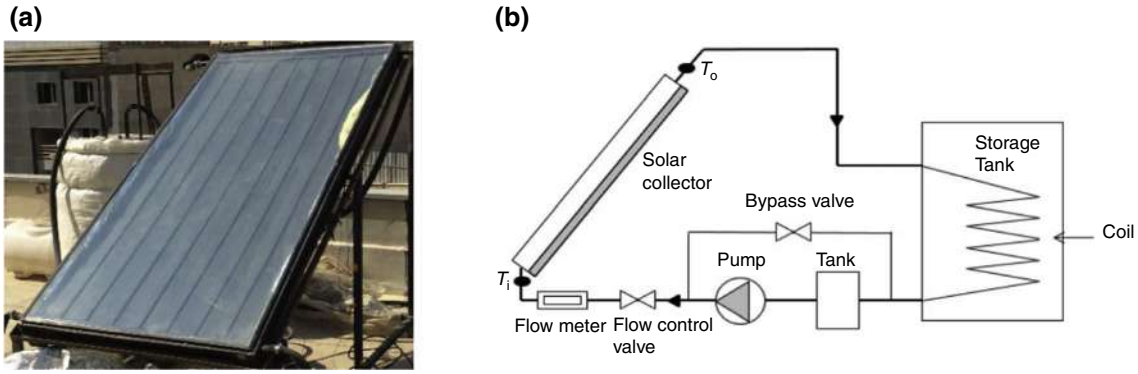

Fig. 23 FPSC system: **a** experimental setup, **b** schematic test device [205]

compared with TiO_2 nanofluid since TiO_2 is more expensive than Al_2O_3. Tahat and Benim [49] experimentally evaluated the influence of using EG and water mixture-based Al2O3-CuO (25:75) hybrid nanofluids on the thermal efficiency of a FPSC system using ASHRAE standards. Several volume concentrations of 0.5%, 1%, 1.5%, and 2% were examined. According to the authors' findings, thermophysical properties (thermal conductivity, viscosity, and density) were increased with nanoparticle concentrations. A similar trend was observed in terms of thermal efficiency leading to a maximum value of 52%. Utilizing the same hybrid nanofluid (Al2O3-CuO/water), Kalbande et al. [206] assessed the thermal performance of a FPSC and energy storage system. They concluded that using hybrid nanofluids is superior to that of conventional working fluids. The useful energy and thermal efficiency of hybrid solar collectors (flat collector and PV system) had been evaluated by Wole-Osho et al. [207] using Al_2O_3-ZnO/water hybrid nanofluids. Several parameters had been tested: ratios of Al_2O_3 in the mixture (0.2–0.8), volume concentrations (0.0001–0.01%), and mass flow rates (0.01–0.1 kg s^{-1}). Researchers stated that changing mixing ratios affected the thermal efficiency of the system leading to an optimum mixing ratio of 0.47 of Al_2O_3. Finally, it was clearly seen that using hybrid nanofluids led to a remarkable improvement in thermal efficiency of 34% compared with water.

Numerical studies

Several researchers have numerically evaluated the influence of utilizing hybrid nanofluids on the energy and exergy performance of FPSCs equipped with other heat transfer enhancing techniques such as turbulators, porous media, and changing tube design. Water-based Al_2O_3-MWCNT hybrid nanofluid in turbulent flow is examined numerically by Ibrahim et al. [208] to determine the exergy efficiency of a FPSC with unique turbulators, shown in Fig. 24. The experiment was carried out on a two-phase water-based Al_2O_3-MWCNT hybrid nanofluid with Reynolds numbers ranging from 5000 to 20,000, volume fractions ranging from 1 to 3%, and torsion ratios of 0.05–0.25 at heights of (5–20 mm) using a novel turbulator. Based on the results obtained, the maximum exergy efficiency occurred at Re of 20,000 and volume concentration of 3% at a turbulator height of 5 mm and a torsion ratio of 0.05. A numerical investigation of the thermal performance of a FPSC system using Cu-Al_2O_3 hybrid nanofluids and porous media had been carried out by Yegane and Kasaeian [209]. The results showed that at a constant nanoparticles volume fraction, a mixture of Cu and Al_2O_3 with equal volume concentration performs better than pure Al_2O_3 nanoparticles in terms of heat transfer. Further, increasing pore density and decreasing porosity led to augmentation in heat transfer rate and friction factor. A numerical investigation of Cu-fly ash hybrid nanofluids on the thermal performance of a FPSC was conducted by Azimy et al. [210]. In this study, authors have considered changing the design of the absorber pipe from straight to zigzag. The influence of fluid temperature, volume concentrations, and mass flow rate on thermal performance have been studied. Based on findings, thermal efficiency of the FPSC increased by using the proposed absorber design, and also by increasing these three parameters, the Nusselt number augmented. In another investigation, Xiong et al. [211] numerically examined the effect of combing Ag-Al_2O_3 hybrid nanofluid with porous media on the hydrothermal performance of FPSC employing the finite element method (FEM), shown in Fig. 25. The proposed study was carried out as a function of hybrid nanofluid concentrations, porosity coefficient, Reynolds number, Darcy number, Brownian motion parameter, radiation parameter, thermophoresis parameter, Schmidt number, and ratio of porous media to hybrid nanofluid thermal conductivity. Authors revealed that the heat transfer rate was augmented by increasing porosity coefficient and lowering Darcy number, radiation parameter, and thermal conductivity ratio. Also, using hybrid nanofluid

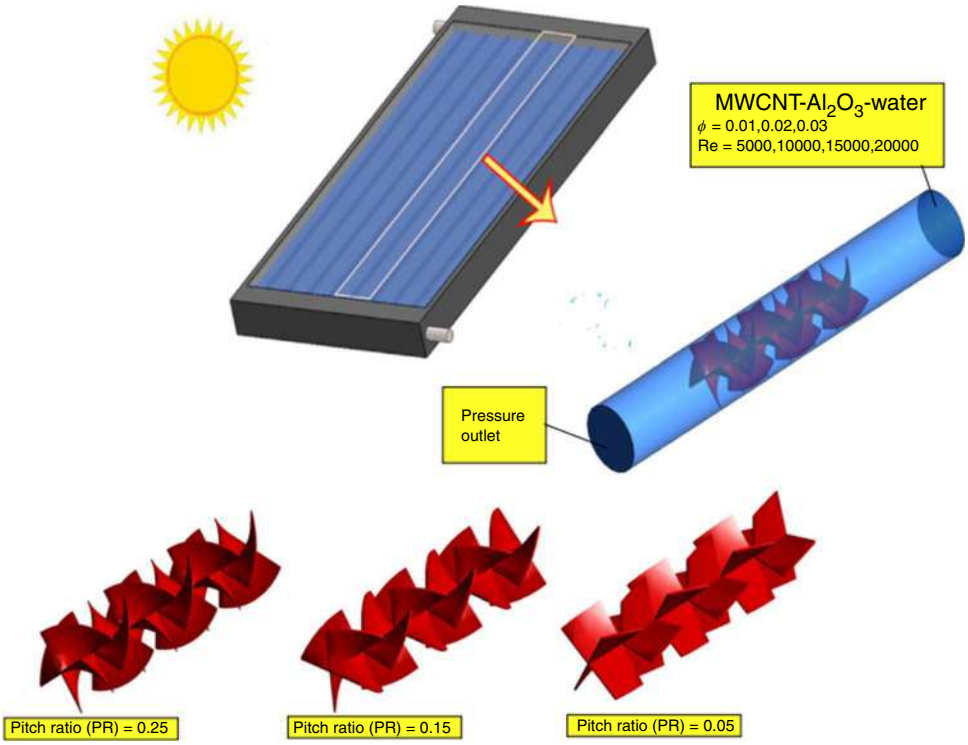

Fig. 24 Schematic of the geometry of the solar collector with turbulators [208]

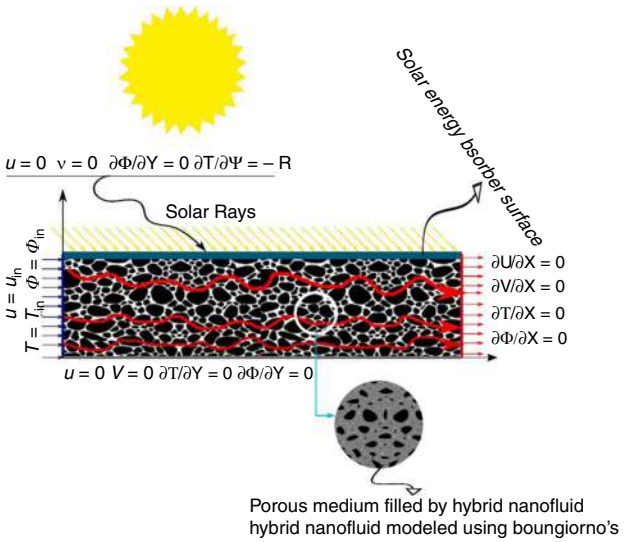

Fig. 25 Schematic of considered FPSC with hybrid nanofluids and porous media [211]

led to a reduction in heat transfer and increased the supply temperature slightly at low Reynolds number.

Nabi et al. [212] tested several turbulence-inducing elements along with hybrid nanofluids that were numerically tested in a FPSC using CFD software. Initially, the influence of a variety of turbulence generating element geometries was assessed for the FPSC. Subsequently, making use of the scenario that resulted in the largest heat transfer, the researchers investigated the impact of two hybrid nanofluids (CuO-MWCNT and CuO-SWCNT) in addition to regular water. In the third step, several concentrations (1–5%) of the fluid that exhibited the maximum rate of heat transfer were tested. According to the findings, the addition of turbulent-inducing features boosted the heat transfer coefficient in all of the analyzed scenarios more than in the base case owing to the creation of a rotating flow and improved mixing. The heat transfer coefficient of hybrid nanofluids at high Reynolds numbers is higher than pure water. Further, the heat transfer coefficient and friction factor increased as the concentration of tested nanofluids increased. The best thermal efficiency was found in SWCNT-CuO/water at a concentration of 1% at Re = 6000, with a 5.16% gain over classic working fluid. In another simulated study, Fattahi and Karimi [213] examined the influence of three parameters affecting the performance of a FPSC, namely Al_2O_3-ZnO-Fe_3O_4 ternary hybrid nanofluids, coating the absorber with a superhydrophobic coating, and wavy absorber. Despite the fact that the ternary nanofluid helped greater heat transfer by increasing the Nusselt number by 50–70%, it yielded a higher friction factor of 11–21%. Also, findings showed that the coating may lower the average Nusselt number by roughly 6% while reducing the friction factor by 45% meaning that it is a useful technique for enhancing hydrothermal performance of FPSC. Alzahrani et al. [214] analyzed numerically the effect of Darcy-Forchheimer and

(CuO-MWCNTs, MgO-MWCNTs) water-based hybrid nanofluids on the thermal performance of an inclined FPSC. Increasing volume concentrations along with increasing thermal radiation parameters exhibited an increase in heat transfer rate which yield an augmentation in Nusselt number.

Theoretical studies

An analytical study of energy and exergy of a FPSC system was carried out by Babu et al. [215] employing mono and hybrid nanofluids (Cu, CuO, and Cu-CuO) employing water as a base fluid. It was noted that there was an enhancement in heat gain by 2.16% for hybrid nanofluids while 1.03%, and 0.91% for Cu/water and CuO/water nanofluids, respectively. The FPSC thermal efficiency was augmented by 2.175% for the hybrid nanofluid and 0.93% and 1.05% for mono nanofluids. On the other hand, a penalty increase in pressure drop was noted: 2.918%, 3.09%, and 2.74% for hybrid and mono nanofluids. Furthermore, in terms of exergy, exergy efficiency was increased by 2.59%, 2.32%, and 2.96% for hybrid and mono nanofluids. It can be concluded that using hybrid nanofluids in the FPSC is superior compared with mono nanofluids. Lee et al. [216] theoretically evaluated three types of solar collectors (flat-plate, vacuum U-tube, and heat pipe solar collectors) employing mono and hybrid nanofluids (MWCNT, CuO, Fe_3O_4, MWCNT-CuO, and MWCNT-Fe_3O_4) water-based. The mass flow rate was fixed at 0.047 kg s^{-1} while volume concentrations and solar radiation were varied with ranges of (0.06–1%) and (650–1000 W m^{-2}). They found that employing MWCNT-CuO and MWCNT-Fe_3O_4 hybrid nanofluids exhibited an improvement in thermal efficiency by 50, 7, and 4% for flat-plate, vacuum U-tube, and heat pipe solar collectors, respectively. In addition, the MWCNT-CuO hybrid nanofluid demonstrated more thermal efficiency than the MWCNT-Fe_3O_4 hybrid nanofluid in three solar collectors. Another thermodynamic investigation of FPSC was performed by Okonkwo et al. [217] on mono and hybrid nanofluids (Al_2O_3/water, Al_2O_3-Fe/water). Different inlet temperatures (25–65 ° C), mass flow rates (0.001–0.07 kg s^{-1}), and volume concentrations (0.05–0.2%) were evaluated employing water as a base fluid. The findings indicated that the implementation of Al_2O_3-water nanofluid at a concentration of 0.1% enhanced the collector's thermal performance by 2.16%; however, the hybrid nanofluids decreased the collector's thermal performance by 1.79% in comparison with water, as exhibited in Fig. 26. Although the hybrid nanofluids have not given a superior thermal alternative to water, they did improve exergetic efficiency by 6.9% compared to 5.7%when utilizing Al_2O_3-water nanofluids. A recent study was performed by Mustafa et al. [218] evaluating the effect of Al_2O_3-Cu/water hybrid nanofluids on thermal performance and the environmental effect of a FPSC. Laminar flow with Reynolds member range of (700–2300) was employed with a volume concentration of nanoparticles of 0.1%. Authors indicated that the thermal efficiency of hybrid nanofluids is higher by 4.23% compared with base fluid (water). Further, environmental pollutants associated with using water is maximized while amounts of emissions is minimal utilizing hybrid nanofluids. Stalin et al. [219] performed a thermodynamic performance analysis on a flat-plate solar thermal collector that utilized single nanofluids and hybrid nanofluids. Heat transfer fluids such as Fe_2O_4/water, Zn-Fe_2O_4/water hybrid nanofluids, and water were used in the experiment. MATLAB codes were developed to solve the collector's thermal model iteratively and evaluate energy and exergetic performance. The results indicated that

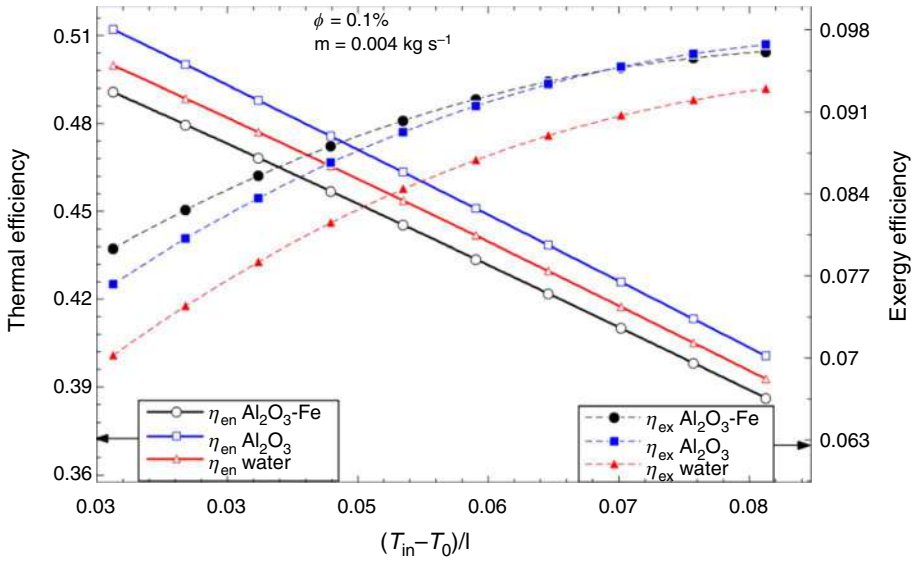

Fig. 26 Thermal and exergetic efficiencies performance of FPSC system [217]

Table 8 A summary of reviewed experimental, numerical, theoretical articles related to employing hybrid nanofluids in FPSCs

Nanoparticles	Base fluids	Type of investigation	Volume or mass fractions	Collector area, m^2	Remarks	References
CuO/MWCNTs Mgo/MWCNTs	Water	Experimental	0.25–2%	0.375	Maximum enhancement in thermal efficiency of FPSC was 18.05% while for CuO hybrid nanofluids, 20.52% enhancement in thermal efficiency was achieved	[47]
CF-GNPs/CF MWCNTs/h-BN	Water	Experimental	0.05–0.1%	1.92	Maximum efficiency of FPSC of 85% was obtained at a mass concentration 0.1% and 4 L min^{-1}, which was 20% higher than water as a working fluid at the same conditions	[199]
hBN/CF-CNTs	Water	Experimental	0.05–0.1%	2.06	Maximum efficiency of FPSC of 87% was obtained	[200]
MWCNT Al_2O_3 MWCNT/Al_2O_3	Water	Experimental	0.005–0.5%	1.94	The results demonstrated that the use of hybrid MWCNT/Al_2O_3 (50:50) led to a considerable increase in efficiency by 29%	[201]
Cu/MWCNTs	Water	Experimental	0.25–2%	0.22	Maximum thermal efficiency of 68.69% was achieved	[202]
Fe_3O_4/MWCNTs	Water	Experimental	0.05–0.3%	3	Thermal efficiency of FPSC was noted to be increased by 28.09% at 0.3 vol% compared with water	[203]
CNC Graphene Graphene/CNC	Water/EG	Experimental	0.1–0.5%	–	At 0.5 vol%, the maximum thermal efficiency of using graphene-CNC hybrid nanofluid was 15.86% while thermal efficiency of using regular water was 4%	[48]
ND/Co_3O_4	Water	Experimental	0.05–0.15%	3	The collector's thermal efficiency was determined to be 59% at 0.15 vol% while it was 48% for pure water	[204]
Al_2O_3 TiO_2 Al_2O_3/TiO_2	Water	Experimental Numerical	0.1–0.2%	1.85	Results indicated that using Al_2O_3, TiO_2, and Al_2O_3/TiO_2 nanofluids led to an augmentation in thermal efficiency of FPSC by 19%, 21%, and 26%, respectively	[205]
Al_2O_3/CuO	Water/EG	Experimental	0.5–2%	2	Maximum thermal efficiency of 52% was obtained using hybrid nanofluids	[49]
Al_2O_3/CuO	Water	Experimental	–	–	Using hybrid nanofluids is superior to that of conventional working fluids	[206]
Al_2O_3/ZnO	Water	Experimental	0.3–1.7%	1.6665	Employing hybrid nanofluids led to a remarkable enhancement in thermal efficiency of 34% compared with water	[207]

Table 8 (continued)

Nanoparticles	Base fluids	Type of investigation	Volume or mass fractions	Collector area, m^2	Remarks	References
Al_2O_3/MWCNT	Water	Numerical	1–3%	0.006	The maximum exergy efficiency occurred at Reynolds number of 20,000 and volume concentration of 3% at a turbulator height of 5 mm and a torsion ratio of 0.05	[208]
Cu/Al_2O_3	Water	Numerical	0.05–0.1%	–	The use of hybrid nanofluids with equal volume fractions is superior to mono nanofluids. Increasing porosity reduces friction factor and Nusselt number	[209]
Cu-fly ash	Water	Numerical	0.5–3.5%	0.225	thermal efficiency of the FPSC increased by using the proposed absorber design	[210]
Ag/Al_2O_3	Water	Numerical	0.005%, 0.1%	–	Hybrid nanofluid led to a reduction in heat transfer and increased the supply temperature slightly at a low Reynolds number	[211]
CuO/MWCNT CuO-SWCNT	Water	Numerical	1–5%	0.09	The best thermal efficiency was found in SWCNT-CuO/water at a concentration of 1% at Re = 6000, with a 5.16% gain over classic working fluid	[212]
Al_2O_3/ZnO/Fe_3O_4	Water	Numerical	0–1%	0.4	Although the ternary nanofluid helped greater heat transfer by increasing the Nusselt number by 50–70%, it yielded a higher friction factor of 11–21%	[213]
CuO/MWCNTs MgO/MWCNTs	Water	Numerical	0–2%	–	Increasing volume concentrations along with increasing thermal radiation parameters exhibited an increase in heat transfer rate which yield an augmentation in Nusselt number	[214]
Cu CuO Cu/CuO	Water	Theoretical	1–5%	0.74	FPSC thermal efficiency was augmented by 2.175% for the hybrid nanofluid and 0.93% and 1.05% for mono nanofluids	[215]
CuO Fe_3O_4 MWCNTs CuO/MWCNTs Fe_3O_4/MWCNTs	Water EG	Theoretical	0.06–0.1%	2.03	MWCNT-CuO hybrid nanofluid demonstrated more thermal efficiency than the MWCNT-Fe_3O_4 hybrid nanofluid in three solar collectors	[216]
Al_2O_3 Al_2O_3/Fe	Water	Theoretical	0.05–0.2%	1.51	hybrid nanofluids decreased the collector's thermal performance by 1.79% as compared to water	[217]

Table 8 (continued)

Nanoparticles	Base fluids	Type of investigation	Volume or mass fractions	Collector area, m^2	Remarks	References
Al_2O_3/Cu	Water	Theoretical	0.1%	2	thermal efficiency of hybrid nanofluids is higher by 4.23% compared with base fluid (water)	[218]
Fe_2O_4 Zn-Fe_2O_4	water	Theoretical	0.02–0.5%	2	Hybrid nanofluids outperformed single nanofluids and water in terms of thermal efficiency	[219]

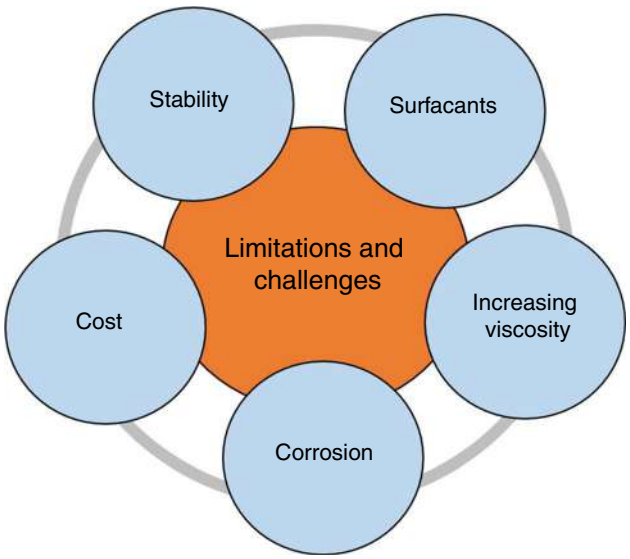

Fig. 27 Limitations and challenges of hybrid nanofluids

hybrid nanofluids outperformed single nanofluids and water in terms of thermal efficiency. Additionally, the hybrid nanofluids demonstrated an 8.24% increase in exergetic efficiency compared to Fe_2O_4/water nanofluids. Table 8 summarizes all reviewed experimental, numerical, theoretical articles related to employing hybrid nanofluids in FPSCs.

Limitations and challenges

Despite the benefits of employing hybrid nanofluids in augmentation of thermal performance of solar collectors among other heat transfer fluids, there are some problems and limitations that need to be addressed and solved to obtain the possible heat transfer efficiency, shown in Fig. 27.

1. Dispersion and long-term stability are essential requirements for hybrid nanofluids. Sustained enhanced thermal conductivity is the result of improved nanofluid stability. It is a technical challenge to create a homogenous suspension of hybrid nanofluids, as nanofluids have a strong propensity to agglomerate due to their strong van der Waals forces. To date, there have been a few studies demonstrating the long-term stability of hybrid nanofluids, as demonstrated by many researchers [79, 80, 99, 117].
2. Numerous experimental investigations have shown that using surfactants enhances the nanoparticles' dispersion and reduces their tendency to agglomerate [55, 117]. However, due to the surfactant's exposure to many cooling and heating cycles, its usage might result in foam formation in the solar collector systems causing a reduction in stability and thermal conductivity via the production of thermal resistance between nanoparticles and base fluids.
3. Viscosity is a crucial factor in heat transfer. As the hybrid nanofluids have a greater viscosity than the base fluids, so the requirement of pumping power needed to circulate the working fluid rises. The rise in pumping power relies on the concentration and morphology of the nanoparticles. With a high concentration of nanoparticles, the use of hybrid nanofluids may result in a substantial rise in pressure drop and, therefore, pumping power consumption [47, 212]. In addition, the increased viscosity may clog the pipes leading to shutting down the entire system. Thus, considerable effort is necessary to develop hybrid nanofluids with low viscosity.
4. The flow of a nanofluid in solar thermal systems may cause contact surfaces to erode and corrode due to the presence of nanoparticles. Few studies have reported how nanofluids erode and corrode in thermal systems, for instance, [220].
5. Nanofluids are much more expensive than classical working fluids. It includes nanoparticle costs as well as preparation costs. Increasing the concentration of hybrid nanofluids leads to further enhancement in thermal conductivity. However, the cost will be high. This is essential to commercialize the employment of hybrid nanofluids in solar thermal applications.

Conclusion and future recommendations

This review presents a comprehensive analysis of preparation methods and characterizations of hybrid nanofluids. Stability evaluations and enhancing methods of hybrid nanofluids have been reviewed along with critically evaluating the enhancement of their thermophysical properties. Further, this review analyzed the utilization of hybrid nanofluids in FPSCs. Based on the literature reviewed in the present study, some important conclusions are stated below:

1. Most scholars used the two-step method for the preparation methods of hybrid nanofluids. Although the one-step method is simple and easy, the two-step method provides control over the volume concentration of hybrid nanofluids.
2. Stability is a critical issue for hybrid nanofluids, especially at high nanoparticle volume concentrations. Nanoparticles tend to agglomerate after a period due to the action of gravity, hence, leading to low stability. This will consequently affect the thermophysical properties of nanofluids by lowering thermal conductivity and increasing viscosity.
3. During hybrid nanofluids preparation, it is essential to employ techniques for enhancing stability such as adding surfactants, controlling pH value, and performing ultrasonication and magnetic string. This will ensure the improvement of hybrid nanofluids stability for long-period.
4. The thermal conductivity of hybrid nanofluids mainly depends on nanoparticle concentration and temperature. Increasing nanoparticle concentration led to the enhancement of thermal conductivity. On the other hand, the viscosity will increase as well.
5. Hybrid combination of nanoparticles containing MWCNTs and GNPs has exhibited higher enhancement in thermal conductivity compared with other types of nanoparticles.
6. Increased viscosity of hybrid nanofluids yields an increase in pumping power and clogs pipes and valves.
7. Artificial neural networks have been offered as an alternative method for predicting the thermophysical properties of hybrid nanofluids due to the accuracy limitation of theoretical models.
8. Hybrid nanofluids have been presented as an alternative to mono nanofluids for the augmentation of the performance of FPSCs. Most of the studies proved that using hybrid nanofluids, compared with single nanofluids and conventional working fluids, enhances the thermal efficiency of FPSCs. However, few investigations revealed that using mono nanofluids in FPSCs exhibited higher thermal efficiency as compared with hybrid nanofluids.
9. Further enhancement of FPSCs thermal performance is achieved using hybrid nanofluids and other heat transfer enhancing techniques like turbulators and porous media.

After an intensive review of the literature and based on the gap found in this current review, several key recommendations are summarized and outlined as follows:

1. The stability of hybrid nanofluids is the key factor in their applications. More research must be performed to study the effect of different factors on the long-term stability of hybrid nanofluids.
2. More investigations should be carried out to optimize the nanoparticles mixing ratios for achieving high thermal conductivity with low viscosity.
3. As the fact that solar thermal collectors work at high temperatures, more investigations should be conducted to observe the thermal conductivity behavior of hybrid nanofluids at high working temperatures.
4. Corrosion and erosion of pipes due to employing hybrid nanofluids for long periods should be deeply addressed in future works.
5. Further investigations are required to be carried out to explore the effect of new types of hybrid nanofluids on the thermal performance of FPSCs.
6. The cost has a crucial impact on the application of hybrid nanofluids in thermal energy transport and storage. The economic feasibility of utilizing hybrid nanofluids should be considered in the future prior to employing them in solar thermal applications.
7. In the literature, some numerical studies used hybrid nanofluids with other heat transfer enhancement techniques such as turbulators and porous media in FPSCs. Using such techniques experimentally, along with hybrid nanofluids, would give more advanced and enhanced thermal performance of FPSCs
8. Employing hybrid nanofluids in FPSCs has proven to provide high thermal efficiency. Now, it is important to perform experiments on real large-scale systems for long-term to observe the sustainability of this technology.

Acknowledgements The authors are grateful to the management of University Technology Malaysia, Universiti Teknologi PETRONAS and University of Malaya for the support to conduct this research works.

References

1. Viral R, Khatod DK. Optimal planning of distributed generation systems in distribution system: a review. Renew Sustain Energy Rev. 2012;16:5146–65.
2. Brini R, Amara M, Jemmali H. Renewable energy consumption, International trade, oil price and economic growth inter-linkages: the case of Tunisia. Renew Sustain Energy Rev. 2017;76:620–7.
3. Farhana K, Kadirgama K, Rahman M, Ramasamy D, Noor M, Najafi G, Samykano M, Mahamude A. Improvement in the performance of solar collectors with nanofluids—A state-of-the-art review. Nano-Structures & Nano-Objects. 2019;18: 100276.
4. Garcia RP, del Rio Oliveira S, Scalon VL. Thermal efficiency experimental evaluation of solar flat plate collectors when introducing convective barriers. Sol Energy. 2019;182:278–85.
5. Zayed M, Zhao J, Du Y, Kabeel AE, Shalaby S. Factors affecting the thermal performance of the flat plate solar collector using nanofluids: a review. Sol Energy. 2019;182:382–96.
6. Alawi OA, Kamar HM, Mallah A, Mohammed HA, Kazi S, Sidik NAC, Najafi G. Nanofluids for flat plate solar collectors: fundamentals and applications. J Clean Prod. 2021;291: 125725.
7. El-Assal B, Irshad K, Ali A. Effect of side reflectors on the performance of flat plate solar collector: a case study for Asir Region, Saudi Arabia. Arab J Sci Eng. 2020;45:1035–50.
8. Visa I, Moldovan M, Duta A. Novel triangle flat plate solar thermal collector for facades integration. Renew Energy. 2019;143:252–62.
9. Sakhaei SA, Valipour MS. Investigation on the effect of different coated absorber plates on the thermal efficiency of the flat-plate solar collector. J Therm Anal Calorim. 2020;140:1597–610.
10. Alami AH, Aokal K. Enhancement of spectral absorption of solar thermal collectors by bulk graphene addition via high-pressure graphite blasting. Energy Convers Manage. 2018;156:757–64.
11. Barbosa EG, de Araujo MEV, de Moraes MJ, Martins MA, Alves BGX, Barbosa EG. Influence of the absorber tubes configuration on the performance of low cost solar water heating systems. J Clean Prod. 2019;222:22–8.
12. Fan M, You S, Gao X, Zhang H, Li B, Zheng W, Sun L, Zhou T. A comparative study on the performance of liquid flat-plate solar collector with a new V-corrugated absorber. Energy Convers Manage. 2019;184:235–48.
13. Ghazanfari V, Imani M, Shadman MM, Amini Y, Zahakifar F. Numerical study on the thermal performance of the shell and tube heat exchanger using twisted tubes and Al_2O_3 nanoparticles. Prog Nucl Energy. 2023;155: 104526.
14. Abolarin S, Everts M, Meyer JP. Heat transfer and pressure drop characteristics of alternating clockwise and counter clockwise twisted tape inserts in the transitional flow regime. Int J Heat Mass Transf. 2019;133:203–17.
15. Balaji K, Iniyan S, Goic R. Thermal performance of solar water heater using velocity enhancer. Renewable Energy. 2018;115:887–95.
16. Abeens M, Meikandan M, Sheriff J, Murunganadhan R. Experimental analysis of convective heat transfer on tubes using twisted tape inserts, louvered strip inserts and surface treated tube. Int J Ambient Energy. 2020;41:540–6.
17. da Silva FA, Dezan DJ, Pantaleao AV, Salviano LO. Longitudinal vortex generator applied to heat transfer enhancement of a flat plate solar water heater. Appl Therm Eng. 2019;158: 113790.
18. Anirudh K, Dhinakaran S. Numerical study on performance improvement of a flat-plate solar collector filled with porous foam. Renew Energy. 2020;147:1704–17.
19. Saedodin S, Zamzamian S, Nimvari ME, Wongwises S, Jouybari HJ. Performance evaluation of a flat-plate solar collector filled with porous metal foam: experimental and numerical analysis. Energy Convers Manage. 2017;153:278–87.
20. Serebryakova M, Zaikovskii A, Sakhapov S, Smovzh D, Sukhinin G, Novopashin S. Thermal conductivity of nanofluids based on hollow γ-Al_2O_3 nanoparticles, and the influence of interfacial thermal resistance. Int J Heat Mass Transf. 2017;108:1314–9.
21. Angayarkanni S, Philip J. Review on thermal properties of nanofluids: recent developments. Adv Coll Interface Sci. 2015;225:146–76.
22. Sharma S, Gupta SM. Preparation and evaluation of stable nanofluids for heat transfer application: a review. Exp Thermal Fluid Sci. 2016;79:202–12.
23. Nasiri A, Shariaty-Niasar M, Rashidi A, Amrollahi A, Khodafarin R. Effect of dispersion method on thermal conductivity and stability of nanofluid. Exp Thermal Fluid Sci. 2011;35:717–23.
24. Hosseini SMS, Dehaj MS. An experimental study on energetic performance evaluation of a parabolic trough solar collector operating with Al_2O_3/water and GO/water nanofluids. Energy. 2021;234: 121317.
25. Sheikholeslami M, Ebrahimpour Z. Thermal improvement of linear Fresnel solar system utilizing Al_2O_3-water nanofluid and multi-way twisted tape. Int J Therm Sci. 2022;176: 107505.
26. Sheikholeslami M, Jafaryar M. Thermal assessment of solar concentrated system with utilizing CNT nanoparticles and complicated helical turbulator. Int J Therm Sci. 2023;184: 108015.
27. Choudhary S, Sachdeva A, Kumar P. Time-based analysis of stability and thermal efficiency of flat plate solar collector using iron oxide nanofluid. Appl Therm Eng. 2021;183: 115931.
28. Sundar LS, Sintie YT, Said Z, Singh MK, Punnaiah V, Sousa AC. Energy, efficiency, economic impact, and heat transfer aspects of solar flat plate collector with Al_2O_3 nanofluids and wire coil with core rod inserts. Sustain Energy Technol Assess. 2020;40: 100772.
29. Eltaweel M, Abdel-Rehim AA. Energy and exergy analysis of a thermosiphon and forced-circulation flat-plate solar collector using MWCNT/Water nanofluid. Case Stud Thermal Eng. 2019;14: 100416.
30. Alawi OA, Kamar HM, Mallah A, Kazi S, Sidik NAC. Thermal efficiency of a flat-plate solar collector filled with Pentaethylene Glycol-treated graphene nanoplatelets: an experimental analysis. Sol Energy. 2019;191:360–70.
31. Sarkar J, Ghosh P, Adil A. A review on hybrid nanofluids: recent research, development and applications. Renew Sustain Energy Rev. 2015;43:164–77.
32. Sajid MU, Ali HM. Thermal conductivity of hybrid nanofluids: a critical review. Int J Heat Mass Transf. 2018;126:211–34.
33. Turcu R, Darabont A, Nan A, Aldea N, Macovei D, Bica D, Vekas L, Pana O, Soran M, Koos A. New polypyrrole-multiwall carbon nanotubes hybrid materials. J Optoelectron Adv Mater. 2006;8:643–7.
34. Kumar V, Tiwari AK, Ghosh SK. Exergy analysis of hybrid nanofluids with optimum concentration in a plate heat exchanger. Mater Res Express. 2018;5: 065022.
35. Shahul Hameed M, Suresh S, Singh RK. Comparative study of heat transfer and friction characteristics of water-based Alumina–copper and Alumina–CNT hybrid nanofluids in laminar flow through pipes. J Thermal Anal Calorimetry. 2019;136:243–53.
36. Sundar LS, Singh MK, Sousa AC. Enhanced heat transfer and friction factor of MWCNT–Fe_3O_4/water hybrid nanofluids. Int Commun Heat Mass Transfer. 2014;52:73–83.
37. Moradi A, Zareh M, Afrand M, Khayat M. Effects of temperature and volume concentration on thermal conductivity of TiO_2-MWCNTs (70–30)/EG-water hybrid nano-fluid. Powder Technol. 2020;362:578–85.
38. Le Ba T, Várady ZI, Lukács IE, Molnár J, Balczár IA, Wongwises S, Szilágyi IM. Experimental investigation of rheological

properties and thermal conductivity of SiO_2–P25 TiO2 hybrid nanofluids. J Therm Anal Calorim. 2021;146:493–507.
39. Xiong Q, Altnji S, Tayebi T, Izadi M, Hajjar A, Sundén B, Li LK. A comprehensive review on the application of hybrid nanofluids in solar energy collectors. Sustain Energy Technol Assess. 2021;47: 101341.
40. Kaska SA, Khalefa RA, Hussein AM. Hybrid nanofluid to enhance heat transfer under turbulent flow in a flat tube. Case Stud Thermal Eng. 2019;13: 100398.
41. Minea AA. Hybrid nanofluids based on Al_2O_3, TiO_2 and SiO_2: numerical evaluation of different approaches. Int J Heat Mass Transf. 2017;104:852–60.
42. Babu JR, Kumar KK, Rao SS. State-of-art review on hybrid nanofluids. Renew Sustain Energy Rev. 2017;77:551–65.
43. Sheikholeslami M. Numerical investigation of solar system equipped with innovative turbulator and hybrid nanofluid. Sol Energy Mater Sol Cells. 2022;243: 111786.
44. Ekiciler R, Arslan K, Turgut O, Kurşun B. Effect of hybrid nanofluid on heat transfer performance of parabolic trough solar collector receiver. J Therm Anal Calorim. 2021;143:1637–54.
45. Henein SM, Abdel-Rehim AA. The performance response of a heat pipe evacuated tube solar collector using MgO/MWCNT hybrid nanofluid as a working fluid. Case Studies in Thermal Engineering. 2022;33: 101957.
46. Shoeibi S, Kargarsharifabad H, Rahbar N, Ahmadi G, Safaei MR. Performance evaluation of a solar still using hybrid nanofluid glass cooling-CFD simulation and environmental analysis. Sustain Energy Technol Assess. 2022;49: 101728.
47. Verma SK, Tiwari AK, Tiwari S, Chauhan DS. Performance analysis of hybrid nanofluids in flat plate solar collector as an advanced working fluid. Sol Energy. 2018;167:231–41.
48. Mahamude ASF, Harun WSW, Kadirgama K, Ramasamy D, Farhana K, Salih K, Yusaf T. Experimental study on the efficiency improvement of flat plate solar collectors using hybrid nanofluids graphene/waste cotton. Energies. 2022;15:2309.
49. Tahat MS, Benim AC. Experimental analysis on thermophysical properties of Al_2O_3/CuO hybrid nano fluid with its effects on flat plate solar collector. Defect and diffusion forum: Trans Tech Publ; 2017. p. 148–56.
50. Babar H, Ali HM. Towards hybrid nanofluids: preparation, thermophysical properties, applications, and challenges. J Mol Liq. 2019;281:598–633.
51. Yang L, Ji W, Mao M, Huang J-N. An updated review on the properties, fabrication and application of hybrid-nanofluids along with their environmental effects. J Clean Prod. 2020;257: 120408.
52. Khan A, Ali M. Thermo-hydraulic behavior of alumina/silica hybrid nanofluids through a straight minichannel heat sink. Case Stud Thermal Eng. 2022;31: 101838.
53. Johari MNI, Zakaria IA, Azmi W, Mohamed W. Green bio glycol Al_2O_3-SiO_2 hybrid nanofluids for PEMFC: the thermal-electrical-hydraulic perspectives. Int Commun Heat Mass Transfer. 2022;131: 105870.
54. Wanatasanapan VV, Abdullah M, Gunnasegaran P. Effect of TiO_2-Al_2O_3 nanoparticle mixing ratio on the thermal conductivity, rheological properties, and dynamic viscosity of water-based hybrid nanofluid. J Market Res. 2020;9:13781–92.
55. Ma M, Zhai Y, Yao P, Li Y, Wang H. Effect of surfactant on the rheological behavior and thermophysical properties of hybrid nanofluids. Powder Technol. 2021;379:373–83.
56. Zhang S, Lu L, Wen T, Dong C. Turbulent heat transfer and flow analysis of hybrid Al_2O_3-CuO/water nanofluid: an experiment and CFD simulation study. Appl Therm Eng. 2021;188: 116589.
57. Malika M, Sonawane SS. The sono-photocatalytic performance of a Fe_2O_3 coated TiO_2 based hybrid nanofluid under visible light via RSM. Colloids Surf, A. 2022;641: 128545.
58. Zainon S, Azmi W. Stability and thermo-physical properties of green bio-glycol based TiO_2-SiO_2 nanofluids. Int Commun Heat Mass Transfer. 2021;126: 105402.
59. Vidhya R, Balakrishnan T, Kumar BS. Investigation on thermophysical properties and heat transfer performance of heat pipe charged with binary mixture based ZnO-MgO hybrid nanofluids. Mater Today: Proc. 2021;37:3423–33.
60. Akilu S, Baheta AT, Said MAM, Minea AA, Sharma K. Properties of glycerol and ethylene glycol mixture based SiO_2-CuO/C hybrid nanofluid for enhanced solar energy transport. Sol Energy Mater Sol Cells. 2018;179:118–28.
61. Li J, Liu C-Y, Xie Z. Synthesis and surface plasmon resonance properties of carbon-coated Cu and Co nanoparticles. Mater Res Bull. 2011;46:743–7.
62. Wei D, Dave R, Pfeffer R. Mixing and characterization of nanosized powders: an assessment of different techniques. J Nanopart Res. 2002;4:21–41.
63. Ma M-Y, Zhai Y-L, Li Z-H, Yao P-T, Wang H. Particle size-dependent rheological behavior and mechanism of Al_2O_3-Cu/W hybrid nanofluids. J Mol Liq. 2021;335: 116297.
64. Suresh S, Venkitaraj K, Selvakumar P, Chandrasekar M. Synthesis of Al_2O_3–Cu/water hybrid nanofluids using two step method and its thermo physical properties. Colloids Surf, A. 2011;388:41–8.
65. Amiri M, Movahedirad S, Manteghi F. Thermal conductivity of water and ethylene glycol nanofluids containing new modified surface SiO_2-Cu nanoparticles: Experimental and modeling. Appl Therm Eng. 2016;108:48–53.
66. Lahari MC, Sai PS, Sharma KV, Narayanaswamy KS. Thermal conductivity and viscosity of glycerine-water based Cu-SiO_2 hybrid nanofluids. Mater Today: Proc. 2022;66:1823–9.
67. Chawhan SS, Barai DP, Bhanvase BA. Investigation on thermophysical properties, convective heat transfer and performance evaluation of ultrasonically synthesized Ag-doped TiO_2 hybrid nanoparticles based highly stable nanofluid in a minichannel. Thermal Sci Eng Progress. 2021;25: 100928.
68. Esfe MH, Arani AAA, Rezaie M, Yan W-M, Karimipour A. Experimental determination of thermal conductivity and dynamic viscosity of Ag–MgO/water hybrid nanofluid. Int Commun Heat Mass Transfer. 2015;66:189–95.
69. Aberoumand S, Jafarimoghaddam A. Tungsten (III) oxide (WO_3)–Silver/transformer oil hybrid nanofluid: preparation, stability, thermal conductivity and dielectric strength. Alex Eng J. 2018;57:169–74.
70. Kishore P, Sireesha V, Harsha VS, Rao VD, Solomon AB. Preparation, characterization and thermo-physical properties of Cu-graphene nanoplatelets hybrid nanofluids. Mater Today: Proc. 2020;27:610–4.
71. Ma X, Song Y, Wang Y, Yao S, Vafai K. Amelioration of pool boiling thermal performance utilizing graphene-silver hybrid nanofluids. Powder Technol. 2022;397:117110.
72. Yarmand H, Gharehkhani S, Ahmadi G, Shirazi SFS, Baradaran S, Montazer E, Zubir MNM, Alehashem MS, Kazi S, Dahari M. Graphene nanoplatelets–silver hybrid nanofluids for enhanced heat transfer. Energy Convers Manage. 2015;100:419–28.
73. Li X, Zeng G, Lei X. The stability, optical properties and solar-thermal conversion performance of SiC-MWCNTs hybrid nanofluids for the direct absorption solar collector (DASC) application. Sol Energy Mater Sol Cells. 2020;206: 110323.
74. Munkhbayar B, Tanshen MR, Jeoun J, Chung H, Jeong H. Surfactant-free dispersion of silver nanoparticles into MWCNT-aqueous nanofluids prepared by one-step technique and their thermal characteristics. Ceram Int. 2013;39:6415–25.
75. Sundar LS, Ramana EV, Graça M, Singh MK, Sousa AC. Nanodiamond-Fe3O4 nanofluids: preparation and measurement of

viscosity, electrical and thermal conductivities. Int Commun Heat Mass Transfer. 2016;73:62–74.
76. Sundar LS, Mesfin S, Ramana EV, Said Z, Sousa AC. Experimental investigation of thermo-physical properties, heat transfer, pumping power, entropy generation, and exergy efficiency of nanodiamond+ Fe_3O_4/60: 40% water-ethylene glycol hybrid nanofluid flow in a tube. Thermal Sci Eng Progress. 2021;21: 100799.
77. Said Z, Jamei M, Sundar LS, Pandey A, Allouhi A, Li C. Thermophysical properties of water, water and ethylene glycol mixture-based nanodiamond+ Fe_3O_4 hybrid nanofluids: an experimental assessment and application of data-driven approaches. J Mol Liq. 2022;347: 117944.
78. Saleh B, Sundar LS. Entropy generation and exergy efficiency analysis of ethylene glycol-water based nanodiamond+ Fe_3O_4 hybrid nanofluids in a circular tube. Powder Technol. 2021;380:430–42.
79. Tiwari AK, Pandya NS, Said Z, Chhatbar SH, Al-Turki YA, Patel AR. 3S (Sonication, surfactant, stability) impact on the viscosity of hybrid nanofluid with different base fluids: an experimental study. J Mol Liq. 2021;329: 115455.
80. Tiwari AK, Pandya NS, Said Z, Öztop HF, Abu-Hamdeh N. 4S consideration (synthesis, sonication, surfactant, stability) for the thermal conductivity of CeO_2 with MWCNT and water based hybrid nanofluid: an experimental assessment. Colloids Surf, A. 2021;610: 125918.
81. Said Z, Sharma P, Sundar LS, Afzal A, Li C. Synthesis, stability, thermophysical properties and AI approach for predictive modelling of Fe_3O_4 coated MWCNT hybrid nanofluids. J Mol Liq. 2021;340: 117291.
82. Harandi SS, Karimipour A, Afrand M, Akbari M, D'Orazio A. An experimental study on thermal conductivity of F-MWCNTs–Fe3O4/EG hybrid nanofluid: effects of temperature and concentration. Int Commun Heat Mass Transfer. 2016;76:171–7.
83. Alklaibi A, Sundar LS, Mouli KVC. Experimental investigation on the performance of hybrid Fe_3O_4 coated MWCNT/Water nanofluid as a coolant of a Plate heat exchanger. Int J Therm Sci. 2022;171: 107249.
84. Alawi OA, Kamar HM, Hussein OA, Mallah A, Mohammed HA, Khiadani M, Roomi AB, Kazi S, Yaseen ZM. Effects of binary hybrid nanofluid on heat transfer and fluid flow in a triangular-corrugated channel: an experimental and numerical study. Powder Technol. 2022;395:267–79.
85. M Safi, A Ghozatloo, NM SHARIATY, A Hamidi, Preparation of MWNT/TiO_2 nanofluids and study of its thermal conductivity and stability, (2014).
86. Bakhtiari R, Kamkari B, Afrand M, Abdollahi A. Preparation of stable TiO_2-Graphene/Water hybrid nanofluids and development of a new correlation for thermal conductivity. Powder Technol. 2021;385:466–77.
87. Shajan S, Baiju V, Krishnakumar T, Andrew G, Thomas L, Alex M, Safeer MB. Experimental investigation on thermophysical properties of Therminol® 55 based hybrid nanofluids with alumina and graphene nanoplatelets for medium temperature applications. Thermal Sci Eng Progress. 2021;26: 101116.
88. Askari S, Lotfi R, Rashidi A, Koolivand H, Koolivand-Salooki M. Rheological and thermophysical properties of ultra-stable kerosene-based Fe_3O_4/Graphene nanofluids for energy conservation. Energy Convers Manage. 2016;128:134–44.
89. Mechiri SK, Vasu V, Venu GA. Investigation of thermal conductivity and rheological properties of vegetable oil based hybrid nanofluids containing Cu–Zn hybrid nanoparticles. Experiment Heat Transfer. 2017;30(3):205–17.
90. Kumar MS, Vasu V, Gopal AV. Thermal conductivity and rheological studies for Cu–Zn hybrid nanofluids with various basefluids. J Taiwan Inst Chem Eng. 2016;66:321–7.
91. Mechiri SK, Vasu V, Babu S. Thermal conductivity of Cu-Zn hybrid newtonian nanofluids: experimental data and modeling using neural network. Procedia Eng. 2015;127:561–7.
92. Paul G, Philip J, Raj B, Das PK, Manna I. Synthesis, characterization, and thermal property measurement of nano-Al95Zn05 dispersed nanofluid prepared by a two-step process. Int J Heat Mass Transf. 2011;54:3783–8.
93. Abbas F, Ali HM, Shaban M, Janjua MM, Shah TR, Doranehgard MH, Ahmadlouydarab M, Farukh F. Towards convective heat transfer optimization in aluminum tube automotive radiators: potential assessment of novel Fe_2O_3-TiO_2/water hybrid nanofluid. J Taiwan Inst Chem Eng. 2021;124:424–36.
94. Mousavi S, Esmaeilzadeh F, Wang X. A detailed investigation on the thermo-physical and rheological behavior of MgO/TiO_2 aqueous dual hybrid nanofluid. J Mol Liq. 2019;282:323–39.
95. Devendiran DK, Amirtham VA. A review on preparation, characterization, properties and applications of nanofluids. Renew Sustain Energy Rev. 2016;60:21–40.
96. Syam Sundar L, Mesfin S, Tefera Sintie Y, Punnaiah V, Chamkha AJ, Sousa A. A review on the use of hybrid nanofluid in a solar flat plate and parabolic trough collectors and its enhanced collector thermal efficiency. J Nanofluids. 2021;10:147–71.
97. Nabil M, Azmi W, Hamid K, Zawawi N, Priyandoko G, Mamat R. Thermo-physical properties of hybrid nanofluids and hybrid nanolubricants: a comprehensive review on performance. Int Commun Heat Mass Transfer. 2017;83:30–9.
98. Sandhya M, Ramasamy D, Kadirgama K, Harun W, Saidur R. Experimental study on properties of hybrid stable & surfactant-free nanofluids GNPs/CNCs (Graphene nanoplatelets/cellulose nanocrystal) in water/ethylene glycol mixture for heat transfer application. J Mol Liq. 2022;348: 118019.
99. Zhang H, Qing S, Xu J, Zhang X, Zhang A. Stability and thermal conductivity of TiO_2/water nanofluids: a comparison of the effects of surfactants and surface modification. Colloids Surf A. 2022;641: 128492.
100. Hazra S, Michael M, Nandi T. Investigations on optical and photo-thermal conversion characteristics of BN-EG and BN/CB-EG hybrid nanofluids for applications in direct absorption solar collectors. Sol Energy Mater Sol Cells. 2021;230: 111245.
101. Hamid KA, Azmi W, Nabil M, Mamat R, Sharma K. Experimental investigation of thermal conductivity and dynamic viscosity on nanoparticle mixture ratios of TiO_2-SiO2 nanofluids. Int J Heat Mass Transf. 2018;116:1143–52.
102. Singh J, Kumar R, Gupta M, Kumar H. Thermal conductivity analysis of GO-CuO/DW hybrid nanofluid. Mater Today: Proc. 2020;28:1714–8.
103. Li X, Zou C, Lei X, Li W. Stability and enhanced thermal conductivity of ethylene glycol-based SiC nanofluids. Int J Heat Mass Transf. 2015;89:613–9.
104. Jin C, Wu Q, Yang G, Zhang H, Zhong Y. Investigation on hybrid nanofluids based on carbon nanotubes filled with metal nanoparticles: Stability, thermal conductivity, and viscosity. Powder Technol. 2021;389:1–10.
105. Wanatasanappan VV, Abdullah M, Gunnasegaran P. Thermophysical properties of Al_2O_3-CuO hybrid nanofluid at different nanoparticle mixture ratio: An experimental approach. J Mol Liq. 2020;313: 113458.
106. M. Tekir, E. Gedik, K. Arslan, H.K. Pazarlıoğlu, B. Aksu, E. Taskesen, Hydrothermal behavior of hybrid magnetite nanofluid flowing in a pipe under bi-directional magnetic field with different wave types. Thermal Sci Eng Progress 2022; 101399.

107. Singh R, Sah NK, Sharma V. Development and characterization of unitary and hybrid Al_2O_3 and ZrO dispersed Jatropha oil-based nanofluid for cleaner production. J Clean Prod. 2021;317: 128365.
108. Daungthongsuk W, Wongwises S. A critical review of convective heat transfer of nanofluids. Renew Sustain Energy Rev. 2007;11:797–817.
109. Mane NS, Tripathi S, Hemadri V. Effect of biopolymers on stability and properties of aqueous hybrid metal oxide nanofluids in thermal applications. Colloids Surf A. 2022;643: 128777.
110. Chamsa-Ard W, Brundavanam S, Fung CC, Fawcett D, Poinern G. Nanofluid types, their synthesis, properties and incorporation in direct solar thermal collectors: a review. Nanomaterials. 2017;7:131.
111. Yu H, Hermann S, Schulz SE, Gessner T, Dong Z, Li WJ. Optimizing sonication parameters for dispersion of single-walled carbon nanotubes. Chem Phys. 2012;408:11–6.
112. Chakraborty S, Panigrahi PK. Stability of nanofluid: a review. Appl Therm Eng. 2020;174: 115259.
113. Hamid KA, Azmi W, Nabil M, Mamat R. Experimental investigation of nanoparticle mixture ratios on TiO_2–SiO_2 nanofluids heat transfer performance under turbulent flow. Int J Heat Mass Transf. 2018;118:617–27.
114. Nabil M, Azmi W, Hamid KA, Mamat R, Hagos FY. An experimental study on the thermal conductivity and dynamic viscosity of TiO_2-SiO_2 nanofluids in water: ethylene glycol mixture. Int Commun Heat Mass Transfer. 2017;86:181–9.
115. Garg P, Alvarado JL, Marsh C, Carlson TA, Kessler DA, Annamalai K. An experimental study on the effect of ultrasonication on viscosity and heat transfer performance of multi-wall carbon nanotube-based aqueous nanofluids. Int J Heat Mass Transf. 2009;52:5090–101.
116. Eshgarf H, Kalbasi R, Maleki A, Shadloo MS. A review on the properties, preparation, models and stability of hybrid nanofluids to optimize energy consumption. J Therm Anal Calorim. 2021;144:1959–83.
117. Xian HW, Sidik NAC, Saidur R. Impact of different surfactants and ultrasonication time on the stability and thermophysical properties of hybrid nanofluids. Int Commun Heat Mass Transfer. 2020;110: 104389.
118. Hormozi F, ZareNezhad B, Allahyar H. An experimental investigation on the effects of surfactants on the thermal performance of hybrid nanofluids in helical coil heat exchangers. Int Commun Heat Mass Transfer. 2016;78:271–6.
119. Ghadimi A, Metselaar IH. The influence of surfactant and ultrasonic processing on improvement of stability, thermal conductivity and viscosity of titania nanofluid. Exp Thermal Fluid Sci. 2013;51:1–9.
120. Leong KY, Razali I, Ahmad KK, Ong HC, Ghazali MJ, Rahman MRA. Thermal conductivity of an ethylene glycol/water-based nanofluid with copper-titanium dioxide nanoparticles: an experimental approach. Int Commun Heat Mass Transfer. 2018;90:23–8.
121. Ouabouch O, Kriraa M, Lamsaadi M. Stability, thermophsical properties of nanofluids, and applications in solar collectors: a review. AIMS Mater Sci. 2021;8:659–84.
122. Suresh S, Venkitaraj K, Selvakumar P, Chandrasekar M. Effect of Al_2O_3–Cu/water hybrid nanofluid in heat transfer. Exp Thermal Fluid Sci. 2012;38:54–60.
123. Akilu S, Baheta AT, Sharma K. Experimental measurements of thermal conductivity and viscosity of ethylene glycol-based hybrid nanofluid with TiO_2-CuO/C inclusions. J Mol Liq. 2017;246:396–405.
124. Qing SH, Rashmi W, Khalid M, Gupta T, Nabipoor M, Hajibeigy MT. Thermal conductivity and electrical properties of hybrid SiO_2-graphene naphthenic mineral oil nanofluid as potential transformer oil. Mater Res Express. 2017;4: 015504.
125. Yıldırım ÇV, Şirin Ş, Kıvak T, Sarıkaya M. A comparative study on the tribological behavior of mono&proportional hybrid nanofluids for sustainable turning of AISI 420 hardened steel with cermet tools. J Manuf Process. 2022;73:695–714.
126. Asadi A, Alarifi IM, Ali V, Nguyen HM. An experimental investigation on the effects of ultrasonication time on stability and thermal conductivity of MWCNT-water nanofluid: finding the optimum ultrasonication time. Ultrason Sonochem. 2019;58: 104639.
127. Asadi M, Asadi A. Dynamic viscosity of MWCNT/ZnO–engine oil hybrid nanofluid: an experimental investigation and new correlation in different temperatures and solid concentrations. Int Commun Heat Mass Transfer. 2016;76:41–5.
128. Mukherjee S, Mishra PC, Chaudhuri P. Stability of heat transfer nanofluids–a review. ChemBioEng Reviews. 2018;5:312–33.
129. Toghraie D, Chaharsoghi VA, Afrand M. Measurement of thermal conductivity of ZnO–TiO_2/EG hybrid nanofluid. J Therm Anal Calorim. 2016;125:527–35.
130. Esfe MH, Saedodin S, Biglari M, Rostamian H. Experimental investigation of thermal conductivity of CNTs-Al_2O_3/water: a statistical approach. Int Commun Heat Mass Transfer. 2015;69:29–33.
131. Muneeshwaran M, Srinivasan G, Muthukumar P, Wang C-C. Role of hybrid-nanofluid in heat transfer enhancement–a review. Int Commun Heat Mass Transfer. 2021;125: 105341.
132. Chandrasekar M, Suresh S, Senthilkumar T. Mechanisms proposed through experimental investigations on thermophysical properties and forced convective heat transfer characteristics of various nanofluids–a review. Renew Sustain Energy Rev. 2012;16:3917–38.
133. Kumar V, Sahoo RR. Viscosity and thermal conductivity comparative study for hybrid nanofluid in binary base fluids. Heat Transfer—Asian Research. 2019;48(7):3144-61
134. Ma M, Zhai Y, Yao P, Li Y, Wang H. Synergistic mechanism of thermal conductivity enhancement and economic analysis of hybrid nanofluids. Powder Technol. 2020;373:702–15.
135. Said Z, Sundar LS, Rezk H, Nassef AM, Ali HM, Sheikholeslami M. Optimizing density, dynamic viscosity, thermal conductivity and specific heat of a hybrid nanofluid obtained experimentally via ANFIS-based model and modern optimization. J Mol Liq. 2021;321: 114287.
136. Vărdaru A, Huminic G, Huminic A, Fleacă C, Dumitrache F, Morjan I. Synthesis, characterization and thermal conductivity of water based graphene oxide–silicon hybrid nanofluids: an experimental approach. Alex Eng J. 2022;61:12111–22.
137. Taherialekouhi R, Rasouli S, Khosravi A. An experimental study on stability and thermal conductivity of water-graphene oxide/aluminum oxide nanoparticles as a cooling hybrid nanofluid. Int J Heat Mass Transf. 2019;145: 118751.
138. Arani AAA, Pourmoghadam F. Experimental investigation of thermal conductivity behavior of MWCNTS-Al_2O_3/ethylene glycol hybrid Nanofluid: providing new thermal conductivity correlation. Heat Mass Transf. 2019;55:2329–39.
139. Asadi A, Asadi M, Rezaniakolaei A, Rosendahl LA, Afrand M, Wongwises S. Heat transfer efficiency of Al_2O_3-MWCNT/thermal oil hybrid nanofluid as a cooling fluid in thermal and energy management applications: an experimental and theoretical investigation. Int J Heat Mass Transf. 2018;117:474–86.
140. Pourrajab R, Noghrehabadi A, Behbahani M, Hajidavalloo E. An efficient enhancement in thermal conductivity of water-based hybrid nanofluid containing MWCNTs-COOH and Ag nanoparticles: experimental study. J Therm Anal Calorim. 2021;143:3331–43.

141. Wole-Osho I, Okonkwo EC, Adun H, Kavaz D, Abbasoglu S. An intelligent approach to predicting the effect of nanoparticle mixture ratio, concentration and temperature on thermal conductivity of hybrid nanofluids. J Therm Anal Calorim. 2021;144:671–88.
142. Kanti PK, Sharma K, Said Z, Jamei M, Yashawantha KM. Experimental investigation on thermal conductivity of fly ash nanofluid and fly ash-Cu hybrid nanofluid: prediction and optimization via ANN and MGGP model. Part Sci Technol. 2022;40:182–95.
143. Malika M, Sonawane SS. Application of RSM and ANN for the prediction and optimization of thermal conductivity ratio of water based Fe_2O_3 coated SiC hybrid nanofluid. Int Commun Heat Mass Transfer. 2021;126: 105354.
144. Rostami S, Toghraie D, Esfahani MA, Hekmatifar M, Sina N. Predict the thermal conductivity of SiO_2/water–ethylene glycol (50: 50) hybrid nanofluid using artificial neural network. J Therm Anal Calorim. 2021;143:1119–28.
145. Rostami S, Toghraie D, Shabani B, Sina N, Barnoon P. Measurement of the thermal conductivity of MWCNT-CuO/water hybrid nanofluid using artificial neural networks (ANNs). J Therm Anal Calorim. 2021;143:1097–105.
146. Pourrajab R, Ahmadianfar I, Jamei M, Behbahani M. A meticulous intelligent approach to predict thermal conductivity ratio of hybrid nanofluids for heat transfer applications. J Therm Anal Calorim. 2021;146:611–28.
147. M. Hemmat Esfe, P.M. Behbahani, A.A.A. Arani, M.R. Sarlak, Thermal conductivity enhancement of SiO_2–MWCNT (85: 15%)–EG hybrid nanofluids, J Thermal Anal Calorimetry (2017); 128: 249–258.
148. Esfe MH, Arani AAA, Firouzi M. Empirical study and model development of thermal conductivity improvement and assessment of cost and sensitivity of EG-water based SWCNT-ZnO (30%: 70%) hybrid nanofluid. J Mol Liq. 2017;244:252–61.
149. K Hamid, W Azmi, M Nabil, R Mamat Improved thermal conductivity of TiO_2–SiO_2 hybrid nanofluid in ethylene glycol and water mixture. IOP Conference series: materials science and engineering, IOP Publishing, 2017, pp. 012067.
150. Parsian A, Akbari M. New experimental correlation for the thermal conductivity of ethylene glycol containing Al_2O_3–Cu hybrid nanoparticles. J Therm Anal Calorim. 2018;131:1605–13.
151. Esfahani NN, Toghraie D, Afrand M. A new correlation for predicting the thermal conductivity of ZnO–Ag (50%–50%)/water hybrid nanofluid: an experimental study. Powder Technol. 2018;323:367–73.
152. M. Hemmat Esfe, S. Esfandeh, M. Rejvani, Modeling of thermal conductivity of MWCNT-SiO_2 (30: 70%)/EG hybrid nanofluid, sensitivity analyzing and cost performance for industrial applications. J Thermal Anal Calorimetry (2018); 131 1437–1447.
153. Esfe MH, Rejvani M, Karimpour R, Abbasian Arani AA. Estimation of thermal conductivity of ethylene glycol-based nanofluid with hybrid suspensions of SWCNT–Al_2O_3 nanoparticles by correlation and ANN methods using experimental data. J Thermal Anal Calorimetry. 2017;128:1359–71.
154. Afrand M. Experimental study on thermal conductivity of ethylene glycol containing hybrid nano-additives and development of a new correlation. Appl Therm Eng. 2017;110:1111–9.
155. Shahsavani E, Afrand M, Kalbasi R. Experimental study on rheological behavior of water–ethylene glycol mixture in the presence of functionalized multi-walled carbon nanotubes. J Therm Anal Calorim. 2018;131:1177–85.
156. Sezer N, Atieh MA, Koç M. A comprehensive review on synthesis, stability, thermophysical properties, and characterization of nanofluids. Powder Technol. 2019;344:404–31.
157. Nadooshan AA, Eshgarf H, Afrand M. Measuring the viscosity of Fe_3O_4-MWCNTs/EG hybrid nanofluid for evaluation of thermal efficiency: Newtonian and non-Newtonian behavior. J Mol Liq. 2018;253:169–77.
158. Giwa SO, Sharifpur M, Ahmadi MH, Sohel Murshed SM, Meyer JP. Experimental investigation on stability, viscosity, and electrical conductivity of water-based hybrid nanofluid of MWCNT-Fe_2O_3. Nanomaterials. 2021;11(1):136.
159. Adio SA, Sharifpur M, Meyer JP. Investigation into effective viscosity, electrical conductivity, and pH of γ-Al_2O_3-glycerol nanofluids in Einstein concentration regime. Heat Transfer Eng. 2015;36:1241–51.
160. Zawawi N, Azmi W, Redhwan A, Sharif M, Samykano M. Experimental investigation on thermo-physical properties of metal oxide composite nanolubricants. Int J Refrig. 2018;89:11–21.
161. Giwa SO, Sharifpur M, Meyer JP. Experimental study of thermoconvection performance of hybrid nanofluids of Al_2O_3-MWCNT/water in a differentially heated square cavity. Int J Heat Mass Transf. 2020;148: 119072.
162. Giwa S, Sharifpur M, Meyer JP, Wongwises S, Mahian O. Experimental measurement of viscosity and electrical conductivity of water-based γ-Al_2O_3/MWCNT hybrid nanofluids with various particle mass ratios. J Therm Anal Calorim. 2021;143:1037–50.
163. Zhu Y, Zamani M, Xu G, Toghraie D, Hashemian M, Alizadeh AA. A comprehensive experimental investigation of dynamic viscosity of MWCNT-WO_3/water-ethylene glycol antifreeze hybrid nanofluid. J Molecul Liquid. 2021;1(333):115986.
164. Afrand M, Najafabadi KN, Akbari M. Effects of temperature and solid volume fraction on viscosity of SiO_2-MWCNTs/SAE40 hybrid nanofluid as a coolant and lubricant in heat engines. Appl Therm Eng. 2016;102:45–54.
165. Amini F, Miry SZ, Karimi A, Ashjaee M. Experimental investigation of thermal conductivity and viscosity of SiO_2/multiwalled carbon nanotube hybrid nanofluids. J Nanosci Nanotechnol. 2019;19:3398–407.
166. Hemmat Esfe M, Sarmasti Emami MR, Kiannejad AM. Experimental investigation of effective parameters on MWCNT–TiO_2/SAE50 hybrid nanofluid viscosity. J Thermal Anal Calorimetry. 2019;137:743–57.
167. Moldoveanu GM, Minea AA, Iacob M, Ibanescu C, Danu M. Experimental study on viscosity of stabilized Al_2O_3, TiO_2 nanofluids and their hybrid. Thermochim Acta. 2018;659:203–12.
168. Urmi W, Rahman M, Hamzah W. An experimental investigation on the thermophysical properties of 40% ethylene glycol based TiO_2-Al_2O_3 hybrid nanofluids. Int Commun Heat Mass Transfer. 2020;116: 104663.
169. Wole-Osho I, Okonkwo EC, Kavaz D, Abbasoglu S. An experimental investigation into the effect of particle mixture ratio on specific heat capacity and dynamic viscosity of Al_2O_3-ZnO hybrid nanofluids. Powder Technol. 2020;363:699–716.
170. Asadi A, Alarifi IM, Foong LK. An experimental study on characterization, stability and dynamic viscosity of CuO-TiO_2/water hybrid nanofluid. J Mol Liq. 2020;307: 112987.
171. Dalkılıç AS, Açıkgöz Ö, Küçükyıldırım BO, Eker AA, Lüleci B, Jumpholkul C, Wongwises S. Experimental investigation on the viscosity characteristics of water based SiO_2-graphite hybrid nanofluids. Int Commun Heat Mass Transfer. 2018;97:30–8.
172. Kazemi I, Sefid M, Afrand M. A novel comparative experimental study on rheological behavior of mono & hybrid nanofluids concerned graphene and silica nano-powders: characterization, stability and viscosity measurements. Powder Technol. 2020;366:216–29.
173. Kanti P, Sharma KV, Yashawantha KM, Dmk S. Experimental determination for viscosity of fly ash nanofluid and fly ash-Cu hybrid nanofluid: prediction and optimization using artificial intelligent techniques. Energy Sour Part A: Recov, Utilization, Environ Effects. 2021;I:1–20.

174. Chu Y-M, Ibrahim M, Saeed T, Berrouk AS, Algehyne EA, Kalbasi R. Examining rheological behavior of MWCNT-TiO_2/5W40 hybrid nanofluid based on experiments and RSM/ANN modeling. J Mol Liq. 2021;333: 115969.
175. Toghraie D, Aghahadi MH, Sina N, Soltani F. Application of artificial neural networks (ANNs) for predicting the viscosity of tungsten oxide (WO_3)-MWCNTs/engine oil hybrid nanofluid. Int J Thermophys. 2020;41:1–17.
176. Jamei M, Ahmadianfar I. A rigorous model for prediction of viscosity of oil-based hybrid nanofluids. Physica A. 2020;556: 124827.
177. Said Z, Cakmak NK, Sharma P, Sundar LS, Inayat A, Keklikcioglu O, Li C. Synthesis, stability, density, viscosity of ethylene glycol-based ternary hybrid nanofluids: experimental investigations and model-prediction using modern machine learning techniques. Powder Technol. 2022;400: 117190.
178. Dardan E, Afrand M, Isfahani AM. Effect of suspending hybrid nano-additives on rheological behavior of engine oil and pumping power. Appl Therm Eng. 2016;109:524–34.
179. Moldoveanu GM, Minea AA. Specific heat experimental tests of simple and hybrid oxide-water nanofluids: proposing new correlation. J Mol Liq. 2019;279:299–305.
180. Gao Y, Xi Y, Zhenzhong Y, Sasmito AP, Mujumdar AS, Wang L. Experimental investigation of specific heat of aqueous graphene oxide Al_2O_3 hybrid nanofluid. Therm Sci. 2021;25:515–25.
181. Tiwari AK, Pandya NS, Shah H, Said Z. Experimental comparison of specific heat capacity of three different metal oxides with MWCNT/water-based hybrid nanofluids: proposing a new correlation. Appl Nanosci. 2020;I:1–11.
182. de Oliveira LR, Ribeiro SR, Reis MH, Cardoso VL, Bandarra Filho EP. Experimental study on the thermal conductivity and viscosity of ethylene glycol-based nanofluid containing diamond silver hybrid material. Diamond Related Mater 2019; 96: 216-30.
183. S Akilu, A Baheta, K Sharma, M Said, Experimental determination of nanofluid specific heat with SiO_2 nanoparticles in different base fluids. AIP conference proceedings, AIP Publishing LLC, 2017, pp. 090001
184. Çolak AB, Yıldız O, Bayrak M, Tezekici BS. Experimental study for predicting the specific heat of water based Cu-Al_2O_3 hybrid nanofluid using artificial neural network and proposing new correlation. Int J Energy Res. 2020;44:7198–215.
185. Kumar V, Pare A, Tiwari AK, Ghosh SK. Efficacy evaluation of oxide-MWCNT water hybrid nanofluids: an experimental and artificial neural network approach. Colloids Surf, A. 2021;620: 126562.
186. Sepehrnia M, Mohammadzadeh K, Veyseh MM, Agah E, Amani M. Rheological behavior of engine oil based hybrid nanofluid containing MWCNTs and ZnO nanopowders: experimental analysis, developing a novel correlation, and neural network modeling. Powder Technol. 2022;404: 117492.
187. Mahian O, Bellos E, Markides CN, Taylor RA, Alagumalai A, Yang L, Qin C, Lee BJ, Ahmadi G, Safaei MR. Recent advances in using nanofluids in renewable energy systems and the environmental implications of their uptake. Nano Energy. 2021;86: 106069.
188. Ajeena AM, Víg P, Farkas I. A comprehensive analysis of nanofluids and their practical applications for flat plate solar collectors: Fundamentals, thermophysical properties, stability, and difficulties. Energy Rep. 2022;8:4461–90.
189. Shamsul Azha NI, Hussin H, Nasif MS, Hussain T. Thermal performance enhancement in flat plate solar collector solar water heater: a review. Processes. 2020;8(7):756.
190. SA Kalogirou, Solar energy engineering: processes and systems, 1st edition, Academic press, 2009
191. Choudhary S, Sachdeva A, Kumar P. Investigation of the stability of MgO nanofluid and its effect on the thermal performance of flat plate solar collector. Renew Energy. 2020;147:1801–14.
192. Tong Y, Chi X, Kang W, Cho H. Comparative investigation of efficiency sensitivity in a flat plate solar collector according to nanofluids. Appl Therm Eng. 2020;174: 115346.
193. Liu S, Afan HA, Aldlemy MS, Al-Ansari N, Yaseen ZM. Energy analysis using carbon and metallic oxides-based nanomaterials inside a solar collector. Energy Rep. 2020;6:1373–81.
194. Ahmadlouydarab M, Ebadolahzadeh M, Ali HM. Effects of utilizing nanofluid as working fluid in a lab-scale designed FPSC to improve thermal absorption and efficiency. Physica A. 2020;540: 123109.
195. Akram N, Sadri R, Kazi S, Ahmed S, Zubir M, Ridha M, Soudagar M, Ahmed W, Arzpeyma M, Tong GB. An experimental investigation on the performance of a flat-plate solar collector using eco-friendly treated graphene nanoplatelets–water nanofluids. J Therm Anal Calorim. 2019;138:609–21.
196. Moravej M, Bozorg MV, Guan Y, Li LK, Doranehgard MH, Hong K, Xiong Q. Enhancing the efficiency of a symmetric flat-plate solar collector via the use of rutile TiO_2-water nanofluids. Sustainable Energy Technol Assess. 2020;40: 100783.
197. Vincely DA, Natarajan E. Experimental investigation of the solar FPC performance using graphene oxide nanofluid under forced circulation. Energy Convers Manage. 2016;117:1–11.
198. Hawwash A, Rahman AKA, Nada S, Ookawara S. Numerical investigation and experimental verification of performance enhancement of flat plate solar collector using nanofluids. Appl Therm Eng. 2018;130:363–74.
199. Hussein OA, Habib K, Muhsan AS, Saidur R, Alawi OA, Ibrahim TK. Thermal performance enhancement of a flat plate solar collector using hybrid nanofluid. Sol Energy. 2020;204:208–22.
200. Ahmed M, Meteab MM, Salih QO, Mohammed HA, Alawi OA. Experimental investigation on the thermophysical and rheological behavior of aqueous dual hybrid nanofluid in flat plate solar collectors. Energies. 2022;15:8541.
201. Elshazly E, Abdel-Rehim AA, El-Mahallawi I. 4E study of experimental thermal performance enhancement of flat plate solar collectors using MWCNT, Al_2O_3, and hybrid MWCNT/Al2O3 nanofluids. Results in Engineering. 2022;16: 100723.
202. Mausam K, Pare A, Ghosh SK, Tiwari A. Thermal performance analysis of hybrid-nanofluid based flat plate collector using grey relational analysis (GRA): an approach for sustainable energy harvesting. Thermal Sci Eng Progress. 2023;37: 101609.
203. Saleh B, Sundar LS. Thermal efficiency, heat transfer, and friction factor analyses of MWCNT+ Fe_3O_4/water hybrid nanofluids in a solar flat plate collector under thermosyphon condition. Processes. 2021;9:180.
204. Syam Sundar L, Misganaw AH, Singh MK, Sousa AC, Ali HM. Efficiency analysis of thermosyphon solar flat plate collector with low mass concentrations of ND–Co_3 O_4 hybrid nanofluids: an experimental study. J Thermal Anal Calorimetry. 2021;143:959–72.
205. Farajzadeh E, Movahed S, Hosseini R. Experimental and numerical investigations on the effect of Al_2O_3/TiO_2H_2O nanofluids on thermal efficiency of the flat plate solar collector. Renew Energy. 2018;118:122–30.
206. Kalbande VP, Walke PV, Rambhad K, Nandanwar Y, Mohan M. Performance evaluation of energy storage system coupled with flat plate solar collector using hybrid nanofluid of CuO+ Al2O3/water. In : J Phys: Conf Ser 2021 May 1 (Vol. 1913, No. 1, p. 012067). IOP Publishing
207. Wole-Osho I, Adun H, Adedeji M, Okonkwo EC, Kavaz D, Dagbasi M. Effect of hybrid nanofluids mixture ratio on the performance of a photovoltaic thermal collector. Int J Energy Res. 2020;44:9064–81.

208. Ibrahim M, Berrouk AS, Algehyne EA, Saeed T, Chu Y-M. Numerical evaluation of exergy efficiency of innovative turbulators in solar collector filled with hybrid nanofluid. J Therm Anal Calorim. 2021;145:1559–74.
209. Aghili Yegane SP, Kasaeian A. Thermal performance assessment of a flat-plate solar collector considering porous media, hybrid nanofluid and magnetic field effects. J Thermal Anal Calorimetry. 2020;141:1969–80.
210. Azimy N, Saffarian MR, Noghrehabadi A. Thermal performance analysis of a flat-plate solar heater with zigzag-shaped pipe using fly ash-Cu hybrid nanofluid: CFD approach. Environ Sci Pollut Res. 2022;I:1–19.
211. Xiong Q, Tayebi T, Izadi M, Siddiqui AA, Ambreen T, Li LK. Numerical analysis of porous flat plate solar collector under thermal radiation and hybrid nanoparticles using two-phase model. Sustain Energy Technol Assess. 2021;47: 101404.
212. Nabi H, Pourfallah M, Gholinia M, Jahanian O. Increasing heat transfer in flat plate solar collectors using various forms of turbulence-inducing elements and CNTs-CuO hybrid nanofluids. Case Stud Thermal Eng. 2022;33: 101909.
213. Fattahi A, Karimi N. Numerical simulation of the effects of superhydrophobic coating in an oval cross-sectional solar collector with a wavy absorber filled with water-based Al2O3-ZnO-Fe_3O_4 ternary hybrid nanofluid. Sustain Energy Technol Assess. 2022;50: 101881.
214. Alzahrani AK, Ullah MZ, Alshomrani AS, Gul T. Hybrid nanofluid flow in a Darcy-Forchheimer permeable medium over a flat plate due to solar radiation. Case Stud Thermal Eng. 2021;26: 100955.
215. Rb JA. Thermodynamic analysis of hybrid nanofluid based solar flat plate collector. World J Eng. 2018;15(1):27–39.
216. Lee M, Shin Y, Cho H. Theoretical study on performance comparison of various solar collectors using binary nanofluids. J Mech Sci Technol. 2021;35:1267–78.
217. Okonkwo EC, Wole-Osho I, Kavaz D, Abid M, Al-Ansari T. Thermodynamic evaluation and optimization of a flat plate collector operating with alumina and iron mono and hybrid nanofluids. Sustain Energy Technol Assess. 2020;37: 100636.
218. Mustafa J, Alqaed S, Sharifpur M. Evaluation of energy efficiency, visualized energy, and production of environmental pollutants of a solar flat plate collector containing hybrid nanofluid. Sustain Energy Technol Assess. 2022;53: 102399.
219. Stalin PMJ, Arjunan TV, Almeshaal M, Murugesan P, Prabu B, Kumar PM. Utilization of zinc-ferrite/water hybrid nanofluids on thermal performance of a flat plate solar collector—a thermal modeling approach. Environ Sci Pollut Res. 2022;29:78848–61.
220. Bubbico R, Celata GP, D'Annibale F, Mazzarotta B, Menale C. Experimental analysis of corrosion and erosion phenomena on metal surfaces by nanofluids. Chem Eng Res Des. 2015;104:605–14.